# Combining Microwave Links and IMERG-L for Improved Rainfall Estimation in Tropical Regions

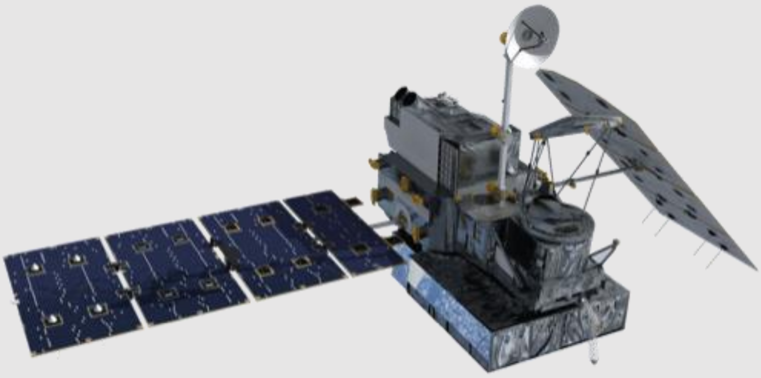


## Zina Janssen


**23-06-2022**


**Supervised by:**
Hidde Leijnse
Linda Bogerd


**MSc thesis**
**Hydrology and Quantitative Water Management Group**
**Wageningen University and Research**

# Abstract

Accurate rainfall measurements are a critical component in many hydrological and agricultural applications. Tropical regions often lack the infrastructure for measuring rainfall at high spatial and temporal resolutions.
Commercial Microwave Links (CML) provide opportunities for high-resolution rainfall measurements in tropical regions. As their standalone applicability is limited by various sources of error and their distribution in space they should be complemented with additional sources of rainfall measurements. For that purpose, this study uses rainfall estimations from the Integrated Multi-satellitE Retrievals for GPM (IMERG) V06 Late Half Hourly. CML and IMERG-derived rainfall estimations between September and December 2019 for Sri Lanka are combined through Kriging with External Drift (KED). This study was the first one to attempt to merge CML and satellite data and found that KED is not suitable. Using KED does not increase performance compared to IMERG or CML as standalone methods. Overall, KED underestimates rainfall and contains more errors than IMERG and CML, due to the low correlation between CML and IMERG and the strong variation over the domain. Validations using a gauge data set showed some seasonal, but no spatial patterns. Future research should implement methods that rely less on assumptions such as Double Kernel Density Smoothing or Geographically Weighted Regression Kriging. Additionally, improving understanding of precipitation and landscape characteristics allows more effective tailoring of the merging method.

# Contents

# 1 | Introduction

## 1.1 Context and motivation

Accurate rainfall monitoring is required for applications such as flood prediction and management, agricultural modelling, and weather forecasting (Grum et al., 2005; Brauer et al., 2016; Gaona et al., 2018; Chwala and Kunstmann, 2019; Overeem et al., 2021). Additionally, precipitation data can be used to assess the effects of climate change (Skofronick-Jackson et al., 2018). Because of its high variability in both time and space, rainfall is notoriously difficult to measure on large scales (Grum et al., 2005; Chwala and Kunstmann, 2019; Overeem et al., 2021). Especially in developing countries with tropical climates, rainfall estimation remains a hefty challenge (Tapiador et al., 2021). The rainfall regimes in tropical climates are characterised by high spatial and temporal variability (Wong and Jim, 2014). However, developing regions usually lack measuring networks that can accurately capture the diversity in precipitation intensity and location (Gosset et al., 2016).

Various methods to estimate rainfall over large areas exist, such as rain gauges, satellites, weather radar and commercial microwave links (CML), each with different benefits and drawbacks. Rain gauges, for example, are able to directly measure rain but are negatively affected by wind, evaporation, and snow and usually have limited spatial coverage (Brauer et al., 2016). Regional rainfall estimates interpolated using sparse gauge networks are shown to contain large errors due to the limited sampling density (Shao et al., 2021).

Weather radars can continuously measure precipitation with a radius of  200 kilometres but are costly to install and maintain and often not present in economically underdeveloped regions. Radar estimations are also affected by errors such as ground clutter and beam blockage (Todini and Mazzetti, 2006).

Satellites provide global estimates, often being the only source of precipitation estimation in developing regions. However, satellite estimations of precipitation are known to be afflicted by errors and bias and can have very low accuracy. The quality of the estimations is mainly impacted by instrumental, algorithmic and sampling errors (Zhao et al., 2022). Additionally, most satellite products have coarse resolutions, both on spatial and temporal scales (Gaona et al., 2018). This severely limits the stand-alone applicability of satellites for precipitation measurements (Overeem et al., 2016a).

CML are recognized as a valuable opportunistic source of precipitation estimations (e.g. Leijnse et al. (2007); Overeem et al. (2016b); Gaona et al. (2018); Christofilakis et al. (2020); Graf et al. (2020)). The frequency of the emitted electromagnetic waves from telephone towers is sensitive to attenuation by rainfall (figure 1.1).

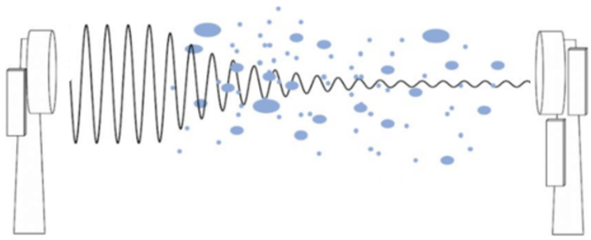

Figure 1.1: Workings of CML. Adapted from Polz et al. (2021). Karlsruhe Institute of Technology.

Records of the transmitted and received signal level (RSL) allow the estimation of a path averaged rain rate based on a power-law attenuation equation (equation 1.1), where $A$ is the attenuation, $R$ is the path averaged rain rate and $a$ and $b$ are functions of the drop size distribution and signal frequency and polarisation (Zinevich et al., 2008).

$$A = aR^b \tag{1.1}$$

The difference in RSL of the emitted and received microwave between wet and dry events allows for estimation of path-averaged rainfall rates (Overeem et al., 2016b). Overeem et al. (2013) found that around 90% of the land area of the world is covered by telecommunication networks, resulting in the low additional costs and global applicability of this technique.

CML derived rainfall data also knows drawbacks. Signal strength is not only affected by precipitation, but also by fog, dust, wet antenna attenuation, and reflection of the beam by objects such as buildings (Gaona et al., 2018; Overeem et al., 2021). The accuracy of the estimation depends on the number of links present and the density of radio towers strongly correlates with population density. This results in CML estimations being most accurate in and around urban areas, but generally much less so in remote regions (Gaona et al., 2017; Chwala and Kunstmann, 2019). As stated by David et al. (2021), the associated sources of error and the unequal spatial distribution means that CML should be supplemented with other data sources, especially when used in remote areas.

Efforts to improve precipitation estimation worldwide are made through NASA's and JAXA's Global Precipitation Mission (GPM). Their Multi-satellitE Retrievals for GPM (IMERG) product offers a gridded global precipitation data set that is available at 30 minute intervals. While IMERG has been a big step towards tackling accurate precipitation measurements, the product does contain significant bias and error. Anjum et al. (2019) found that IMERG tends to underestimate low-intensity events and fails to capture light rainfall. Subsequently, multiple studies have found that IMERG fails to record high-intensity events, underestimating the total amount of precipitation (Foelsche et al., 2017; Maranan et al., 2020; Bogerd et al., 2021). However, validations of IMERG in the West African forest zone and the Merapi basin in Indonesia have shown promising results regarding IMERG's performance in tropical climate regimes (Maranan et al., 2020; Rahmawati et al., 2021). Additionally, Skofronick-Jackson et al. (2017) have confirmed IMERG's capability to capture monsoon dynamics in India. IMERG is thus a viable candidate to supplement CML in tropical regions. However, as mentioned by Sunilkumar et al. (2019), evaluation results differ between regions and region-specific evaluation is advisable prior to using IMERG precipitation estimates.

Merging multiple sources of measurements is a solidified manner to improve rainfall estimation (Liberman et al., 2014; Trömel et al., 2014; Kumah et al., 2020; Shao et al., 2021). Bianchi et al. (2013) have demonstrated that rainfall estimations combining satellite, gauge, radar, and CML derived measurements perform better than the individual methods. For example, Kumah et al. (2021) used satellite data for Wet-Dry classification and estimation of wet path length resulting in improved CML accuracy. Most research on merging rainfall products is conducted on merging gauges and radar, radar and CML, or satellites and gauges (e.g. Krajewski (1987); Sinclair and Pegram (2005); Yuehong et al. (2008); Kim and Yoo (2014); Park et al. (2017)). As radar and gauges are not always available in tropical regions, the current research will merge CML and satellites, which is, as far as the author is aware, the first attempt at doing so.

Merging can be done using a panoply of methods (Safont et al., 2019). Some examples are a mean field bias (MFB) adjustment (Cummings et al., 2009), a distance weighted algorithm (Liberman et al., 2014), various types of Kriging (Haberlandt, 2007; Cantet, 2017; Eisele et al., 2021), a Kalman filter (Trömel et al., 2014), Kernel density smoothing (Li and Shao, 2010; Long et al., 2016) and by integrating some of the previously mentioned methods (Shao et al., 2021). Simplistic methods such as using an MFB adjustment, Inverse Distance Weighting and Nearest Neighbours usually fail to capture the variability of the rainfall field (Haberlandt, 2007; Trömel et al., 2014; Liberman et al., 2014). Approaches using calculus of variation such as described by Bianchi et al. (2013), are complex and difficult to implement for large data sets.

In the existing literature, Kriging is reported as one of the best methods for merging different sources of rainfall measurements when using a sufficiently large number of observations. Non-stationary types of Kriging that combine a regression of the dependent variable, an auxiliary variable, and the spatial autocorrelation between the residuals such as Kriging with External Drift (KED) show the most favourable performance compared to some of the other methods mentioned above. When used for large regions, these non-stationary Kriging methods are able to capture the dynamic nature of rainfall and produce lower errors and inaccuracies (Goudenhoofdt and Delobbe, 2009; Sideris et al., 2014; Park et al., 2017). Implementing a merged product in tropical regions can significantly improve rainfall estimation. The current research uses multiple sources of rainfall estimation to create such a merged product, combining IMERG and CML using KED.

## 1.2 Research questions

This research will study the potential of a merged IMERG-CML based rainfall product. The input measurements need to be evaluated on their performance to identify sources of bias and error that can propagate into the merged product. Initially, the performance of IMERG in Sri Lanka should be evaluated. For the evaluation of the performance of CML, the results from Overeem et al. (2021) will be used, which examine the same area and period as the current research. These evaluations will be used to assess whether combining of CML and IMERG leads to improved estimation compared to the individual products. From this objective, the following research questions are formulated.

1. How accurate are IMERG precipitation estimates over Sri Lanka?
2. What is the potential of a merged product using KED for estimating rainfall in Sri Lanka?
   a) How does the performance of the merged product compare to the rain gauge measurements and CML and IMERG individually?
   b) What are the most important precipitation characteristics and spatial factors associated with errors and biases in the merged product?

## 1.3 Thesis contents

This thesis is divided into five chapters. Chapter 2 addresses the data and methods used and describes the area under evaluation. In this chapter the site characteristics of the study area are discussed. Additionally, the studied data sets, preprocessing steps and implemented methods are described. Subsequently, the chapter describes the methods used. Chapter 3 describes the results of the previously described methods. In chapter 4, the limitations of the current research as well as suggestions for future research are presented. The last chapter, chapter 5, provides the conclusion of the research.

# 2 | Materials and Methods

## 2.1 Field Site

The research area comprises Sri Lanka, an island nation located in the Indian Ocean. The yearly average temperature is 27° C and the country has a tropical monsoon climate. The Sri Lankan monsoon climate is characterised by intense precipitation events, as stated by Thambyahpillay (1954): "It never rains, it pours."

The precipitation pattern is subject to strong temporal and spatial variation, with mean annual rainfall below 900 mm in the southeast and northwest and above 5000 mm on the western slopes of the mountains in the south (Overeem et al., 2021). Following the classification of Karunaweera et al. (2014), the country is divided into three climatic zones: wet, dry, and intermediate (figure 2.1).

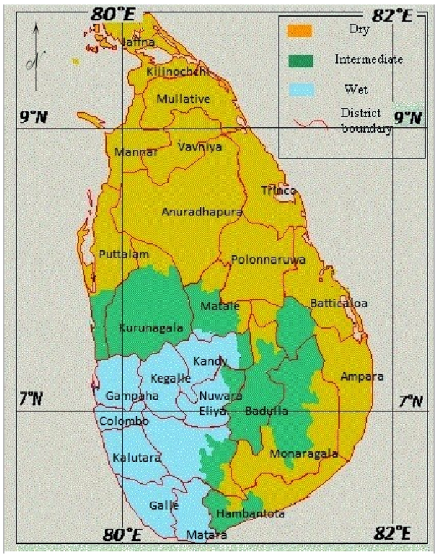


Figure 2.1: Climatic regions Sri Lanka. Adapted from Karunaweera et al. (2014)

Rainfall characteristics such as intensity and drop size distribution influence the accuracy of measurements, understanding the different drivers of the Sri Lankan weather patterns thus increases understanding of validation results.

The period under review spans from 12 September to 31 December 2019. This period captures the last part of the southwest monsoon (SWM) -from May until September-, the second inter-monsoon period (IMP) -between October and November-, and the first part of the northeast monsoon (NEM), between December and February (Thambyahpillay, 1954).

During the SWM the monsoon brings moisture from the Indian Ocean and causes intense precipitation, up to 2500 mm per month, on the southwest coast. Additionally, heavy rains occur on the windward (southwestern) side of the mountains, while there is very little rain on the leeward (northeastern) side.

Within the IMP, rainfall most of Sri Lanka receives 400 mm of rain. In the same period, the southwestern slopes are subject to rainfall sums of up to 1200 mm. Furthermore, this period is characterized by strong winds, thunderstorms, and high-intensity precipitation events. These are influenced by the southward migration of the Inter Tropical Convergence Zone over Sri Lanka, tropical depressions, and cyclones.

During the NEM, the west coast receives relatively little rain, while heavier precipitation occurs in the northeastern part. The windward slopes of the mountain range experience rainfall up to 2500 mm (Marambe et al., 2015; Overeem et al., 2021).

## 2.2 Data

Three sources of rainfall data are used: CML, satellite, and gauge measurements. CML and satellite measurements will be merged and the gauge data is used for the validation of the merged product and IMERG. These sources will be described in the following section.

### CML derived rainfall measurements

Path averaged rainfall rates derived from the CMLs are retrieved using the R package RAINLINK[1]. Using the maximum and minimum signal level over a period of 15 minutes, the maximum and minimum RSL are determined which are converted to mean rainfall intensities. To estimate rainfall rates, RAINLINK follows a five-step process: 1. Wet-Dry classification, 2. reference level calculation, 3. outlier filtering, 4. conversion to signal attenuation, and 5. path averaged rainfall intensity calculation. These steps are shortly explained in the following paragraph.

Firstly, to prevent rainfall overestimation during dry periods, wet-dry classification using the nearby link approach is employed to separate wet and dry periods (step 1). If at least half of the links in the vicinity (i.e., within 10 km) are experiencing a decrease in RSL, the link for that time step is classified as wet. Secondly, a Reference Signal Level is computed (step 2) after which outliers

[1]The package can be found on GitHub https://github.com/overeem11/RAINLINK

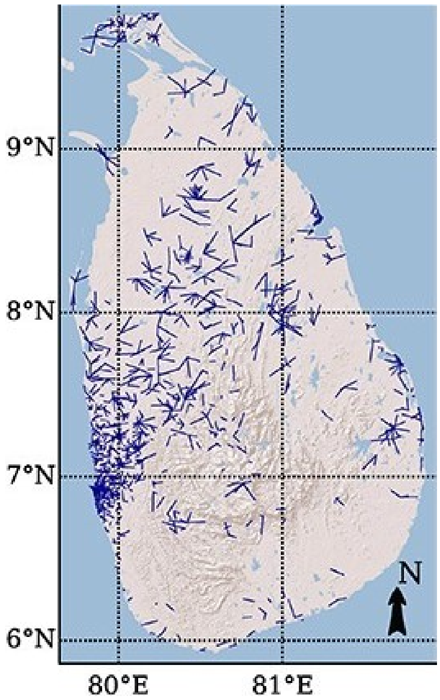


Figure 2.2: Cml locations. Adapted from Overeem et al. (2021)

are removed based on a Received Power Threshold (step 3). Subsequently, the minimum and maximum received powers are converted to attenuations using the reference signal level (step 4). Lastly, the path averaged rainfall intensities are computed from these corrected and filtered attenuations (step 5). For more details on RAINLINK, consult Overeem et al. (2016a).

The minimum and maximum RSL used for producing rainfall rates for Sri Lanka are provided by Dialog Sri Lanka for 1326 link paths at 15-minute intervals (Overeem et al., 2021). Although RAINLINKs parameters such as the nearby link search radius, wet antenna attenuation, and the outlier filter threshold are calibrated for the Netherlands, Overeem et al. (2021) found that this does not severely impact RAINLINKs performance for Sri Lanka. This is likely due to the smaller relative importance of wet antenna attenuation and errors in dry-wet classification as a result of the generally higher rainfall intensity in Sri Lanka. Additionally, Gaona et al. (2017) found that differences in climatology do not strongly affect the power-law relation (equation 1.1) used to retrieve rainfall rates. This renders RAINLINK useful and effective for estimating rainfall in tropical regions.

### Satellite rainfall measurements

For the satellite measurements the GPM IMERG product is used, of which the most current version is V06. IMERG is a combination of observations from the GPM Core Observatory satellite, the GPM constellation, and reanalysis data[2]. Gaps in the observations are filled using morphing algorithms (consult Huffman et al. (2015b); Tan et al. (2019); Huffman et al. (2015a) for a more in-depth description of IMERG). Additionally, temporal interpolation is done using displacement vectors derived from infrared measurements (Tan et al., 2016; Maranan et al., 2020). This combination allows for precipitation estimation at 30-minute intervals at a 0.1° resolution (~120km$^2$). 1066 IMERG pixels are considered in the current research, depicted in figure 2.3 (Foelsche et al., 2017).

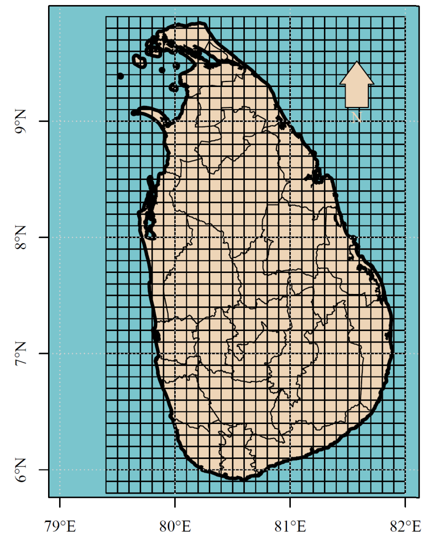


Figure 2.3: IMERG pixel location over Sri Lanka

Three types of IMERG products exist, IMERG Early (IMERG-E), IMERG Late (IMERG-L) and IMERG Final (IMERG-F). Their respective latencies are three hours, twelve hours, and three months. Selecting the most appropriate version of IMERG is subject to several considerations, regarding their performance and temporal availability.

Bogerd et al. (2021) describes that IMERG-L performs better than IMERG-E, due to the inclusion of additional sources of data and the usage of both forward and backward propagation, instead of only forward interpolation. The IMERG-F product is regarded as the most accurate version, due to its calibration using gauges from the Global Precipitation Climate Centre (GPCC) (Huffman et al., 2015a). However, these GPCC gauges are unequally spread. As Brocca et al. (2020) have found, IMERG-L outperforms IMERG-F in gauge-poor areas. As the number of GPCC gauges in Sri Lanka is limited and the latency of IMERG-L is much lower than that of IMERG-F, 14 hours versus 3 months, IMERG-L is assumed to perform best and is chosen. The prod-

[2] Reanalysis data is a combination of past short-term forecasts and observations through assimilation, used in meteorology.

uct is available both on half-hourly and daily timescales. The current research uses the V06 IMERG-L half-hourly product, hereafter referred to as IMERG.

#### Rain gauge measurements

A rain gauge network provided by the Sri Lanka Department of Meteorology is used to validate both IMERG and the merged precipitation estimates. Two sets of gauge measurements are available, one containing the data for September-December 2019, and one data set for the whole of 2020. Both contain stations that take hourly and/or daily measurements. Daily measurements span from 08:30-08:30 (+5:30 UTC) the following day.

The location of the gauges is shown in figure 2.4. Not all gauges provide consistent measurements due to instrument errors, in which case no data is available for that time step. The stations, months for which data is available, and the percentage of time intervals where rainfall data was recorded (availability) are displayed in table 2.1. The 2019 data serves as validation for the final product, whereas the 2020 data only serves as validation for IMERG.

Table 2.1: Available data

| Measurement Interval | Months | Year | Nr. of stations | Availability |
|---|---|---|---|---|
| Hourly | Sept-Dec | 2019 | 12 | 86% |
| Daily | Sept-Dec | 2019 | 11 | 100% |
| Hourly | Jan-Aug | 2020 | 19 | 99% |
| Daily | Jan-Dec | 2020 | 428 | 100% |

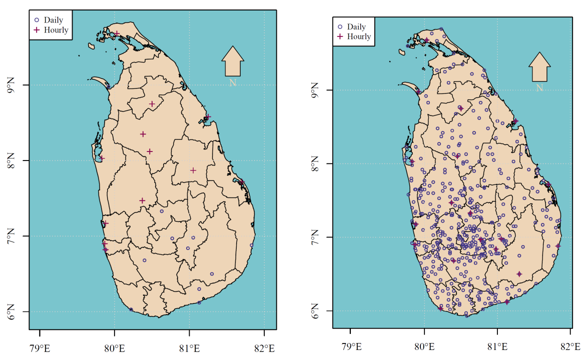


(a) Gauge data 2019 (b) Gauge data 2020

Figure 2.4: Hourly and daily rain gauge measurement locations

## 2.3 Methods

This section describes the preprocessing of the data, the method used for merging CML and IMERG predictions, and the subsequent validation. To increase insight into the performance of IMERG in Sri Lanka and the sources of error in the merged product, a separate validation of IMERG is conducted, also explained in this section.

### 2.3.1 Merging CML and IMERG precipitation measurements

For combining the gridded IMERG and the CML point estimations, Kriging with External drift (KED) is used. To avoid confusion, it should be mentioned that KED is mathematically very similar to and thus sometimes also called Regression Kriging or Universal Kriging. Kriging is a statistical method that describes the unknown value $\hat{Z}$ as a weighted combination of observations and a trend.

KED is an extension of Kriging that uses a drift function to describe a non-constant trend, allowing for the interpolation of non-stationary variables, such as rainfall (Cantet, 2017). KED utilises the correlation between measurements of the variable to be interpolated at location $s$, $Z(s)$, and a second variable $Y(s)$ to construct the drift function. The drift function represents a linear model of the prediction of $Z(s)$ by $Y$, where $Y$ is well known and accurately sampled. Additionally, $Z$ and $Y$ are assumed to strongly correlate over the whole domain.

After the construction of the drift function, the residuals are computed. Using the covariance structure of these residuals, the variogram that captures the spatial autocorrelation of the residuals of $Z(s)$ is constructed. Local differences in $Z(s)$ that are not captured with the drift function, are modelled by this variogram. This autocorrelation is described by the variogram parameters: the nugget, which represents random error, the highly local variation between observations, the range, which is the maximum distance over which there is correlation, and the sill, the variance in the observations at the range distance. Additionally, there are multiple shapes of variogram models such as Gaussian, exponential, and linear. Using the drift function and the spatial autocorrelation $\hat{Z}$ is estimated (Haberlandt, 2007).

As IMERG data is available for the whole country, it represents $Y(s)$, while the CML derived measurements represent the value to be estimated, $Z(s)$. Prior to merging, path averaged rainfall rates are converted to points in the middle of the link path to simplify the interpolation procedure. Additionally, the CML measurements are averaged from measurements of every 15 minutes to half-hourly measurements to match the temporal resolution of IMERG. KED requires some variation in the value of $Z(s)$ for the construction of the variogram. Following Grimes and Pardo-Igúzquiza (2010), only time steps with at least 0.1% of CML measurements indicating precipitation over 0.001 mm were interpolated. Instances with lower precipitation do not yield meaningful KED results and are considered as dry.

Using KED for rainfall estimation faces two important challenges. Fitting variograms on rainfall data is complex because of the variable nature of precipitation events, where the spatial autocorrelation of one time step can strongly differ from the autocorrelation at the next. As such, constructing a variogram from observations for every subsequent time step leads to improved performance of KED. This requires sufficient data, with a minimum of 300 measurements of $Z(s)$. The data provides at least 500 measurements per time step, which makes the continuous fitting of the variogram possible.

For every iteration, the linear model is constructed, the residuals are computed, and the variogram is drawn up. This will increase processing time but improve accuracy (Grimes and Pardo-Igúzquiza, 2010). The automated variogram fitting is done for every iteration using the automap package in R[3]. The variogram parameters are determined for every time step separately, which results in unique variograms with a different nugget, sill, range, and model structure. An overview of the variogram parameters can be found in the appendix **??**.

To further complicate matters, rainfall is strongly non-normal and Kriging assumes Gaussianity (Goovaerts et al., 1997). This is all the more important for KED, as it requires the residuals to be Gaussian as well. Normalising rainfall is complex due to the large number of zero values and extremes, causing the high possibility of introducing bias when back transforming the data.

Cecinati et al. (2017) compared different normalisation techniques when merging rainfall measurements through KED. It was concluded that a Box-Cox transform with $\lambda = 0.25$ provides the best trade-off between improving Gaussianity and avoiding high bias introduced through the back transform after the interpolation. Box-Cox transformation is a well-known method and is defined as follows

$$y^* = \begin{cases} \frac{y^\lambda - 1}{\lambda} & \lambda \neq 0 \\ \log(y) & \lambda = 0 \end{cases} \tag{2.1}$$

here $y$ represents the untransformed variable of interest and $y*$ is the same variable after transformation (Box and Cox, 1964). IMERG and CML derived measurements are both normalised using the Box-Cox transform with $\lambda = 0.25$. Normalised CML and IMERG measurements are then interpolated on a 0.02° grid. These interpolated values are back-transformed to obtain rainfall intensities at half-hour temporal resolutions. Regular back transformation produces the median of the variable. When interpolation is done, the interpolation variance can be used to decrease bias in the back transform, after which the back-transformed mean is produced using equation 2.2.

$$\begin{cases} (\lambda\mu + 1)^{1/\lambda}\left[1 + \frac{\sigma^2(1-\lambda)}{2(\lambda\mu+1)^2}\right] & \text{if } \lambda \neq 0 \\ e^{\mu}\left[1 + \frac{\sigma^2}{2}\right] & \text{if } \lambda = 0 \end{cases} \tag{2.2}$$

Using the Kriging variances, the KED derived measurements are back transformed.

KED derived measurements below zero are set to zero as negative rainfall is physically impossible. Additionally, rainfall intensity values over 500 mm/h are removed for the same reason.

### 2.3.2 Performance measures

The validation of rainfall measurements consists of two parts. Firstly, the wet-dry classification is assessed, which relates to the skill of signalling rainfall, irrespective of the amount. This classification is followed by an appraisal of the rainfall intensity estimation. Both evaluations are conducted for IMERG and KED predictions. Rain gauge measurements are compared to both measurements. As mentioned before, some stations provide daily measurements while others provide hourly measurements. As these are not always the same station nor provide the same amount of measurements, the hourly and daily data are evaluated separately. As the stations used for the daily and hourly evaluations are not the same (table 2.1), the performance scores, apart from the HSS, cannot easily be compared between the hourly and daily evaluations. The HSS is normalised by the complete range of of possible improvement over the standard, thus this metric can be compared.

#### Wet-Dry classification

Evaluation of the wet-dry classification is conducted as follows. IMERG and KED predictions are averaged to match the temporal resolution of the gauges. IMERG and KED values are extracted at the location of the gauges and compared.

Based on a threshold of at least 0.1 mm/h to distinguish between wet and dry, following Gaona et al. (2017), IMERG and KED predictions are compared to the gauge measurements and classified as Hit (H), Miss (M), False Alarm (FA), and Correct Negative (CN). H represents a correctly classified wet event, CN a correctly classified dry event, M is a wet event which is classified as dry, and FA defines dry events classified as dry. These performance scores are combined to obtain several contingency

[3] The documentation on this package can be found on: https://cran.r-project.org/web/packages/automap/automap.pdf.

metrics, following Kumah et al. (2020): Probability of Detection (POD), Probability of False Alarm (POFA), Accuracy (ACC) and Heike Skill Score (HSS).

Formulas for these metrics are shown in table 2.2. The POD represents the fraction of rain correctly detected, the POFA (also known as False Alarm Ratio) is the fraction of no rain incorrectly detected, and ACC is the fraction of rain and no rain correctly detected. The HSS compares the performance of the forecast to random chance. A POFA of 0 and POD of 1 indicate that rain is always correctly classified. The optimal score for HSS and ACC is 1, representing flawless forecasting and perfect accuracy of the forecasting respectively.

Table 2.2: Metrics for evaluating Wet-Dry classification of IMERG and KED

| Metric | Formula | Range | Optimum |
|---|---|---|---|
| *POD* | $\frac{H}{H+M}$ | 0 to 1 | 1 |
| *POFA* | $\frac{FA}{H+FA}$ | 0 to 1 | 0 |
| *ACC* | $\frac{H+CN}{H+CN+M+FA}$ | 0 to 1 | 1 |
| *HSS* | $\frac{2(H*CN-FA*M)}{(H+M)(M+CN)+(H+FA)(FA+CN)}$ | $-\infty$ to 1 | 1 |

### Statistical evaluation

The estimations of rainfall intensity by IMERG and the KED are compared to the gauge measurements. Performance of the rainfall depth estimation is evaluated using the Normalized Mean Absolute Error (NMAE) and the Relative Bias (RB).

The NMAE is the Mean Absolute Error (MAE), normalized using the mean. The MAE expresses the total amount of error between the sample and the prediction. The normalisation is applied to be able to compare the metric between different scales. Not all stations and measurement periods have the same data availability, so the normalisation allows for comparison between the different months, stations, and time intervals. The RB indicates the average systematic error. A RB smaller than 0 and over 0 indicate under and over estimation respectively. An NMAE and RB of 0 would indicate perfect agreement between the gauges and the estimation (table 2.3).

To compare the performance of KED and IMERG with the CML data as evaluated by Overeem et al. (2021), additional metrics, found in that paper, are used. These are the coefficient of determination, $r^2$ and the coefficient of variation of the residuals, CV. Comparison between CML and gauge values is done by constructing a simple linear model, describing the relationship between the two measurements. CML estimations are treated as the predictor variable and the gauge measurements are the measured variable. From this linear model the $r^2$ and the CV are calculated. Model fit is described by the $r^2$, where 0 indicates no skill and 1 indicates perfect skill. CV captures the spread of the residuals of the model around the regression line, the maximum value depends on the values in the data set. A CV of 0 indicates perfect agreement between the predictor and measured variable.

Table 2.3: Statistical metrics for evaluating IMERG and the merged product

| Metric | Formula | Range | Optimum |
|---|---|---|---|
| *NMAE* | $\frac{\sum_{i=1}^{n} \lvert R_{IMERG,i} - R_{gauge,i} \rvert}{\sum_{i=1}^{n} R_{gauge,i}}$ | 0 to $-\infty$ | 0 |
| *RB* | $\frac{\sum_{i=1}^{n} (R_{IMERG,i} - R_{gauge,i})}{\sum_{i=1}^{n} R_{gauge,i}} * 100\%$ | $-\infty$ to $\infty$ | 0 |
| *CV* | $\sqrt{\frac{\sum_{i=1}^{n} (Y_i - \hat{Y}_i)^2}{\mathrm{df}}}$ | - | 0 |
| $r2$ | $1 - \frac{SS_{\mathrm{res}}}{SS_{\mathrm{tot}}}$ | 0 to 1 | 1 |

Previous research has shown that IMERG performance depends on rainfall intensity, which varies with location and season (e.g Bogerd et al., 2021). As briefly mentioned before, CML are mainly present around urban areas and thus, CML-derived rainfall measurements are not equally spread over the country. Additionally, not all links consistently provide trustworthy power levels, resulting in a variable number of usable links over time. Thus both the availability and the performance of CML and IMERG vary over time and space.

This spatial and temporal variability of CML and IMERG can propagate into the KED estimations. To discover whether bias and error in IMERG and the KED estimation is linked to season or location, all evaluations are carried out on the complete data set, on data aggregated per month, and data aggregated per location. For a more in-depth evaluation of IMERG, the measurements are also compared against the 2020 gauge data set. To conduct spatial evaluation for 2020, aggregation is done based on the three climatic regions as seen on figure 2.1.

KED measurements are compared to the performance evaluation of IMERG and the CML evaluation as provided by Overeem et al. (2021). Furthermore, as KED is based upon assumptions regarding the input data, these assumptions are checked. These assumptions constitute the strong correlation between the auxiliary variable and the variable to be estimated and the anisotropy of the data. Investigating the validity of these assumptions for the current data sets improves understanding of the results.

# 3 | Results

This section consists of four parts. Firstly, overall performance scores and statistical metrics are presented. Secondly, metrics are compared between months to uncover seasonal effects. Thirdly, evaluations are conducted between stations for the 2019 evaluations and per climatic region for the validation of IMERGs performance in 2020. Lastly, four rainfall maps derived from KED and IMERG are presented to appreciate rainfall patterns produced by IMERG and KED and possible sources for errors are discussed.

## 3.1 Evaluation overall performance

Firstly, the Wet-Dry classification is assessed. This relates to the ability to distinguish between rain and no rain. The results of the evaluations of IMERG in 2019 serve as a benchmark for the later evaluation of the KED derived rainfall (referred to as KED). Also, the evaluations of IMERG in 2020 are used for general conclusions on the performance of IMERG in Sri Lanka.

### 3.1.1 Wet-Dry Classification

The Wet-Dry classification is evaluated by comparing the POD, POFA, ACC, and HSS (table 2.2). The aggregated scores are shown in table 3.1.

The POD and POFA indicate that IMERG can accurately distinguish between wet and dry time days. Hourly variations are classified a lot more poorly. As hourly rainfall is a lot more variable, classification per hour is more challenging than classification per day, partly explaining this difference (Haberlandt, 2007). IMERG has a low HSS, especially for hourly measurements, with almost no improvement of skill compared to random guessing. When considering the performance of IMERG in 2020, the discrepancy between the hourly and daily evaluation is again striking. The HSS between 2019 and 2020 is similar. This indicates that the time period does not strongly impact IMERG's country wide Wet-Dry classification. ACC and HSS are comparable for daily IMERG between 2019 and 2020, while slightly worse for hourly in 2019. IMERG has a overall high accuracy, which can be accounted to IMERGs skill at correctly classifying no rain.

The latter is further investigated and confirmed by calculating the same performance scores after the removal of rainfall events below 1 mm, using the gauge measurements as the indicator. From table 3.2, it can be seen that the ACC and HSS decrease, this effect is most pronounced for the daily evaluations. Performance for daily and hourly measurements become more similar.

Table 3.1: Performance scores IMERG

| **Scores 2019** | **POD** | **POFA** | **ACC** | **HSS** |
|---|---|---|---|---|
| Daily | 0.83 | 0.35 | 0.71 | 0.42 |
| Hourly | 0.34 | 0.73 | 0.64 | 0.06 |
| **Scores 2020** | | | | |
| Daily | 0.67 | 0.47 | 0.76 | 0.43 |
| Hourly | 0.27 | 0.84 | 0.84 | 0.12 |

Table 3.2: Performance scores IMERG when solely considering rainfall depths > 1 mm

| **Scores 2019** | **ACC** | **HSS** |
|---|---|---|
| Daily | 0.69 | 0.22 |
| Hourly | 0.58 | 0.19 |
| **Scores 2020** | | |
| Daily | 0.65 | 0.16 |
| Hourly | 0.64 | 0.06 |

When considering KED performance scores, daily Wet-Dry classification is somewhat decreased compared to IMERG (table 3.3). POD and POFA are similar and there is a small decrease in ACC and HSS. Hourly variations are captured slightly better with KED. All hourly performance scores have increase with respect to IMERG. However, HSS is still very low, indicating skill on par with random guessing.

Table 3.3: Performance scores KED

| **Scores** | **POD** | **POFA** | **ACC** | **HSS** |
|---|---|---|---|---|
| Daily | 0.76 | 0.37 | 0.66 | 0.32 |
| Hourly | 0.43 | 0.80 | 0.73 | 0.13 |

Performance scores change when only considering rainfall depths over 1 mm. The difference with the full evaluation for KED is smaller than for IMERG. Both for IMERG and KED, the HSS is more favourable in the filtered evaluations, albeit this effect is more pronounced for IMERG. In general, neither IMERG nor KED display high skill in Wet-Dry classification, regardless of the inclusion of light rainfall.

Table 3.4: Performance scores KED with rainfall depths > 1 mm

| **Scores** | **ACC** | **HSS** |
|---|---|---|
| Daily | 0.72 | 0.12 |
| Hourly | 0.67 | 0.2 |

### 3.1.2 Statistical evaluation

For a more quantitative evaluation the NMAE, RB, CV, and $r^2$ are computed (table 2.3). Scatter plots indicating the correlation between gauge measurements and IMERG are shown in figure 3.1. From the figures, it can be seen that while the NMAE is rather low, the measurements are not aligned with the 1:1 line. For the hourly measurements, there is a strong scatter around the zero rainfall values for both years. This can stem from local variations at the location of the gauges not captured by IMERG. Overall, the RB indicates that IMERG slightly overestimates rainfall, apart from the hourly measurements in 2019, which show an underestimation of 10.6%.

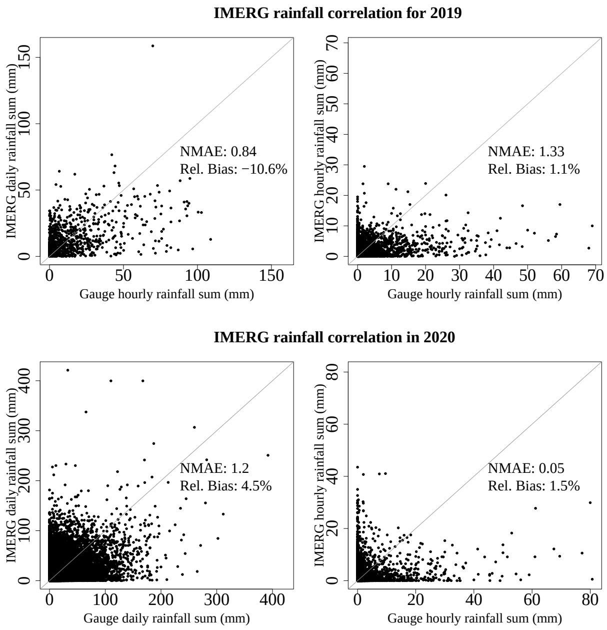


Figure 3.1: Scatter plots for IMERG rainfall depth correlation

Figure 3.2 shows that KED performs worse at estimating rainfall sums than IMERG. Generally, the NMAE is quite low an comparable for both intervals and measurements, with KED measurements having higher NMAE for both hourly and daily gauge values. The RB shows that daily rainfall is underestimated and hourly rainfall is overestimated. This pattern is also visible in IMERG. The hourly measurements show significant disagreement with the 1:1 line, with strong scatter at zero rainfall values, both for IMERG and KED.

In Overeem et al. (2021), scatter plots displaying the correlation between CML and gauge measurements can be found. To compare the patterns, these plots are also presented here. The CML measurements show better agreement with the 1:1 line than both IMERG and KED. Additionally, the scatter shows a better skill in estimating correct rainfall depths with non-zero rainfall, which is absent for both KED and IMERG. For the hourly measurements, it can be seen that there are large rainfall depths estimated by KED, CML, and IMERG for near-zero gauge measurements. This is most likely stemming from strong local variability in rainfall or gauge measurement errors, as the same pattern is found in all three measurements and thus originates from the gauges rather than the measurement method. Additionally, from this, the propagation of the rainfall estimation errors in IMERG and CML into KED can be seen.

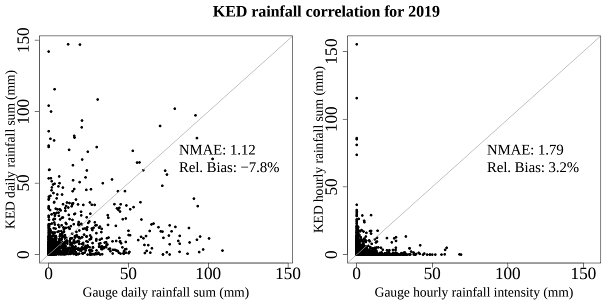


Figure 3.2: Scatter plot for KED rainfall depth correlation

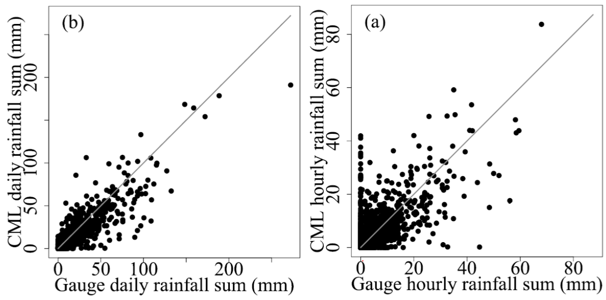


Figure 3.3: Scatter plots for CML rainfall depth. Adapted from Overeem et al. (2021)

This statistical evaluation is concluded by a comparison of metrics from the paper by Overeem et al. (2021), IMERG, and KED. From table 3.6 it can be seen that IMERG and KED are outperformed by CML, with lower $r^2$ and a higher CV. KED shows a decrease in all metrics, while IMERG shows lower $r^2$ and CV but less over- and underestimation for the daily measurements and the hourly measurements respectively. Especially the very low $r^2$ values show that KED has no skill in estimating rainfall depth.

When only considering rainfall $> 1$ mm, both KED and IMERG show further decreased performance. CV slightly improves, but $r^2$ is lower and especially increased underestimation of hourly rainfall is found. It is interesting to note that KED performs significantly worse than both IMERG and CML.

Table 3.5: Comparison of the statistical metrics IMERG, CML and KED

| All rainfall values | | | |
|---|---|---|---|
| **IMERG** | CV | $r^2$ | RB |
| Daily | 1.5 | 0.3 | -10.6% |
| Hourly | 5.7 | 0.2 | 1.1% |
| **CML** | | | |
| Daily | 0.87 | 0.79 | -17.6% |
| Hourly | 4.33 | 0.57 | 2.1% |
| **KED** | | | |
| Daily | 1.70 | 0.07 | -7.8% |
| Hourly | 5.9 | 0.003 | 3.2% |

Table 3.6: Comparison of the statistical metrics IMERG, CML and KED with $>$ 1 mm of rain

| Rainfall values $>$ 1 mm | | | |
|---|---|---|---|
| **IMERG** | | | |
| Daily | 1 | 0.2 | -24.4% |
| Hourly | 2.5 | 0.1 | -60.1% |
| **CML** | | | |
| Daily | 0.87 | 0.79 | -18.6% |
| Hourly | 0.86 | 0.58 | 15.6% |
| **KED** | | | |
| Daily | 1.1 | 0.02 | -11.9% |
| Hourly | 3.5 | 0.001 | -63.4% |

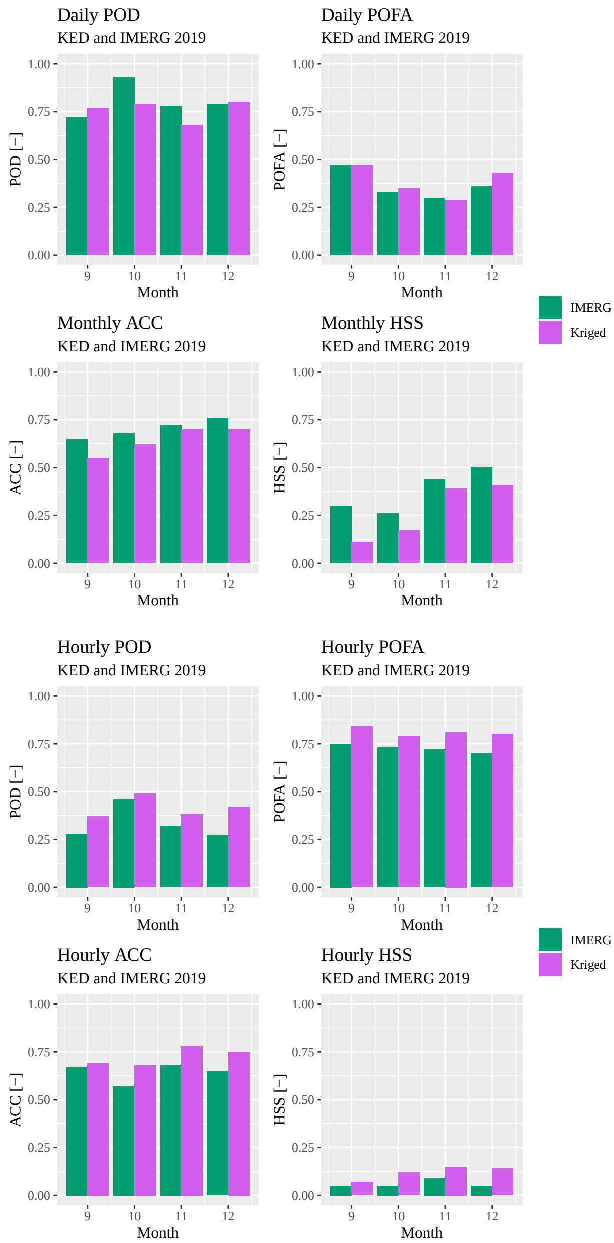


Figure 3.4: Performance skills per month in 2019

### Monthly comparison

To evaluate how seasons affect performance, metrics are aggregated per month as shown in figure 3.4. Recall that the period under review spans three different monsoonal periods, with the first one taking place until September, the second one between October and November and the last one starting in December. From this figure, no clear seasonal pattern is visible. There is some variation between the different months, the most notable is the difference in HSS in KED measurements. December, which coincides with the NEM, has the most favourable ACC and HSS for both IMERG and KED, but the effect is small. The differences between the months do overlap for KED and IMERG, indicating that seasonal effects propagate.

The same comparison is made for 2020, displayed in figure 3.5. The daily rainfall sums are available for the whole year, the hourly only from January until August. There is some difference between the months, with July having the best overall performance and February the worst. Monthly differences between are comparable for the hourly and daily evaluations. Low HSS and ACC are found for March-May, which coincides with the first inter-monsoon period. December still has more favourable scores compared to September - November, comparable to what is seen in figure 3.4. January has the best HSS and ACC, which also falls within the NEM. However, the differences remain small and February, which is also part of the NEM, is characterised with worse performance metrics.

To further explore seasonal effects, metrics per month are shown in figure 3.6. The NMAE is relatively consistent between the months, the figure displays that IMERG is associated with lower error than KED for all months. From the NMAE plots, no pattern is visible. When comparing the NMAE for hourly and daily measurements the small monthly variations are different. For example, NMAE is higher in September than in October for both

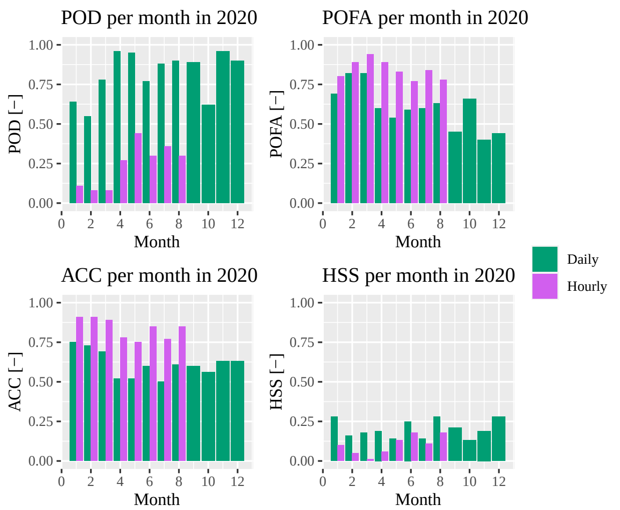


Figure 3.5: IMERG performance skills per month in 2020

IMERG and KED for the daily comparisons. For the hourly evaluations, NMAE is similar for KED and higher in October for IMERG. In case of strong seasonality, its effect should have been visible in both the hourly and daily gauge measurements.

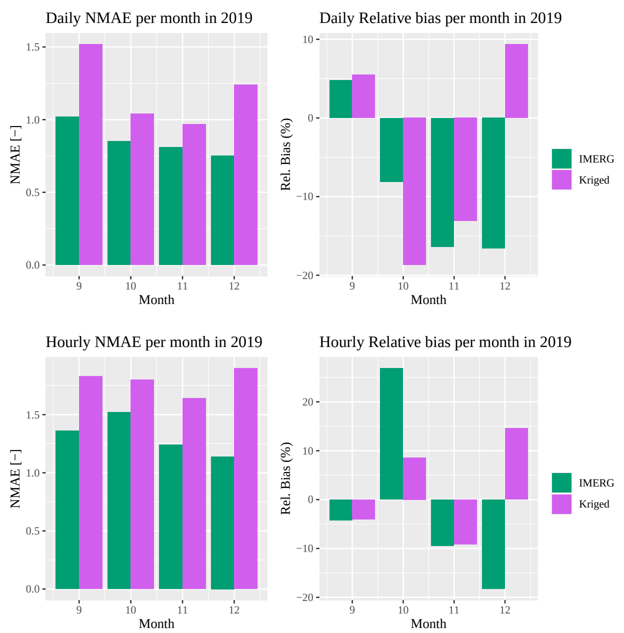


Figure 3.6: Monthly statistical metrics KED and IMERG

The difference in RB between the months is larger. The direction of the bias, albeit not the amount, shows agreement between KED and IMERG performance for September - November, whereas the directions in December are opposite. Agreement between the hourly and daily metrics is variable. The overestimation of KED and underestimation of IMERG in December are present in both plots, but October rainfall is underestimated on a daily interval but overestimated on an hourly one. When considering the patterns found in the Wet-Dry classification, with December having the best performance, these plots show a different outcome. The spikes and dips in IMERG metrics do somewhat correspond to the spikes and dips in the KED metrics, again indicating the propagation of the seasonal effects.

To conclude the monthly validations, the metrics for IMERG in 2020 are displayed in figure 3.7. Here, a strong increase in both NMAE and RB is found between March and May, whereas the rest of the months have comparable scores. These months coincide with the first inter monsoonal period, which runs from the end of February until April. This decreased performance for this season was also found in figure 3.5.

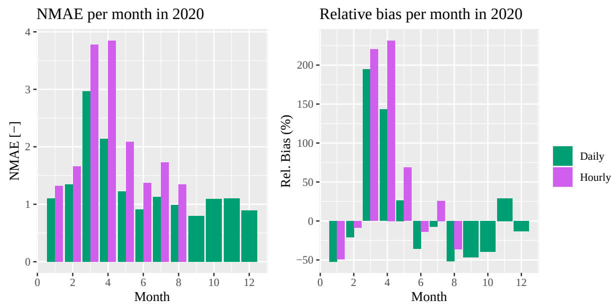


Figure 3.7: Monthly statistical metrics for IMERG in 2020

## Spatial variability

The spatial distribution of the metrics is evaluated by aggregating the data over the whole period per location. For the 2019 data, maps are created displaying the hourly and daily metrics per station (figure 3.8 and figure 3.9).

There is no distinct spatial pattern visible, however, IMERG performs slightly worse in the eastern part of the country, especially at the station that is at the upper part of the eastern coast (Trincomalee). POD, POFA and HSS show worse performance in the dry part of the country (figure 2.1).

The scores of the daily data set are more homogeneous compared to the hourly ones, seen in figure 3.8 and figure 3.10. Additionally, the hourly data are both under and overestimated, while the daily measurements are mainly underestimated. The most favourable scores coincide with the wet region as seen in figure 2.1. The strong difference between the performance scores for the hourly measurements may stem from the highly local hourly rainfall dynamics. The large variation between performance among gauges was also found by Overeem et al. (2021) and can also originate from gauge errors.

The 2020 data sets are aggregated into a wet, intermediate, and dry zone (figure 2.1). The aggregated scores per climatic region in 2020 for the hourly and daily

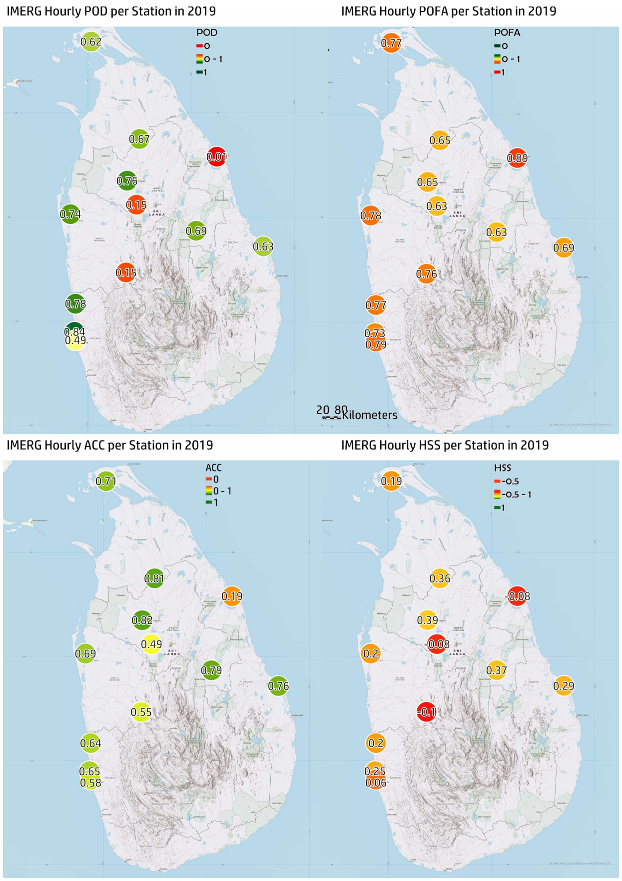


Figure 3.8: Hourly performance metrics per station for IMERG

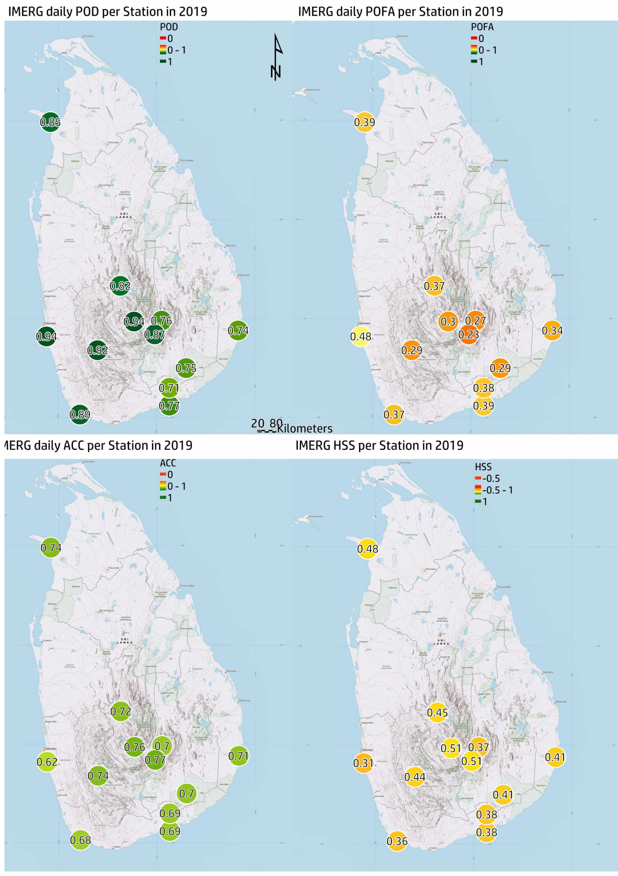


Figure 3.9: Daily performance metrics per station for IMERG

sets are shown in table 3.7. IMERG performs best in the wet zone, with the most striking difference the improved RB for the hourly data. The fact that scores indicating the most optimal IMERG performance in the wet zone and decreased performance elsewhere overlaps with the results as seen in the maps.

Table 3.7: Scores for IMERG in 2020

| Scores (Hourly) | Dry | Intermediate | Wet |
|---|---|---|---|
| *POD* | 0.18 | 0.31 | 0.34 |
| *POFA* | 0.89 | 0.82 | 0.82 |
| *ACC* | 0.87 | 0.82 | 0.80 |
| *HSS* | 0.07 | 0.14 | 0.14 |
| *NMAE* | 2.32 | 2.27 | 1.81 |
| *Rel. Bias* | 75.7 | 78.3 | 27.6 |
| **Scores (Daily)** | **Dry** | **Intermediate** | **Wet** |
| *POD* | 0.86 | 0.88 | 0.86 |
| *POFA* | 0.7 | 0.61 | 0.46 |
| *ACC* | 0.6 | 0.6 | 0.63 |
| *HSS* | 0.23 | 0.26 | 0.3 |
| *NMAE* | 1.36 | 1.31 | 1 |
| *Rel. Bias* | 43.2 | 24.5 | -14.6 |

The KED maps display no particular spatial pattern. The reduced performance in the eastern part of Sri Lanka as seen in figure 3.12 is also visible in the KED performance scores. Again, Wet-Dry classification skill is lowest at the Trincomalee station. From the figure, it can be seen that the locations of the CMLs (figure 2.2) coincide with more favourable performance scores for KED. Especially for the daily performance, the locations with better scores are similar between KED and IMERG, indicating that spatial differences in IMERG performance are somewhat present in KED. Both maps indicate propagation of spatial variability of CML and IMERG into KED.

The same spatial separation is conducted for the hourly RB and NMAE and displayed in figure 3.12. Striking are the two stations with very distinct scores. The most extreme ones are again Trincomalee, on the east coast with an NMAE of 2.13 and an RB of 50.7% and Ratmalana, on the bottom west coast, with an NMAE of 2.12 and an RB of 105.3%. Especially the last one is remarkable, as the stations that are close display significantly better metrics. It is unlikely that the variations in rainfall are that local, the high RB might stem from errors with the gauge. When looking at these metrics, no clear relation with the climatic regions is seen. There is no overlap between the spatial distribution of the performance scores and the metrics. Both maps show strong variation in performance scores per station, indicating that there is a strong spatial variability in the performance of IMERG, with the variation between the hourly

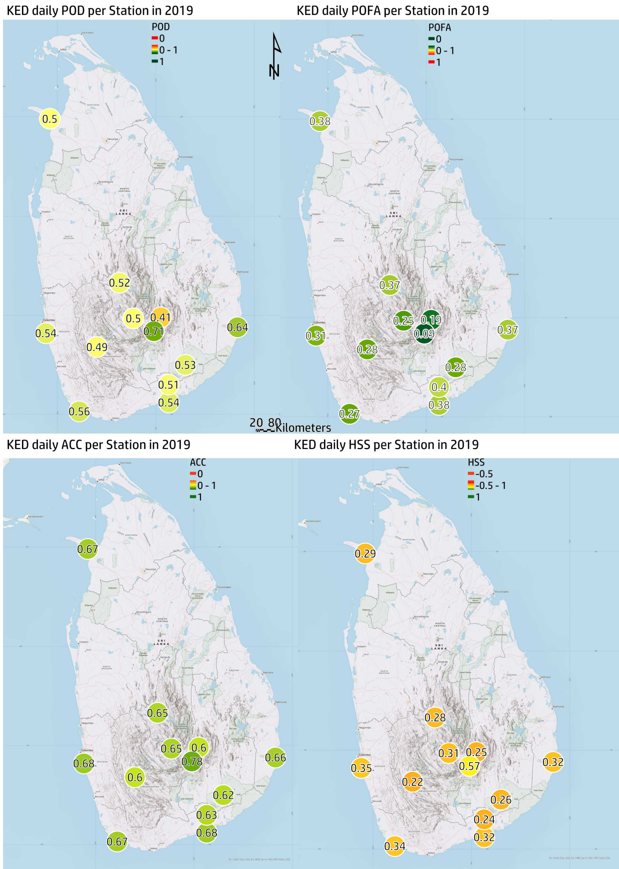


Figure 3.10: Daily performance metrics per station for KED

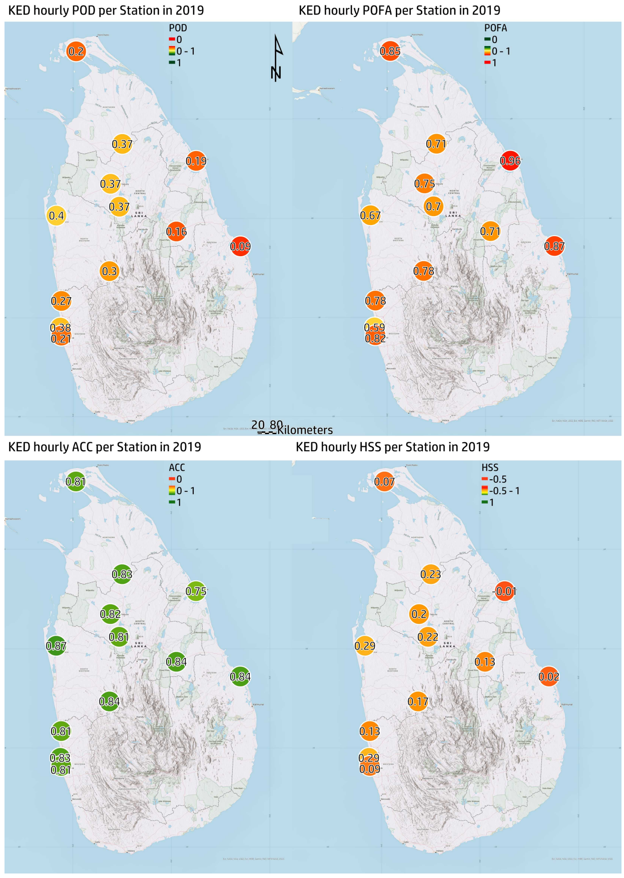


Figure 3.11: Hourly performance metrics per station for KED

measurements once again being greater than the daily ones.

When appreciating the hourly KED map (figure 3.13), the extreme values for the Trincomalee station are even more pronounced with an NMAE of 7.58 and an RB of 503.7% for KED. The Ratmalana station shows less extreme metrics, however, the difference in RB with the stations that are near remains notable.

The daily map, figure 3.15, contains less extreme values but still shows strong variation between the stations. The similarity between scores and their magnitude is less pronounced between the daily evaluation of KED and IMERG as compared to the hourly evaluations (figure 3.9). For example, the station on the bottom has an RB of -79.2% compared to IMERG and an RB of 53.6% compared to KED. The locations with the most links, on the eastern coast, do somewhat coincide with more favourable metrics, but the effect is less pronounced than as seen on the performance score maps.

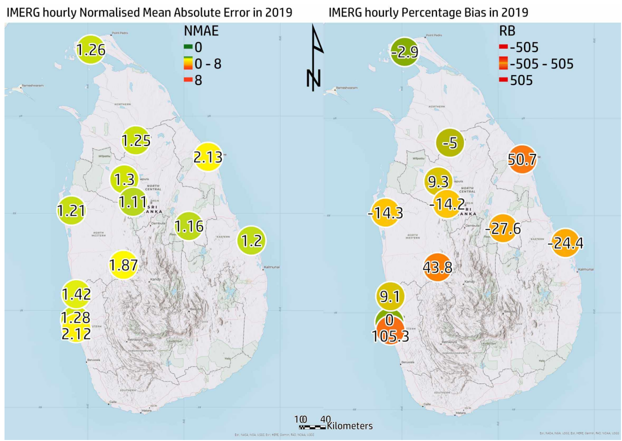


Figure 3.12: Hourly RB and NMAE per station for IMERG

### Rainfall maps

The last part of this results section contains four rainfall maps showing the rainfall patterns over Sri Lanka as derived from IMERG and KED. To increase understanding of the results and possible sources of error, two events are chosen where KED performs well, with differences between the gauges and KED below 0.001 mm/h. Additionally, two events where KED performs bad, with differences over 100 mm/h, are selected.

Figure 3.16 and figure 3.17 show two maps for iterations with small differences between the interpolated and the gauge rainfall. For the event on the 2nd of October (figure 3.16), the location of the rainfall event overlaps partly between IMERG and KED, rainfall on the top part

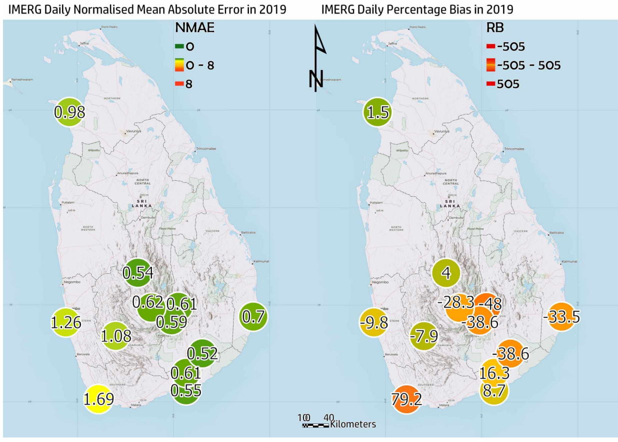


Figure 3.13: Daily RB and NMAE per station for IMERG

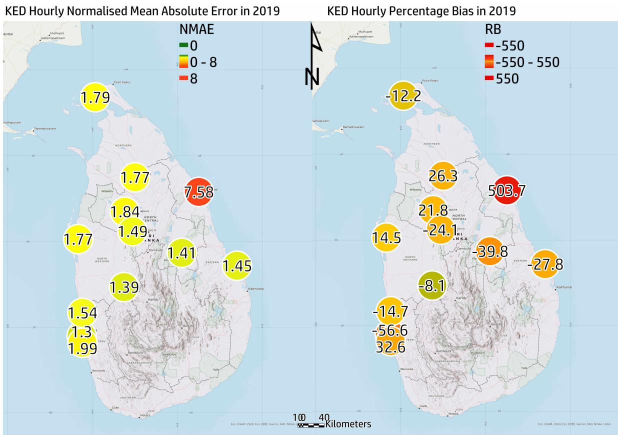


Figure 3.14: Hourly RB and NMAE per station for KED)

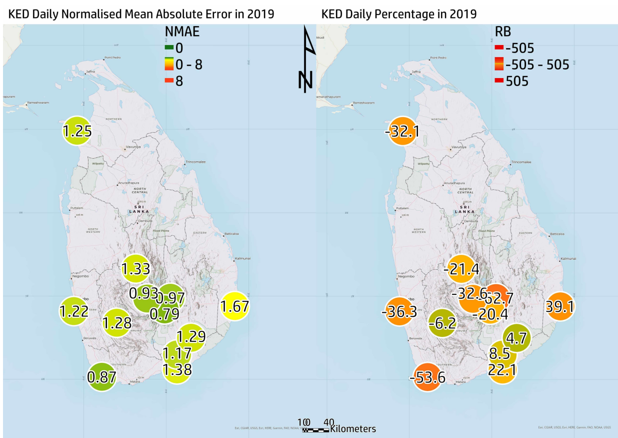


Figure 3.15: Daily RB and NMAE per station for KED)

of the west coast is visible on both maps. Precipitation at the bottom part of the country is not found by KED, this part corresponds to a location with virtually no link coverage. For the other two precipitation events in figure 3.16, the location of the rain is different. When looking at the gauge values in table 3.8, the gauges only indicate zero rainfall values, whereas KED displays very low rainfall values. Non-zero IMERG rainfall values are more sparse in the table but mostly higher than KED. Rainfall as depicted by KED is highly local, IMERG shows more spread-out events.

In figure 3.17 the location of the rainfall is widely different between KED and IMERG. The location of the precipitation event on the current and the previous map is similar for KED but not for IMERG. This might indicate the effect of CML picking up a highly local event or a malfunctioning link. Rainfall as indicated by IMERG is now also highly local and isolated. Again, all gauges indicate zero rainfall, with IMERG estimating less wet instances but with higher values.

The two events where KED performs bad are depicted in figure 3.18 and figure 3.19. The interpolated precipitation intensities on the 25th of October do somewhat coincide with higher precipitation intensities as measured by IMERG. Additionally, the rainfall pattern is comparable, however IMERG estimates rain are more locations and again shows less local rainfall.

Especially for the the 9th of November, the rainfall patterns as depicted by KED are present at locations where IMERG measures very low to no rainfall and vice versa. From table 3.11, it can be seen that KED generally gives estimations close to the zero values as indicated by the gauges, but has one high value, which is the cause for the large overall difference. Note that four all four maps, gauges indicated zero values. It might be the case that IMERG incorrectly detected rainfall, however looking at the intensities, it is more likely that the gauges were affected by measurement errors. Additionally, the location of the precipitation events might not have been close to the gauges.

The KED interpolated rainfall is more local, while the IMERG measurements are more smooth. From the figures, it can be concluded that KED is better at capturing the highly local and intense tropical rainfall patterns, albeit giving possible overly local estimations. Neither IMERG nor KED show very realistic representations of rainfall patterns, however IMERG might have a slightly better performance.

### Violation of Kriging Assumptions

As mentioned in the methods section, KED assumes isotropy and correlation between the variables used in the interpolation. Some interpolated time steps contain very high rainfall values and the overall performance of KED is bad. An attempt at understanding the bad performance of Kriging is made by comparing two directional variograms and two correlation plots. Again, the comparison between a time step with bad and good KED

Table 3.8: Rainfall values for IMERG, KED and gauges

| Station Name | IMERG | KED | Gauge |
|---|---|---|---|
| Colombo | 0.1 | 0.0008 | 0 |
| Jaffna | 0 | 9.1E-07 | 0 |
| Puttalam | 0 | 1.7E-08 | 0 |
| Trincomalee | 0 | 0.63 | |
| Batticaloa | 0 | 0 | 0 |
| Kurunegala | 0.1 | 7.8E-05 | 0 |
| Katunayake | 0 | 0 | 0 |
| Anuradhapura | 1.2 | 1.79E-05 | 0 |
| Mahailluppalama | 0 | 0 | |
| Polonnaruwa | 0 | 0 | 0 |
| Ratmalana | 0.6 | 0 | 0 |
| Vavuniya | 0 | 2.7E-07 | 0 |

Table 3.9: Rainfall values for IMERG, KED and gauges

| Station Name | IMERG | KED | Gauge |
|---|---|---|---|
| Colombo | 0 | 0 | 0 |
| Jaffna | 0 | 0 | 0 |
| Puttalam | 0 | 0 | 0 |
| Trincomalee | 0.4 | 0 | |
| Batticaloa | 0 | 6.08E-14 | 0 |
| Kurunegala | 0 | 9.20E-12 | 0 |
| Katunayake | 0 | 3.26E-10 | 0 |
| Anuradhapura | 0 | 0 | 0 |
| Mahailluppalama | 0 | 3.26E-10 | 0 |
| Polonnaruwa | 0 | 0 | 0 |
| Ratmalana | 0 | 0 | 0 |
| Vavuniya | 0 | 0 | 0 |

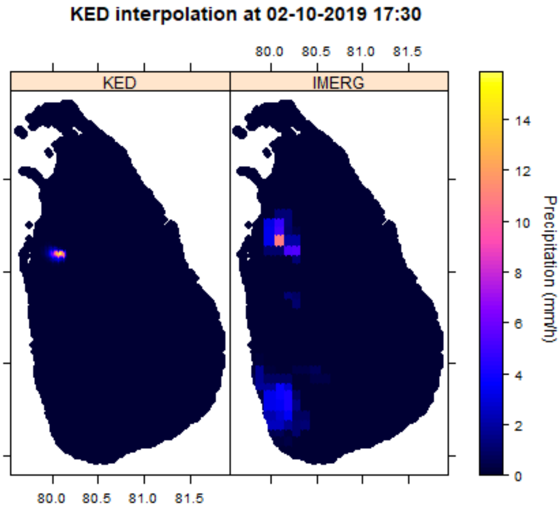


Figure 3.16: Rainfall maps of IMERG and KED on the 2nd of October

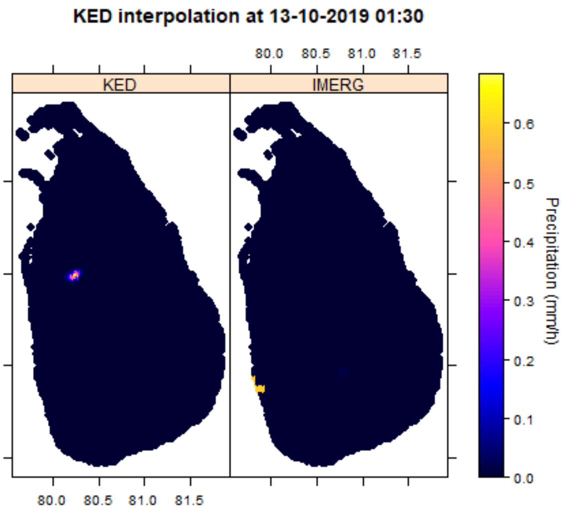


Figure 3.17: Rainfall maps of IMERG and KED on the 13th of October

performance is made. The plots shown here serve as an general example for the time steps not presented, the patterns described are also present in the variograms and scatter plots of events with similar performances.

One of the reasons for the low skill of KED could be anisotropy. Figure 3.21 shows two directional variograms, displaying the spatial autocorrelation of the residuals in multiple directions. In case the variogram displays a strongly differing pattern in one of the directions it indicates anisotropy. The left variogram is based on a time step with good KED performance (see figure 3.18). The variogram shows some anisotropy, with autocorrelation in the 0 direction varying from the other directions. However, when the variogram is compared to the one on the right, it can be seen that its fit is much better. The right plot shows the variogram for the 9th of November, a time step with bad KED performance (figure 3.19). The variogram has distinctly different shapes in the different directions and thus anisotropy is present.

The second Kriging assumption that can be violated in the current research is the strong correlation between the drift and the variable to be interpolated. When looking at figure 3.23, it can be see that the left plot has a low Pearson's correlation. When looking at the scatter, most points are indicating zero rainfall and the scatter indicates good agreement between IMERG and CML, with limited outliers. Looking at the gauge values in figure 3.17, KED, gauge, and IMERG values show good agreement.

The right plot shows a strong deviation from the

Table 3.10: Rainfall values for IMERG, KED and gauges

| Station Name | IMERG | KED | Gauge |
|---|---|---|---|
| Colombo | 1.2 | 1.19E-05 | 0 |
| Jaffna | 0 | 0.15 | 0 |
| Puttalam | 0.3 | 0.3 | 0 |
| Trincomalee | 0.3 | 0.3 | |
| Batticaloa | 0.8 | 0.002 | 0 |
| Kurunegala | 0.3 | 0.3 | 0.4 |
| Katunayake | 0.2 | 0.0005 | 0 |
| Anuradhapura | 0 | 8.22E-05 | 0 |
| Mahailluppalama | 0 | 0.0006 | 0 |
| Polonnaruwa | 1 | 0.0001 | 0 |
| Ratmalana | 0.7 | 0.0004 | 0 |
| Vavuniya | 0.3 | 1.66 | 0 |

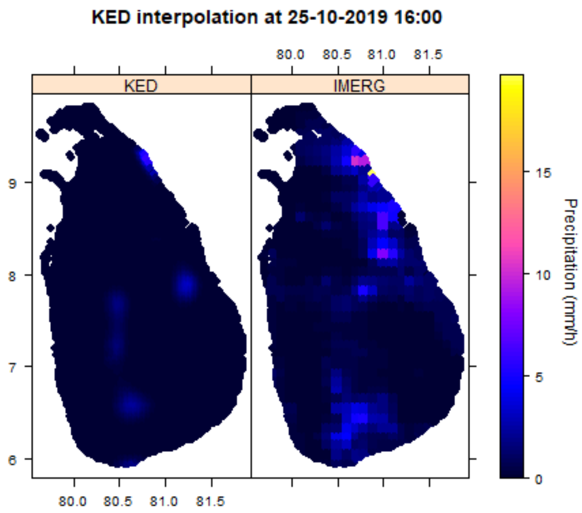


Figure 3.18: Rainfall maps of IMERG and KED on the 25th of October

Table 3.11: Rainfall values for IMERG, KED and gauges

| Station Name | IMERG | KED | Gauge |
|---|---|---|---|
| Colombo | 3.2 | 5.6 | 0 |
| Jaffna | 0.1 | 0.02 | 0 |
| Puttalam | 0.1 | 0.05 | 0 |
| Trincomalee | 0.1 | 0.07 | |
| Batticaloa | 0 | 2.84E-05 | 0 |
| Kurunegala | 0.2 | 0.22 | 0 |
| Katunayake | 0.5 | 0.5 | 0 |
| Anuradhapura | 0.1 | 4.17 | 0 |
| Mahailluppalama | 0 | 0 | 0 |
| Polonnaruwa | 0.2 | 147.34 | 0 |
| Ratmalana | 3.8 | 0.002 | 0 |
| Vavuniya | 0 | 0.0005 | 0 |

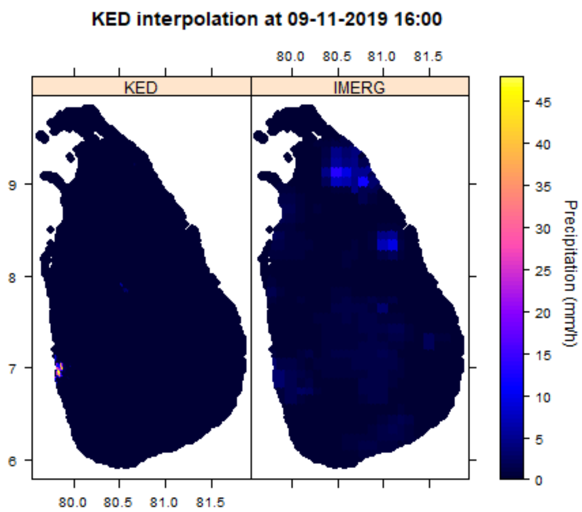


Figure 3.19: Rainfall maps of IMERG and KED on the 9th of November

1:1 line. The scatter portraying a straight line can be explained by the fact that the resolutions of CML and IMERG measurements do not match. Within an IMERG pixel with a single measurement, multiple CML measurements are present. Additionally, the figure shows that CML measures significantly higher rainfall intensities. When comparing the values seen in the scatter plots to the gauge values found in figure 3.19 it can be seen that the gauges and IMERG indicate much lower rainfall intensities than KED. The weak correlation between IMERG and CML measurements can be seen in the different between the location of KED and IMERG rainfall, resulting in the difference between KED and the gauges.

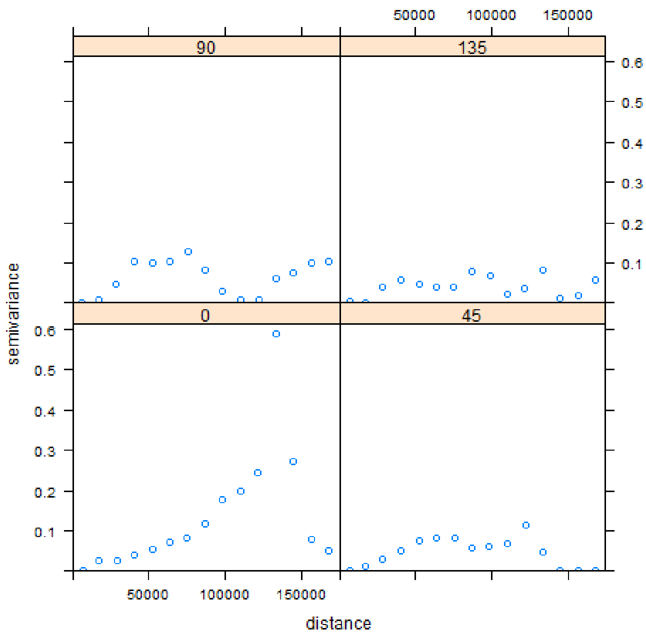


Figure 3.20: Directional variogram for IMERG and CML on 13-10-2019

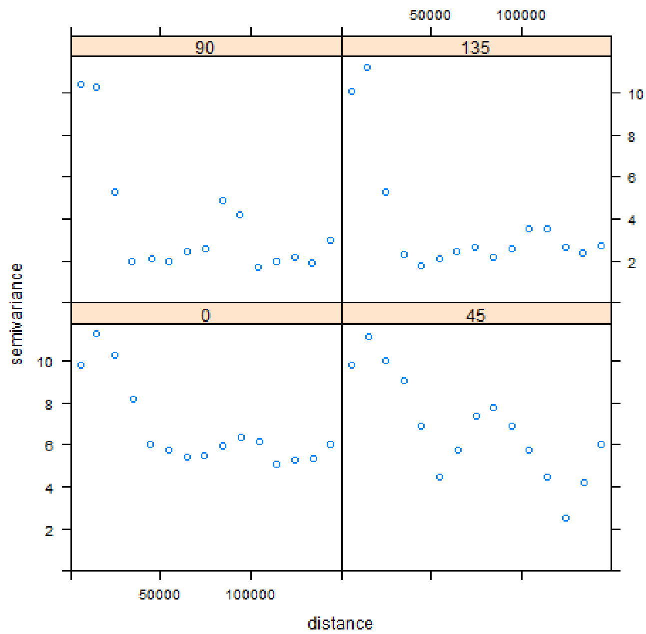


Figure 3.21: Directional variogram for IMERG and CML on 9-11-2019

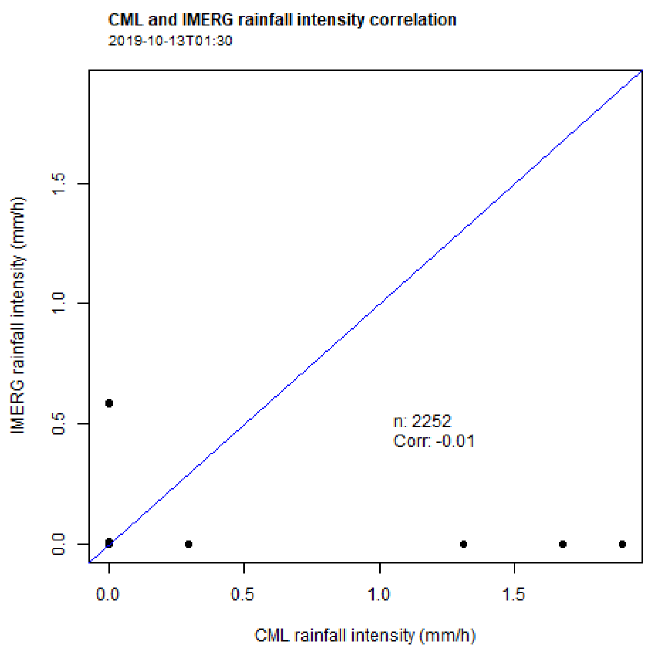


Figure 3.22: Correlation plot for IMERG and CML on 13-10-2019

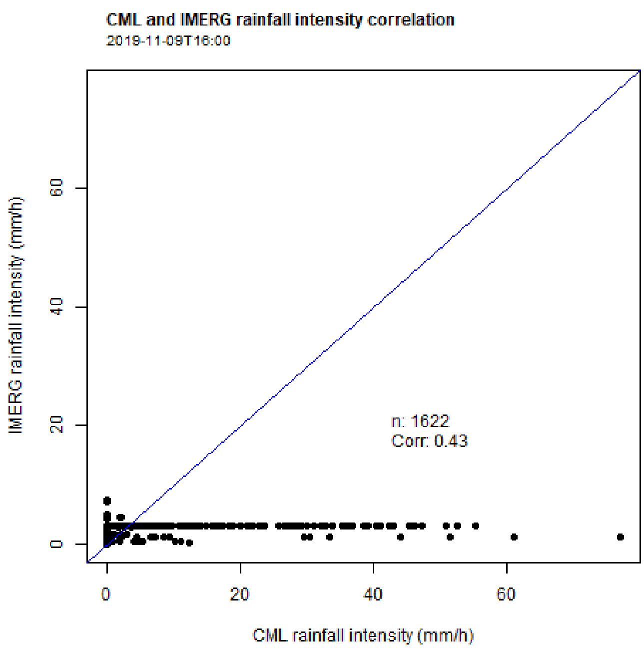


Figure 3.23: Correlation plot for IMERG and CML on 9-11-2019

# 4 | Discussion

First, the limitations of the different sets of data used are discussed, the limitations of KED and the overall methodology are considered. Suggestions for further research are given throughout all sections.

## 4.1 Data limitations

### 4.1.1 IMERG

The applicability of KED used is strongly dependent on the data quality and availability of the drift and interpolation variable. Passive rainfall retrieval such as used in IMERG is intrinsically affected by bias and error which is usually region-specific Maranan et al. (2020). While IMERG has shown to have improved performance compared to KED, CMLs mostly outperformed IMERG, indicating that IMERG provides lower quality estimates. Especially when considering the more variable hourly rainfall, IMERG displayed bad performance.

Uncovering the sources of error and bias in IMERG for Sri Lanka will increase understanding of errors in the final product and allows for tailoring of the merging method (Kumah et al., 2020). The scope of the current research was not covering an in-depth analysis of sources of IMERG errors. A more extensive validation the quasi-real-time products IMERG-E and IMERG-L for Sri Lanka, such as the recent paper by Bandara et al. (2022) will provide opportunities for improving the current method as sources of error and bias can be dealt with accordingly. Furthermore, Li and Shao (2010) found that direct merging using gridded satellites estimate introduces significant bias around the boundaries between consecutive grids. The current study directly used the gridded product, which possibly introduced these boundary errors. A suggestion to circumvent these errors, as presented by Li and Shao (2010), is using a smoothing method such as Kernel Density Smoothing.

Lastly, the release of IMERG V07 is due in near future. This version will likely have improved accuracy and thus the possibility to improve the overall quality of merged estimates in which IMERG is used as a source.

### 4.1.2 CML

As mentioned in the method section, the parameters of RAINLINK were not optimized for Sri Lanka. The discrepancy this causes between the measured and actual rainfall can propagate through the merged product although Overeem et al. (2021) showcased that the effect of this lack of optimization is limited. However, as found by Overeem et al. (2016a), interpolation methods and the link density play a minor, albeit, important role in the total error. Main sources of error are related to the retrieval of the rainfall rates. With the current efforts to reduce errors in CML rainfall retrieval, as stated by Chwala and Kunstmann (2019), future versions of rainfall estimation might produce better quality CML estimations. By extend, this will increase the performance of KED.

### 4.1.3 Gauges

While the rain gauge measurements had good availability, the number of stations was rather limited. The spatial variability in interpolated rainfall map quality may be very large, which is difficult to accurately assess based on the limited coverage of the gauges (Overeem et al., 2021). Additionally, the daily gauges were mainly located in the southern part of the country, preventing an appraisal of the spatial variation in performance over the whole country. The rain gauge measurements in 2020 were more spread, so future research could consider choosing 2020 as their period under review to provide more holistic conclusions on this variation. It is well known that gauges are also subject to errors, and taking them as absolute truth measurements is sometimes incorrect (Haese et al., 2017). However, the gauge data used in this research was sufficient to provide general conclusions.

### 4.1.4 General

Merging different sources of data has the benefit that weak points of a source may be counteracted with the other. In this research, the limited availability of CML measurements in sparsely inhabited regions could potentially be counteracted by the widespread availability of IMERG. However, in case both sources have the same weak points, the weak points can reinforce each other. For example, both IMERG and CMLs are negatively affected by orthography. As described by Tan et al. (2019), the current version of IMERG, used in this study, does not have a scheme to account for orthographic influences on precipitation, leading to decreased accuracy in mountainous areas. CML density in mountains is usually limited.

As the elevated areas in Sri Lanka receive a lot of rain, accurate measurement is vital for applications such as flood and hydrological modelling (Min et al., 2020). For the current research, there was only a limited amount of validation gauges available in mountainous regions, so no clear conclusions can be made on whether the KED interpolation performed worse in mountainous regions. The 2020 gauge data is significantly more extensive and does provide opportunities for evaluation of both IMERG and KED based on elevation. Staying on the topic of elevation, it has shown to be a very effective drift variable in previous studies to be added to the KED interpolation (e.g. Hudson and Wackernagel (1994); Hengl et al. (2007)). By combining different measurement methods with additional drift variables, such as presented in Park et al. (2017), KED performance can be improved.

Assessing the effect of geographical characteristics such as elevation is a valuable extension of the current research. This research addressed spatial variation to some extent, but did not go in-depth on the underlying mechanics. Linking the spatial variance in performance to landscape characteristics may provide additional opportunities for tailoring merging methods. Both IMERG and KED show strong spatial variations, however, it remains unclear what exactly causes this. It is advised that prior to a implementation of different methods of rainfall estimation in Sri Lanka, more research into spatial factors influencing rainfall is conducted.

The Box-Cox transformation with $\lambda = 0.25$ used to normalise the CML and IMERG measurements before interpolation has greatly improved the results of KED. However, as mentioned before, normalisation of rainfall values is tricky. There are many methods available, all with their strengths and weaknesses (Krzysztofowicz, 1997; Cecinati et al., 2017). The current research employed the Box-Cox normalisation, which has provided the best results in previous research, however, it was beyond the scope to compare different methods and quantify the bias introduced through this normalisation. In the future, different methods for normalisation of tropical rainfall prior to interpolation should be conducted.

## 4.2 Limitations of using KED

KED assumes that the drift variable and the variable to interpolated are strongly correlated. However, the correlation between IMERG and CML rainfall measurements is highly variable. This limits the accuracy and consistency of the interpolated rainfall between interpolations. An additional assumption is the requirement that the drift variable is accurately sampled over the whole domain. As mentioned before, IMERG is not always accurate. As found in the scatter plots showing the correlation between IMERG and CML, correlation is often very low. This can partly be explained by the difference in resolution, causing IMERG to fail to capture local rainfall events. Applying methods where this correlation is not required, such as a simplistic mean-field bias Cummings et al. (2009) or a more sophisticated one, like Double Kernel Density Smoothing (Shao et al., 2021), will likely improve results. The anisotropy of rainfall in Sri Lanka violates the second assumption of Kriging. This will decrease the effectiveness of the method for estimating rainfall. However, Haberlandt (2007) and Overeem et al. (2016a) have reported minute decreases in uncertainty related to the anisotropy of the data (e.g.Hudson and Wackernagel, 1994; Goudenhoofdt and Delobbe, 2009). No in-depth evaluation of the effect of anisotropy on the accuracy of Kriging has been done for tropical climates, however. Current results have suggested that anisotropy negatively impacts the KED performance, although the effect is limited. However, the methods mentioned previously do not require isotropy and might thus pose even better candidates for future endeavours.

Most implementations of KED separate wet and dry pixels and only employ KED for the wet pixels. This is motivated by the complication of large amounts of zero values and improves the correlation of the drift variable with $Z(s)$ (Haberlandt, 2007; Park et al., 2017). The exclusion of zero values has the added benefit of making the normalisation and the subsequent back transform more effective. However, as the current research aimed to produce rainfall estimations for the whole country, KED was employed for all locations. Additionally, assuming the aim of creating a method that is applicable to real-life, the creation of country-wide estimations is important. Thus it is advisable to change the method used or alter the parameters, rather than limiting the scope.

Kriging on both wet and dry areas significantly complicates the fitting of the variogram. The added lack of correlation between CML and IMERG prevented the usage of a climatological variogram, such as used by Overeem et al. (2021), as the Kriging function could not be solved. This created the necessity for fitting a new variogram for each iteration. This method can, however, lead to badly fitted variograms, in cases where there is no correlation between CML and IMERG. Additionally, the difference between the variograms for each iteration make the methods unstable and computationally expensive (Haberlandt, 2007). Using an extensive record of IMERG and gauge measurements it is possible to fit a climatological variogram, decreasing the variability between time steps and making KED more robust.

Another limitation of KED is that the matrix is not stable when the covariate does not vary smoothly in space (Goovaerts et al., 1997). Kriging methods that separate the estimation of the trend from the interpolation of the residuals, such as Regression Kriging, avoid this by using more complex forms of regression (Park et al., 2017). Furthermore, KED does not allow user-defined weights to be given. For example, for the current research, it could have improved performance if locations with a dense CML network could have had a higher weight for CML measurements and vice versa. IMERG has shown to be outperformed by CML, and it would thus be favourable to apply such weights. Geographically Weighted Regression Kriging, as described by Kumar et al. (2012), is a good choice between using different sources of measurements as well as other covariates and knowledge about the data and the field site. This know-how can subsequently be used to construct a tailor-made merging algorithm, as presented by Zinevich et al. (2008).

# 5 | Conclusion

The current section will provide conclusions on the performanco of IMERG for Sri Lanka in both 2019 and 2020. Next, the performance of KED is discussed. This section will answer the research questions as posed in chapter 1.2.

## 5.1 IMERG

IMERG shows good Wet-Dry classification for daily measurements but fails to capture the more variable hourly rainfall. This is signified by the large difference in performance when comparing the hourly and daily measurements. The same difference can be seen when evaluating the statistical metrics, however, IMERG then performs somewhat better at measuring hourly rainfall intensities. Especially when compared to the hourly gauge measurements, performance is good, with an RB close to 0 and a low NMAE. IMERG does show variation in performance between different months, but no distinct seasonal effects are found within the period under review. When considering the whole year, some seasonal variation is found. Especially when considering the RB and NMAE, IMERG appears to be unable to accurately capture rainfall during the first IMP. The results suggest a slightly improved performance in the NEP and a decreased performance in the second IMP. This does correspond with the behaviour of IMERG as described in previous literature. IMERG is unable to capture the highly local and intense showers of the second IMP, while dryer NEM with more moderate rainfall is captured better. However, the results show only minimal change between months, and the pattern is not sufficiently clear to warrant strong claims. With regards to the spatial variability, IMERGs performance in the wet region of Sri Lanka, the southwestern part, is better than in the other regions. However, no distinct spatial patterns are found. Understanding of the topography and the effect of other factors on precipitation patterns is very valuable for future research. The strong spatial variation in KED and IMERG indicate strong spatial rainfall variability over Sri Lanka. Future attempts at merging multiple sources of data need to be able to address this challenge.

## 5.2 KED

Rainfall interpolation using KED with CML derived values and IMERG is not able to capture rainfall better than CML or IMERG alone. In general, KED underestimates rainfall. Compared to the performance of IMERG and CML, all metrics point towards a decreased performance. Especially the statistical metrics show a strongly decreased performance with respect to CML. KED performs well at Wet-Dry classification, but still does not perform significantly better than IMERG.

Seasonality does not seem to affect the performance of KED, with all performance metrics similar between different months. While the difference in RB is large when considering the separate months, no distinct pattern is visible in the metrics. Spatially, more pronounced patterns are recognized, mainly coinciding with the climatic regions. Additionally, the events in locations within regions with high link density are captured better. This further limits the applicability of KED for Sri Lanka, as one of the main potential benefits was its perceived ability to estimate rainfall in rural areas with limited amounts of links present. The quality of estimations by KED strongly varies over the country, complicating any solid conclusions on its overall performance. However, as it has not garnered improvements compared to existing methods, merging IMERG and CML can best be done with a different method.

Considering the rainfall maps, it can be seen that KED maps rainfall events in a highly local manner. Furthermore, KED interpolated rainfall intensities can be very high. While these very local and intense precipitation events are present in tropical climates, the extreme amounts of precipitation render the maps unlikely to represent reality. KED is also not able to realistically capture rainfall patterns.

From this research, it can be concluded that the current implementation of KED is not suitable for estimating rainfall in Sri Lanka. While KED does perform well for some events, the performance is not consistent and varies strongly. In some instances, impossibly high values are estimated. Overall, the current research has contributed to the understanding of the performance of IMERG and the difficulties of constructing a merging algorithm for Sri Lanka.

The method presented in the current research can be improved upon by constructing a more robust variogram, with climatologically derived parameters. This will prevent the large variation between time steps. Additionally, different normalisation methods should be employed to uncover the possible negative effects of the Box-Cox transform as used in this study. Future research should aim to employ merging methods that have fewer assumptions associated with them, such as Double Kernel Density Smoothing or methods that allow differentiation on covariate weighing such as Geographically Weighted Regression Kriging. The rather simplistic regression model as used in KED is not able to capture the complicated relationship between the CML and IMERG measurements. Furthermore, an important suggestion is the extensive evaluation of seasonal and spatial factors prior to merging different sources of data is very important for understanding and improving results. Building upon the method as presented in the current research will further understanding of weaknesses in methods used and allow for effective improvements.

# Acknowledgements

I have received a great deal of support and guidance during the writing of my thesis. Firstly, I would like to thank my supervisors, Linda and Hidde, for their time and support. You helped me structure my working processes and taught me a great deal about academic research. I am greatly indebted to for your guidance, constructive feedback and continuous encouragement throughout the project.

Subsequently I would like to thank Aart Overeem, GSMA Sri Lanka and Dialog Sri Lanka for the data they have so kindly provided me with. The gauge data sets provided by GSMA, the RSL data sets from Dialog, and Aart who prepared and retrieved the data were all a vital part of this research.

Lastly I would like all staff members of HWM and the participants of the thesis ring for reading my work and providing insightful feedback as well as be a friendly space to ask questions. My thanks goes out especially to all Valkers for increasing the locations atmosphere. While the Valk is not the most inspiring environment, your presence made it all the more bearable.

# Bibliography

Anjum, M.N., Ahmad, I., Ding, Y., Shangguan, D., Zaman, M., Ijaz, M.W., Sarwar, K., Han, H., Yang, M., 2019. Assessment of imerg-v06 precipitation product over different hydro-climatic regimes in the tianshan mountains, north-western china. Remote Sensing 11, 2314.

Bandara, U., Agarwal, A., Srinivasan, G., Shanmugasundaram, J., Jayawardena, I.S., 2022. Intercomparison of gridded precipitation datasets for prospective hydrological applications in sri lanka. International Journal of Climatology 42, 3378–3396.

Bianchi, B., Jan van Leeuwen, P., Hogan, R.J., Berne, A., 2013. A variational approach to retrieve rain rate by combining information from rain gauges, radars, and microwave links. Journal of Hydrometeorology 14, 1897–1909.

Bogerd, L., Overeem, A., Leijnse, H., Uijlenhoet, R., 2021. A comprehensive five-year evaluation of imerg late run precipitation estimates over the netherlands. Journal of Hydrometeorology .

Box, G.E., Cox, D.R., 1964. An analysis of transformations. Journal of the Royal Statistical Society: Series B (Methodological) 26, 211–243.

Brauer, C.C., Overeem, A., Leijnse, H., Uijlenhoet, R., 2016. The effect of differences between rainfall measurement techniques on groundwater and discharge simulations in a lowland catchment. Hydrological Processes 30, 3885–3900.

Brocca, L., Massari, C., Pellarin, T., Filippucci, P., Ciabatta, L., Camici, S., Kerr, Y.H., Fernández-Prieto, D., 2020. River flow prediction in data scarce regions: soil moisture integrated satellite rainfall products outperform rain gauge observations in west africa. Scientific Reports 10, 1–14.

Cantet, P., 2017. Mapping the mean monthly precipitation of a small island using kriging with external drifts. Theoretical and Applied Climatology 127, 31–44.

Cecinati, F., Wani, O., Rico-Ramirez, M.A., 2017. Comparing approaches to deal with non-gaussianity of rainfall data in kriging-based radar-gauge rainfall merging. Water Resources Research 53, 8999–9018.

Christofilakis, V., Tatsis, G., Chronopoulos, S.K., Sakkas, A., Skrivanos, A.G., Peppas, K.P., Nistazakis, H.E., Baldoumas, G., Kostarakis, P., 2020. Earth-to-earth microwave rain attenuation measurements: A survey on the recent literature. Symmetry 12, 1440.

Chwala, C., Kunstmann, H., 2019. Commercial microwave link networks for rainfall observation: Assessment of the current status and future challenges. WIREs Water 6, e1337.

Cummings, R., Upton, G.J., Holt, A., Kitchen, M., 2009. Using microwave links to adjust the radar rainfall field. Advances in water resources 32, 1003–1010.

David, N., Liu, Y., Kumah, K.K., Hoedjes, J.C., Su, B.Z., Gao, H.O., 2021. On the power of microwave communication data to monitor rain for agricultural needs in africa. Water 13, 730.

Eisele, M., Graf, M., El Hachem, A., Seidel, J., Chwala, C., Kunstmann, H., Bárdossy, A., 2021. Rainfall estimates from opportunistic sensors in germany across spatio-temporal scales-geostatistical interpolation framework, in: EGU General Assembly Conference Abstracts, pp. 1229–1245.

Foelsche, U., Kirchengast, G., Fuchsberger, J., Tan, J., Petersen, W.A., 2017. Evaluation of gpm imerg early, late, and final rainfall estimates using wegenernet gauge data in southeastern austria. Hydrology and Earth System Sciences 21, 6559–6572.

Gaona, R., F, M., Overeem, A., Brasjen, A., Meirink, J.F., Leijnse, H., Uijlenhoet, R., 2017. Evaluation of rainfall products derived from satellites and microwave links for the netherlands. IEEE Transactions on Geoscience and Remote Sensing 55, 6849–6859.

Gaona, R., F, M., Overeem, A., Raupach, T.H., Leijnse, H., Uijlenhoet, R., 2018. Rainfall retrieval with commercial microwave links in são paulo, brazil. Atmospheric Measurement Techniques 11, 4465–4476.

Goovaerts, P., et al., 1997. Geostatistics for natural resources evaluation. Oxford University Press on Demand.

Gosset, M., Kunstmann, H., Zougmore, F., Cazenave, F., Leijnse, H., Uijlenhoet, R., Chwala, C., Keis, F., Doumounia, A., Boubacar, B., 2016. Improving rainfall measurement in gauge poor regions thanks to mobile telecommunication networks. Bulletin of the American Meteorological Society 97, ES49–ES51.

Goudenhoofdt, E., Delobbe, L., 2009. Evaluation of radar-gauge merging methods for quantitative precipitation estimates. Hydrology and Earth System Sciences 13, 195–203.

Graf, M., Chwala, C., Polz, J., Kunstmann, H., 2020. Rainfall estimation from a german-wide commercial microwave link network: optimized processing and validation for 1 year of data. Hydrology and Earth System Sciences 24, 2931–2950.

Grimes, D.I., Pardo-Igúzquiza, E., 2010. Geostatistical analysis of rainfall. . Geographical analysis 42, 136–160.

Grum, M., Krämer, S., Verworn, H.R., Redder, A., 2005. Combined use of point rain gauges, radar, microwave link and level measurements in urban hydrological modelling. Atmospheric Research 77, 313–321.

Haberlandt, U., 2007. Geostatistical interpolation of hourly precipitation from rain gauges and radar for a large-scale extreme rainfall event. Journal of Hydrology 332, 144–157.

Haese, B., Hörning, S., Chwala, C., Bárdossy, A., Schalge, B., Kunstmann, H., 2017. Stochastic reconstruction and interpolation of precipitation fields using combined information of commercial microwave links and rain gauges. Water Resources Research 53, 10740–10756.

Hengl, T., Heuvelink, G.B., Rossiter, D.G., 2007. About regression-kriging: From equations to case studies. Computers & geosciences 33, 1301–1315.

Hudson, G., Wackernagel, H., 1994. Mapping temperature using kriging with external drift: theory and an example from scotland. International journal of Climatology 14, 77–91.

Huffman, G.J., Bolvin, D.T., Braithwaite, D., Hsu, K., Joyce, R., Xie, P., Yoo, S.H., 2015a. Nasa global precipitation measurement (gpm) integrated multi-satellite retrievals for gpm (imerg). Algorithm Theoretical Basis Document (ATBD) Version 4, 26.

Huffman, G.J., Bolvin, D.T., Nelkin, E.J., Tan, J., 2015b. Integrated multi-satellite retrievals for gpm (imerg) technical documentation. NASA/GSFC Code 612, 2019.

Karunaweera, N.D., Galappaththy, G.N., Wirth, D.F., 2014. On the road to eliminate malaria in sri lanka: lessons from history, challenges, gaps in knowledge and research needs. Malaria Journal 13, 1–10.

Kim, J., Yoo, C., 2014. Use of a dual kalman filter for real-time correction of mean field bias of radar rain rate. Journal of Hydrology 519, 2785–2796.

Krajewski, W.F., 1987. Cokriging radar-rainfall and rain gage data. Journal of Geophysical Research: Atmospheres 92, 9571–9580.

Krzysztofowicz, R., 1997. Transformation and normalization of variates with specified distributions. Journal of Hydrology 197, 286–292.

Kumah, K.K., Hoedjes, J.C., David, N., Maathuis, B.H., Gao, H.O., Su, B.Z., 2020. Combining mwl and msg seviri satellite signals for rainfall detection and estimation. Atmosphere 11, 884.

Kumah, K.K., Hoedjes, J.C., David, N., Maathuis, B.H., Gao, H.O., Su, B.Z., 2021. The msg technique: Improving commercial microwave link rainfall intensity by using rain area detection from meteosat second generation. Remote Sensing 13, 3274.

Kumar, S., Lal, R., Liu, D., 2012. A geographically weighted regression kriging approach for mapping soil organic carbon stock. Geoderma 189, 627–634.

Leijnse, H., Uijlenhoet, R., Stricker, J., 2007. Rainfall measurement using radio links from cellular communication networks. Water resources research 43.

Li, M., Shao, Q., 2010. An improved statistical approach to merge satellite rainfall estimates and raingauge data. Journal of Hydrology 385, 51–64.

Liberman, Y., Samuels, R., Alpert, P., Messer, H., 2014. New algorithm for integration between wireless microwave sensor network and radar for improved rainfall measurement and mapping. Atmospheric Measurement Techniques 7, 3549–3563.

Long, Y., Zhang, Y., Ma, Q., 2016. A merging framework for rainfall estimation at high spatiotemporal resolution for distributed hydrological modeling in a data-scarce area. Remote Sensing 8, 599.

Marambe, B., Punyawardena, R., Silva, P., Premalal, S., Rathnabharathie, V., Kekulandala, B., Nidumolu, U., Howden, S., 2015. Climate, Climate Risk, and Food Security in Sri Lanka: Need for Strengthening Adaptation Strategies. chapter 4. pp. 1759–1789.

Maranan, M., Fink, A.H., Knippertz, P., Amekudzi, L.K., Atiah, W.A., Stengel, M., 2020. A process-based validation of gpm imerg and its sources using a mesoscale rain gauge network in the west african forest zone. Journal of Hydrometeorology 21, 729–749.

Min, X., Yang, C., Dong, N., 2020. Merging satellite and gauge rainfalls for flood forecasting of two catchments under different climate conditions. Water 12, 802.

Overeem, A., Leijnse, H., van Leth, T.C., Bogerd, L., Priebe, J., Tricarico, D., Droste, A., Uijlenhoet, R., 2021. Tropical rainfall monitoring with commercial microwave links in sri lanka. Environmental Research Letters 16, 074058.

Overeem, A., Leijnse, H., Uijlenhoet, R., 2013. Country-wide rainfall maps from cellular communication networks. Proceedings of the National Academy of Sciences 110, 2741–2745.

Overeem, A., Leijnse, H., Uijlenhoet, R., 2016a. Retrieval algorithm for rainfall mapping from microwave links in a cellular communication network. Atmospheric Measurement Techniques 9, 2425–2444.

Overeem, A., Leijnse, H., Uijlenhoet, R., 2016b. Two and a half years of country-wide rainfall maps using radio links from commercial cellular telecommunication networks. Water Resources Research 52, 8039–8065.

Park, N.W., Kyriakidis, P.C., Hong, S., 2017. Geostatistical integration of coarse resolution satellite precipitation products and rain gauge data to map precipitation at fine spatial resolutions. Remote Sensing 9, 255.

Polz, J., Schmidt, L., Glawion, L., Graf, M., Werner, C., Chwala, C., Mollenhauer, H., Rebmann, C., Kunstmann, H., Bumberger, J., 2021. Supervised and unsupervised machine-learning for automated quality control of environmental sensor data.

Rahmawati, N., Rahayu, K., Yuliasari, S.T., 2021. Performance of daily satellite-based rainfall in groundwater basin of merapi aquifer system, yogyakarta. Theoretical and Applied Climatology 146, 173—–190.

Safont, G., Salazar, A., Vergara, L., 2019. Multiclass alpha integration of scores from multiple classifiers. Neural Computation 31, 806–825.

Shao, Y., Fu, A., Zhao, J., Xu, J., Wu, J., 2021. Improving quantitative precipitation estimates by radar-rain gauge merging and an integration algorithm in the yishu river catchment, china. Theoretical and Applied Climatology 144, 611–623.

Sideris, I., Gabella, M., Erdin, R., Germann, U., 2014. Real-time radar–rain-gauge merging using spatio-temporal co-kriging with external drift in the alpine terrain of switzerland. Quarterly Journal of the Royal Meteorological Society 140, 1097–1111.

Sinclair, S., Pegram, G., 2005. Combining radar and rain gauge rainfall estimates using conditional merging. Atmospheric Science Letters 6, 19–22.

Skofronick-Jackson, G., Kirschbaum, D., Petersen, W., Huffman, G., Kidd, C., Stocker, E., Kakar, R., 2018. The global precipitation measurement (gpm) mission's scientific achievements and societal contributions: reviewing four years of advanced rain and snow observations. Quarterly Journal of the Royal Meteorological Society 144, 27–48.

Skofronick-Jackson, G., Petersen, W.A., Berg, W., Kidd, C., Stocker, E.F., Kirschbaum, D.B., Kakar, R., Braun, S.A., Huffman, G.J., Iguchi, T., et al., 2017. The global precipitation measurement (gpm) mission for science and society. Bulletin of the American Meteorological Society 98, 1679–1695.

Sunilkumar, K., Yatagai, A., Masuda, M., 2019. Preliminary evaluation of gpm-imerg rainfall estimates over three distinct climate zones with aphrodite. Earth and Space Science 6, 1321–1335.

Tan, J., Huffman, G.J., Bolvin, D.T., Nelkin, E.J., 2019. Imerg v06: Changes to the morphing algorithm. Journal of Atmospheric and Oceanic Technology 36, 2471–2482.

Tan, J., Petersen, W.A., Tokay, A., 2016. A novel approach to identify sources of errors in imerg for gpm ground validation. Journal of Hydrometeorology 17, 2477–2491.

Tapiador, F.J., Villalba-Pradas, A., Navarro, A., García-Ortega, E., Lim, K.S.S., Kim, K., Ahn, K.D., Lee, G., 2021. Future directions in precipitation science. Remote Sensing 13, 1074.

Thambyahpillay, G., 1954. The rainfall rhythm in ceylon .

Todini, E., Mazzetti, C., 2006. A bayesian multisensor combination approach to rainfall estimate, in: Proceedings of the 2nd International Symposium on Communications, Control and Signal Processing, Marrakech, Morocco, pp. 13–15.

Trömel, S., Ziegert, M., Ryzhkov, A.V., Chwala, C., Simmer, C., 2014. Using microwave backhaul links to optimize the performance of algorithms for rainfall estimation and attenuation correction. Journal of Atmospheric and Oceanic Technology 31, 1748–1760.

Wong, G.K., Jim, C.Y., 2014. Quantitative hydrologic performance of extensive green roof under humid-tropical rainfall regime. Ecological engineering 70, 366–378.

Yuehong, S., Wanchang, Z., Yonghe, L., Jingying, Z., 2008. Analysis of quantitative estimation of precipitation using different algorithms with doppler radar data, in: 2008 International Workshop on Education Technology and Training & 2008 International Workshop on Geoscience and Remote Sensing, IEEE. pp. 372–375.

Zhao, B., Dai, Q., Zhuo, L., Mao, J., Zhu, S., Han, D., 2022. Accounting for satellite rainfall uncertainty in rainfall-triggered landslide forecasting. Geomorphology 398, 108051.

Zinevich, A., Alpert, P., Messer, H., 2008. Estimation of rainfall fields using commercial microwave communication networks of variable density. Advances in water resources 31, 1470–1480.

Table A.1: Table of performance scores for IMERG for hourly and daily gauge sums in 2019

| **Station Name (D)** | **POD** | **POFA** | **ACC** | **HSS** |
|---|---|---|---|---|
| *Badulla* | 0.99 | 0.16 | 0.85 | 0.48 |
| *Bandarawela* | 0.99 | 0.15 | 0.85 | 0.35 |
| *Galle* | 0.99 | 0.33 | 0.67 | 0.075 |
| *Hambantota* | 0.96 | 0.29 | 0.72 | 0.3 |
| *Katugastota* | 0.94 | 0.25 | 0.75 | 0.39 |
| *Mannar* | 0.93 | 0.41 | 0.64 | 0.28 |
| *Mattala* | 0.93 | 0.23 | 0.77 | 0.43 |
| *Monaragala* | 0.95 | 0.24 | 0.77 | 0.4 |
| *Pottuvil* | 0.9 | 0.26 | 0.73 | 0.34 |
| *Ratmalana* | 0.98 | 0.26 | 0.73 | 0.09 |
| **Station Name (H)** | | | | |
| *Anuradhapura* | 0.76 | 0.65 | 0.82 | 0.39 |
| *Batticaloa* | 0.63 | 0.69 | 0.76 | 0.29 |
| *Colombo* | 0.84 | 0.73 | 0.65 | 0.25 |
| *Jaffna* | 0.62 | 0.77 | 0.71 | 0.19 |
| *Katunayake* | 0.78 | 0.77 | 0.64 | 0.2 |
| *Kurunegala* | 0.15 | 0.76 | 0.55 | -0.1 |
| *Mahailluppalama* | 0.15 | 0.63 | 0.49 | -0.08 |
| *Polonnaruwa* | 0.69 | 0.63 | 0.79 | 0.37 |
| *Puttalam* | 0.74 | 0.78 | 0.69 | 0.2 |
| *Ratmalana* | 0.49 | 0.79 | 0.58 | 0.06 |
| *Trincomalee* | 0.006 | 0.89 | 0.19 | -0.008 |
| *Vavuniya* | 0.67 | 0.65 | 0.81 | 0.36 |

Table A.2: Table of variogram parameters

| month | day | hour | minute | model | nugget | sill | range |
|---|---|---|---|---|---|---|---|
| 09 | 12 | 08 | 00 | Matern | 0.005589113296940393 | 0.22808828202229586 | 37093.76962561694 |
| 09 | 12 | 09 | 00 | Spherical | 9.108982867930609e-4 | 1.7442658266845914 | 24087.094274913215 |
| 09 | 12 | 10 | 00 | Matern | 0.11629149051076963 | 2.393756560980867 | 13250.691374731437 |
| 09 | 12 | 11 | 00 | Matern | 0.14475087625975383 | 1.3138379616419995 | 56502.65991561526 |
| 09 | 12 | 12 | 00 | Matern | 0.02760509021869387 | 1.4361796877420916 | 109873.94272171016 |
| 09 | 12 | 13 | 00 | Matern | 0.02622728431563996 | 0.7650065302432604 | 113598.00409708492 |
| 09 | 12 | 14 | 00 | Matern | 0.04444916953462991 | 163554.44115965505 | 125705300.38014339 |
| 09 | 12 | 15 | 00 | Matern | 0.026087366560612762 | 36.291295131955096 | 3624407.979533299 |
| 09 | 12 | 16 | 00 | Matern | 0.018352783528233295 | 14.93075019043334 | 2177061.7517854203 |
| 09 | 12 | 08 | 30 | Matern | 0.15660771044110217 | 1.2735160986768024 | 20871.770960232774 |
| 09 | 12 | 09 | 30 | Matern | 0.14091591834874637 | 2.182773284164124 | 23507.944781831502 |
| 09 | 12 | 10 | 30 | Gaussian | 0.13756126218188103 | 1.6615060821005074 | 14672.126124672532 |
| 09 | 12 | 11 | 30 | Matern | 0 | 0.8461446936080963 | 42466.65460655821 |
| 09 | 12 | 12 | 30 | Matern | 0.02659634985688147 | 1.519937256564354 | 121806.44626193121 |
| 09 | 12 | 13 | 30 | Matern | 0.0931228468413834 | 5209.457441062224 | 28243378.61393427 |
| 09 | 12 | 14 | 30 | Matern | 0.0362013896716372 | 9293.726559949495 | 95217704.16102463 |
| 09 | 12 | 15 | 30 | Matern | 0.03290956305084913 | 31203.12060827257 | 144188035.56019634 |
| 09 | 13 | 00 | 00 | Spherical | 0.043871694282218675 | 0.2904052247435692 | 10589.718389510532 |
| 09 | 13 | 01 | 00 | Matern | 0.013434120010583698 | 0.5726533690532423 | 3830.273951568925 |
| 09 | 13 | 03 | 00 | Matern | 0.010578982378703944 | 0.07859522085043992 | 12787.026708105463 |

| | | | | | | | |
|---|---|---|---|---|---|---|---|
| 09 | 13 | 04 | 00 | Spherical | 0.14191354812914747 | 0.1590788681420222 | 10579.762821669017 |
| 09 | 13 | 05 | 00 | Matern | 0.11862774940163215 | 9.750003772236205 | 16249836.157411609 |
| 09 | 13 | 06 | 00 | Matern | 0.004264754149204802 | 0.4545141296508821 | 99701.68660262576 |
| 09 | 13 | 07 | 00 | Matern | 0.0023998617785729193 | 0.16426288062784541 | 236029.35121864392 |
| 09 | 13 | 08 | 00 | Matern | 4.073003704944881e-4 | 0.8320460223101129 | 495468.21157689404 |
| 09 | 13 | 13 | 00 | Matern | 0.03290760659477636 | 1.0975510463622589 | 76736.89483070375 |
| 09 | 13 | 14 | 00 | Matern | 0.03425373808222919 | 2.3504366111227935 | 169888.94077901338 |
| 09 | 13 | 15 | 00 | Matern | 0.04692326364923575 | 2.2751506847411505 | 189158.48112663097 |
| 09 | 13 | 16 | 00 | Matern | 0 | 3.411940489719586 | 170671.16816819334 |
| 09 | 13 | 17 | 00 | Matern | 0 | 3.371632481623456 | 369914.488617324 |
| 09 | 13 | 18 | 00 | Matern | 0 | 5.865476404875405 | 700502.2393197595 |
| 09 | 13 | 19 | 00 | Matern | 0.026219208193515794 | 4.2557728410588656 | 365284.39865969925 |
| 09 | 13 | 20 | 00 | Matern | 0.012336696478755214 | 427.40624247163225 | 14800899.124390485 |
| 09 | 13 | 21 | 00 | Matern | 0.004901622329359081 | 112.41720995821083 | 29574233.834928755 |
| 09 | 13 | 22 | 00 | Matern | 0.002338630462109691 | 0.4926449736547378 | 465529.1915910043 |
| 09 | 13 | 00 | 30 | Matern | 0 | 0.7500910917781517 | 3947.269119405594 |
| 09 | 13 | 02 | 30 | Gaussian | 0.11510736220222723 | 0.28558401074731166 | 11089.040432894533 |
| 09 | 13 | 03 | 30 | Spherical | 0.0773608726083181 | 0.0773608726083181 | 52481.320630991075 |
| 09 | 13 | 04 | 30 | Gaussian | 0.12264459335890895 | 0.20581826563848432 | 8687.525831417968 |
| 09 | 13 | 05 | 30 | Gaussian | 0.0066906884643854235 | 0.6284890075259095 | 80723.58685457896 |
| 09 | 13 | 06 | 30 | Matern | 0.0025233743509108387 | 0.19763606522597468 | 123632.75215784264 |
| 09 | 13 | 08 | 30 | Matern | 0.0015316209182140996 | 0.15324130519403512 | 212651.4685670108 |
| 09 | 13 | 10 | 30 | Matern | 0.13033325580577954 | 0.5198493959117958 | 109124.46521420394 |
| 09 | 13 | 11 | 30 | Matern | 0 | 5.187418894937304 | 2145.938587924779 |
| 09 | 13 | 12 | 30 | Matern | 0.05760945805256919 | 0.4734830945976607 | 33739.071537891046 |
| 09 | 13 | 13 | 30 | Matern | 0.05597941801266831 | 1.5724880947680893 | 112910.46182586126 |
| 09 | 13 | 14 | 30 | Matern | 0.021133282126118043 | 1.678649126322971 | 112570.25108595767 |
| 09 | 13 | 15 | 30 | Matern | 0 | 2.861478283541106 | 116122.34411512964 |
| 09 | 13 | 16 | 30 | Matern | 6.709293889288557e-5 | 4.687347101375042 | 346504.3658174571 |
| 09 | 13 | 17 | 30 | Matern | 0.0026497391754595778 | 2.8506700603725434 | 347157.1760629948 |
| 09 | 13 | 18 | 30 | Matern | 0.017607569637519103 | 3.4219783371646115 | 625206.2949443264 |
| 09 | 13 | 19 | 30 | Matern | 0.012121346966840323 | 13225.388717550957 | 110043858.16746694 |
| 09 | 13 | 20 | 30 | Matern | 0.026269058401594103 | 16.418590039341463 | 1167655.665062557 |
| 09 | 13 | 21 | 30 | Matern | 0.0010237301244571061 | 0.8390026223794483 | 1057361.0722065743 |
| 09 | 13 | 23 | 30 | Spherical | 0.02470867478512847 | 0.03835309043277651 | 13956.532587310638 |
| 09 | 14 | 00 | 00 | Spherical | 0.003560164951640842 | 0.21574714839801978 | 8163.522718890576 |
| 09 | 14 | 01 | 00 | Matern | 0.04465791680424408 | 0.5201374417357496 | 6717.500898539507 |
| 09 | 14 | 02 | 00 | Matern | 0.021385207339336822 | 0.3688500542023622 | 5231.943676179357 |
| 09 | 14 | 03 | 00 | Matern | 0.002066771247072911 | 0.009170227571176692 | 126676.88207482292 |
| 09 | 14 | 04 | 00 | Spherical | 0.030981051057682785 | 0.06689345937218788 | 9926.076195762305 |
| 09 | 14 | 05 | 00 | Matern | 0.011256635897083901 | 0.43569142932934013 | 148188.06948663856 |
| 09 | 14 | 06 | 00 | Gaussian | 0.013114642925173848 | 0.15438435806471226 | 11891.031626101309 |
| 09 | 14 | 07 | 00 | Gaussian | 0.03487519056317878 | 0.8051691946425105 | 7781.718182265326 |
| 09 | 14 | 12 | 00 | Matern | 0.014653628253794671 | 0.395336019825134 | 19493.522856874348 |
| 09 | 14 | 13 | 00 | Matern | 4.0351206483911275 | 4.0351206483911275 | 52481.320630991075 |
| 09 | 14 | 15 | 00 | Gaussian | 0.008451703282734965 | 0.7297205141739828 | 55290.535595499845 |
| 09 | 14 | 16 | 00 | Matern | 0.01652743938528187 | 3.432919425916824 | 109850.28052432691 |

| | | | | | | | |
|---|---|---|---|---|---|---|---|
| 09 | 14 | 17 | 00 | Matern | 0.026491289711495433 | 0.5675047002231008 | 108707.57623179411 |
| 09 | 14 | 18 | 00 | Matern | 0.029035560929566367 | 2024507.6670864122 | 891557223.6059744 |
| 09 | 14 | 21 | 00 | Matern | 0 | 6.690078352858552 | 1719.751911564051 |
| 09 | 14 | 22 | 00 | Matern | 0.012732853503672982 | 0.1958203571309129 | 21139.418405829754 |
| 09 | 14 | 23 | 00 | Gaussian | 0.24050227223834925 | 0.3008906591705131 | 10791.710952074936 |
| 09 | 14 | 00 | 30 | Spherical | 0.02585728461176075 | 0.3649512424255654 | 9731.894467410802 |
| 09 | 14 | 01 | 30 | Spherical | 0.03336174603658578 | 0.27585500925172013 | 12862.31400047627 |
| 09 | 14 | 02 | 30 | Matern | 0.011421993872482604 | 0.21874421226053306 | 11000.061323719437 |
| 09 | 14 | 03 | 30 | Spherical | 0.022120374781945513 | 0.03504842882666172 | 4204.067992551638 |
| 09 | 14 | 04 | 30 | Matern | 0.022536952767828654 | 0.3793946788376613 | 289463.97639601707 |
| 09 | 14 | 05 | 30 | Matern | 0.009361829574413384 | 0.3155863276877768 | 89080.88781933318 |
| 09 | 14 | 06 | 30 | Matern | 0.17096604272898952 | 1.342571176553752 | 8900.033185239752 |
| 09 | 14 | 11 | 30 | Gaussian | 0.027751178136248937 | 1.2796156262064662 | 20311.899234207656 |
| 09 | 14 | 12 | 30 | Gaussian | 0.031411051475494424 | 1.1502483164653117 | 28508.120585574135 |
| 09 | 14 | 13 | 30 | Matern | 3.972682825762235 | 3.972682825762235 | 52481.320630991075 |
| 09 | 14 | 14 | 30 | Matern | 0.0030642684626006346 | 0.43588436487981574 | 36177.719408631434 |
| 09 | 14 | 15 | 30 | Matern | 0.07116241338122399 | 1.9839717025902108 | 110728.80740763077 |
| 09 | 14 | 16 | 30 | Matern | 0.02188243357882313 | 2.1445476256773297 | 114674.91725762002 |
| 09 | 14 | 17 | 30 | Matern | 0.037155850039377714 | 6.6525412789787115 | 1132175.7852364553 |
| 09 | 14 | 18 | 30 | Matern | 0.0014931535202049255 | 196.88872956200314 | 142825893.55683863 |
| 09 | 14 | 20 | 30 | Matern | 0.07304503614694756 | 0.28785281033761884 | 8250.362672721616 |
| 09 | 14 | 21 | 30 | Matern | 0.09112759977027332 | 1.5541802464468142 | 4949.408251164205 |
| 09 | 14 | 23 | 30 | Spherical | 0.13031779191328308 | 8.747092875101828 | 11120.990238330283 |
| 09 | 15 | 01 | 00 | Spherical | 1.664755022163072 | 3.7452098715952022 | 5461.946472969574 |
| 09 | 15 | 02 | 00 | Spherical | 0.31654325921320137 | 3.0883949043866137 | 8656.927269830727 |
| 09 | 15 | 03 | 00 | Gaussian | 0.002837584647252193 | 0.2170034902221573 | 41957.24910797407 |
| 09 | 15 | 04 | 00 | Gaussian | 0 | 3.956978150822941 | 2870.2211361943882 |
| 09 | 15 | 05 | 00 | Matern | 3.3052590140277545 | 5.782877813387364 | 5032.091107050195 |
| 09 | 15 | 07 | 00 | Gaussian | 0.015281517300591624 | 1.7753602255567402 | 32214.07369688844 |
| 09 | 15 | 08 | 00 | Matern | 0.2464042491244648 | 1.242932761418269 | 50099.43821168277 |
| 09 | 15 | 09 | 00 | Spherical | 0.5202571935680501 | 5.202012755412935 | 13242.7497698185 |
| 09 | 15 | 10 | 00 | Gaussian | 0.11808141910818094 | 2.7906220766261733 | 24549.774201499124 |
| 09 | 15 | 11 | 00 | Gaussian | 0.13138713504400037 | 4.75607455797949 | 42679.951747038736 |
| 09 | 15 | 12 | 00 | Matern | 0 | 8.139185093036204 | 2960.646137293945 |
| 09 | 15 | 13 | 00 | Gaussian | 0.6655417641989952 | 4.988635230467254 | 12120.450768679153 |
| 09 | 15 | 14 | 00 | Gaussian | 0.5082834054322412 | 4.4612058509899235 | 15619.49415164038 |
| 09 | 15 | 15 | 00 | Matern | 0.5771823865305962 | 6.80795145438758 | 14127.87782491997 |
| 09 | 15 | 16 | 00 | Matern | 0 | 8.205820852211282 | 9709.076545847387 |
| 09 | 15 | 17 | 00 | Spherical | 1.9350891171029072 | 5.599785945401907 | 25945.428217626246 |
| 09 | 15 | 18 | 00 | Gaussian | 0.6436486817208876 | 8.514966651985501 | 23375.262716052443 |
| 09 | 15 | 19 | 00 | Gaussian | 0.6405626347051917 | 3.9699727258505635 | 15676.264193919093 |
| 09 | 15 | 20 | 00 | Gaussian | 0.060511183965724746 | 1.938111629103513 | 53366.30388505557 |
| 09 | 15 | 21 | 00 | Matern | 0 | 5.846412940956025 | 822.962999876781 |
| 09 | 15 | 22 | 00 | Matern | 0.9817310059799246 | 8.740138901004968 | 4566.981109852034 |
| 09 | 15 | 23 | 00 | Gaussian | 0.8018413626531378 | 8.896220766983928 | 12200.875013869803 |
| 09 | 15 | 00 | 30 | Matern | 0 | 5.3791763263210415 | 2343.340885979444 |
| 09 | 15 | 01 | 30 | Matern | 0 | 6.000860156653075 | 1892.281288924534 |

| | | | | | | | |
|---|---|---|---|---|---|---|---|
| 09 | 15 | 02 | 30 | Gaussian | 0.21972378857969208 | 1.4405542675692844 | 8938.4751641998555 |
| 09 | 15 | 04 | 30 | Spherical | 2.327052740433223 | 6.743270970949419 | 5476.445868590423 |
| 09 | 15 | 05 | 30 | Matern | 0.3696242937842659 | 5.3957457757991 | 6503.500634459961 |
| 09 | 15 | 06 | 30 | Matern | 0.03296128748453878 | 1.4883357976830824 | 26298.72900771672 |
| 09 | 15 | 07 | 30 | Gaussian | 0.03459329677280134 | 1.7985585503008354 | 30984.447830558798 |
| 09 | 15 | 08 | 30 | Spherical | 4.0169375736341335 | 10.094006626410202 | 5588.155679956225 |
| 09 | 15 | 09 | 30 | Gaussian | 1.5126729983040121 | 5.905334811580134 | 12997.309032295569 |
| 09 | 15 | 10 | 30 | Gaussian | 0.08384538371171503 | 3.8830000907358664 | 41134.3653583551 |
| 09 | 15 | 11 | 30 | Gaussian | 0.3898528508971826 | 5.518915470361039 | 40406.68116873687 |
| 09 | 15 | 12 | 30 | Matern | 3.0298891927190144 | 7.9293079928982095 | 5269.464318566251 |
| 09 | 15 | 13 | 30 | Gaussian | 0.8386175944078029 | 6.771797312672123 | 12899.829538759877 |
| 09 | 15 | 14 | 30 | Matern | 0.30344810328074817 | 5.028732801095265 | 31418.94336647328 |
| 09 | 15 | 15 | 30 | Spherical | 1.823105786175702 | 6.591335964626316 | 12577.014704714968 |
| 09 | 15 | 16 | 30 | Matern | 1.0912388170036051 | 9.007543286639798 | 15008.036841315077 |
| 09 | 15 | 17 | 30 | Gaussian | 0.6258298543413818 | 8.135212344960571 | 20942.67235881631 |
| 09 | 15 | 18 | 30 | Gaussian | 1.328202029954648 | 5.913320957691936 | 9519.616464761295 |
| 09 | 15 | 19 | 30 | Gaussian | 0.0821982845917098 | 2.677193426748599 | 32416.07836154832 |
| 09 | 15 | 20 | 30 | Spherical | 0.012066380906055222 | 0.8302480134868488 | 13171.276235950252 |
| 09 | 15 | 21 | 30 | Gaussian | 1.1483850831110303 | 9.514665605511082 | 17071.977932880014 |
| 09 | 15 | 22 | 30 | Gaussian | 0.43919105441010226 | 9.65734809741283 | 11375.42251187517 |
| 09 | 15 | 23 | 30 | Gaussian | 3.1541057651381172 | 9.529572753069552 | 10703.336461522149 |
| 09 | 16 | 00 | 00 | Gaussian | 0.851904244015224 | 7.182210417250013 | 8782.61956142162 |
| 09 | 16 | 01 | 00 | Matern | 0.3926715277965749 | 5.659211944662687 | 7331.593359266849 |
| 09 | 16 | 02 | 00 | Spherical | 1.0451201565257677 | 5.805111297090514 | 10148.84306737889 |
| 09 | 16 | 03 | 00 | Spherical | 1.708259412689852 | 9.491364394613104 | 10569.08012918675 |
| 09 | 16 | 04 | 00 | Spherical | 0.6508074078470915 | 6.081907138230068 | 11522.514275136322 |
| 09 | 16 | 05 | 00 | Gaussian | 1.6619952528118083 | 10.832567696493296 | 14896.039639415674 |
| 09 | 16 | 06 | 00 | Gaussian | 1.1613207876255565 | 6.268225087810425 | 12376.377290710916 |
| 09 | 16 | 07 | 00 | Exponential | 0.03906587591907812 | 1.9012530943344392 | 13002.67751232707 |
| 09 | 16 | 08 | 00 | Gaussian | 0.23574550278336143 | 3.067790083194583 | 17376.425202188668 |
| 09 | 16 | 09 | 00 | Spherical | 1.0661166386115388 | 5.217141639886485 | 9179.283642647251 |
| 09 | 16 | 10 | 00 | Spherical | 0.36387648003920436 | 2.5379363424975456 | 6588.055557508096 |
| 09 | 16 | 11 | 00 | Matern | 0.890272421762698 | 9.563544358353465 | 11945.327972510242 |
| 09 | 16 | 12 | 00 | Matern | 0.4936473369843119 | 6.348285371142297 | 9950.387547507464 |
| 09 | 16 | 13 | 00 | Gaussian | 0.5667024950394973 | 6.119236206475015 | 14173.162914492068 |
| 09 | 16 | 14 | 00 | Gaussian | 0.2034075608062672 | 6.871863576429865 | 21857.115374256646 |
| 09 | 16 | 15 | 00 | Gaussian | 0.20999129293284058 | 1.5999235329215904 | 19623.91234816813 |
| 09 | 16 | 16 | 00 | Matern | 0.15802385723636522 | 1.7664633805899632 | 18004.59558749113 |
| 09 | 16 | 17 | 00 | Gaussian | 0.006696581249990704 | 0.44534713455367675 | 39052.783971050485 |
| 09 | 16 | 18 | 00 | Gaussian | 0.0010703206896878722 | 0.09440528839106722 | 35937.34979243763 |
| 09 | 16 | 20 | 00 | Spherical | 0.11275976994666859 | 0.6458658561014987 | 30790.832304364045 |
| 09 | 16 | 21 | 00 | Matern | 0.0457163041113285 | 0.6615256023565161 | 12007.87481741814 |
| 09 | 16 | 22 | 00 | Matern | 0.004627071145116426 | 1207.0624994763239 | 180886558.02277657 |
| 09 | 16 | 23 | 00 | Spherical | 0 | 6.393228510941886 | 6041.5600936355 |
| 09 | 16 | 00 | 30 | Spherical | 1.990007660156444 | 8.094408211389327 | 5205.136289660271 |
| 09 | 16 | 01 | 30 | Spherical | 1.3466070287716092 | 5.650197745433562 | 9145.465695431929 |
| 09 | 16 | 02 | 30 | Gaussian | 0.3985123055553032 | 4.2384991973215955 | 17294.535906807043 |

| | | | | | | | |
|---|---|---|---|---|---|---|---|
| 09 | 16 | 03 | 30 | Matern | 0.772587872843198 | 5.950696331683707 | 16731.32517011128 |
| 09 | 16 | 04 | 30 | Spherical | 0.6540361970840701 | 5.825332297942259 | 12468.566032288383 |
| 09 | 16 | 05 | 30 | Spherical | 0.42478125192409855 | 7.584589466880576 | 18346.35621203936 |
| 09 | 16 | 06 | 30 | Gaussian | 0.35209964869703086 | 2.469976046504316 | 13509.910612474076 |
| 09 | 16 | 07 | 30 | Gaussian | 0.3045887470242687 | 1.7920980852173958 | 16465.231691863788 |
| 09 | 16 | 08 | 30 | Gaussian | 1.8311432007353632 | 3.8482772978636133 | 16679.95436072353 |
| 09 | 16 | 09 | 30 | Spherical | 2.4440751701637082 | 4.3399919860358 | 8732.19428850519 |
| 09 | 16 | 10 | 30 | Spherical | 0.044172956643249946 | 7.65128578624522 | 14159.386821742293 |
| 09 | 16 | 11 | 30 | Spherical | 1.0617542436806755 | 8.698632290543491 | 8961.290467120883 |
| 09 | 16 | 12 | 30 | Matern | 0.316638526528566 | 4.410351991050686 | 13979.79343434031 |
| 09 | 16 | 13 | 30 | Gaussian | 0.2637009102350866 | 7.460292316377346 | 14737.95277647152 |
| 09 | 16 | 14 | 30 | Gaussian | 0.12070570181266374 | 3.8803942298854714 | 26886.115866050284 |
| 09 | 16 | 15 | 30 | Spherical | 0 | 0.8736970027965618 | 21773.242909155284 |
| 09 | 16 | 16 | 30 | Gaussian | 0.12677691243585748 | 1.245509377145921 | 20533.580575573003 |
| 09 | 16 | 17 | 30 | Gaussian | 0.0017874138371281416 | 0.3431519389715304 | 43539.271130886715 |
| 09 | 16 | 19 | 30 | Exponential | 0.006366800661046432 | 0.20296853554254746 | 10040.19342816082 |
| 09 | 16 | 20 | 30 | Gaussian | 0.12970931028015686 | 1.5118032402853658 | 12541.559615457067 |
| 09 | 16 | 21 | 30 | Matern | 0.0012597294450217005 | 9.058470793890745 | 2709841.8817998916 |
| 09 | 16 | 22 | 30 | Spherical | 0.18440828652878072 | 0.601403015697427 | 7144.354520752205 |
| 09 | 16 | 23 | 30 | Gaussian | 0.5576238821231458 | 3.9313058407765746 | 8596.33953645466 |
| 09 | 17 | 00 | 00 | Gaussian | 0.019604087125814573 | 0.8256597446108036 | 24673.3260360379 |
| 09 | 17 | 01 | 00 | Matern | 0.05604881898064395 | 0.6070461944041768 | 3965.4216360624146 |
| 09 | 17 | 02 | 00 | Matern | 0.10235082419006127 | 1.1498197398448495 | 19284.541979975143 |
| 09 | 17 | 03 | 00 | Matern | 0.01692236682721618 | 0.4575199216562882 | 49837.723942886405 |
| 09 | 17 | 04 | 00 | Matern | 0.10139952701197621 | 1.0655541734244538 | 12399.655465494316 |
| 09 | 17 | 05 | 00 | Gaussian | 0.07136610032108003 | 1.8982208520659591 | 18047.52068389618 |
| 09 | 17 | 06 | 00 | Gaussian | 0.031319585233449514 | 0.9219926911391315 | 24525.87716114735 |
| 09 | 17 | 07 | 00 | Matern | 0.0115371241690275 | 0.47433387768298485 | 55075.81092062763 |
| 09 | 17 | 08 | 00 | Gaussian | 0.09718390315855681 | 0.5393010939922279 | 18707.16454715752 |
| 09 | 17 | 09 | 00 | Spherical | 0 | 10.755185280117685 | 5608.241939169323 |
| 09 | 17 | 10 | 00 | Gaussian | 0.008761721460975674 | 0.47896930333057297 | 36755.85057466649 |
| 09 | 17 | 11 | 00 | Matern | 0.009604279727517703 | 0.38372320243591523 | 59075.08963734897 |
| 09 | 17 | 12 | 00 | Gaussian | 0.06431960289345262 | 1.7203501475205432 | 35682.146691086156 |
| 09 | 17 | 13 | 00 | Gaussian | 0.0701472954065501 | 1.4642890101662656 | 46283.54510391105 |
| 09 | 17 | 14 | 00 | Matern | 0.01977275083793046 | 0.5910799290115457 | 48154.59113810638 |
| 09 | 17 | 15 | 00 | Matern | 0.001328003211138066 | 0.6090382308988371 | 133495.50982236487 |
| 09 | 17 | 16 | 00 | Matern | 5.44093090158777 | 5.44093090158777 | 52481.320630991075 |
| 09 | 17 | 17 | 00 | Spherical | 1.9099384370946728 | 6.153556410903861 | 5527.497341698233 |
| 09 | 17 | 18 | 00 | Gaussian | 0.0017770394387856478 | 0.5056035583156617 | 28406.869858486865 |
| 09 | 17 | 21 | 00 | Matern | 4.649773477272244e-4 | 0.336318003452068 | 93017.19152861505 |
| 09 | 17 | 22 | 00 | Spherical | 0 | 2.442093143996777 | 5711.68011908497 |
| 09 | 17 | 23 | 00 | Matern | 0.07164188896000516 | 1.4713545593785904 | 10417.281864143004 |
| 09 | 17 | 00 | 30 | Spherical | 0.0778346421612881 | 0.42708414088626845 | 14555.474284530817 |
| 09 | 17 | 01 | 30 | Spherical | 0.06868264177172258 | 1.0574185502736386 | 20035.22892401423 |
| 09 | 17 | 02 | 30 | Matern | 0.04264517289065021 | 0.7713125825460352 | 29465.93948947446 |
| 09 | 17 | 03 | 30 | Matern | 0.005559971825853433 | 0.5886601508016434 | 43694.47663600873 |
| 09 | 17 | 04 | 30 | Matern | 0.2661798991271013 | 5.071373248974309 | 15148.454229795823 |

| | | | | | | | |
|---|---|---|---|---|---|---|---|
| 09 | 17 | 05 | 30 | Gaussian | 0.013800172570686078 | 0.6026944276231493 | 44781.95076768043 |
| 09 | 17 | 07 | 30 | Gaussian | 0.1822687886308093 | 1.05714125521867 | 15640.516986522098 |
| 09 | 17 | 08 | 30 | Gaussian | 3.1176589707931264 | 122608.99948892496 | 23793320.903864257 |
| 09 | 17 | 09 | 30 | Matern | 0.30935285088491465 | 2.7056742918517127 | 10290.418761950072 |
| 09 | 17 | 10 | 30 | Matern | 2.5383699223239235e-4 | 0.6223619535047227 | 46279.25282650647 |
| 09 | 17 | 11 | 30 | Gaussian | 0.07449269948343094 | 0.5909275222747615 | 41296.188385858506 |
| 09 | 17 | 12 | 30 | Gaussian | 0.05039766234351575 | 3.20911665932465 | 42947.43916557151 |
| 09 | 17 | 13 | 30 | Gaussian | 0.034870927932473254 | 1.205034405523964 | 47430.09734777981 |
| 09 | 17 | 14 | 30 | Matern | 0 | 1.2208656457146685 | 276109.8451040436 |
| 09 | 17 | 15 | 30 | Matern | 0.015442307240381217 | 12.184050674879353 | 2306175.2953646034 |
| 09 | 17 | 16 | 30 | Matern | 1.5219859917297045 | 8.814425978792864 | 8350.898070892572 |
| 09 | 17 | 18 | 30 | Matern | 0.0012777948746909196 | 0.08118074041808314 | 35303.11951509534 |
| 09 | 17 | 20 | 30 | Matern | 0.0011557630354518433 | 0.1056003566463532 | 80964.3479281099 |
| 09 | 17 | 22 | 30 | Matern | 0.3362482028545626 | 3.9198047800299873 | 5600.849945538584 |
| 09 | 17 | 23 | 30 | Matern | 0.0030585605610411893 | 0.18034863797205775 | 31658.49347717342 |
| 09 | 18 | 00 | 00 | Matern | 0.018630861493938645 | 0.30757745078661447 | 13589.867294327327 |
| 09 | 18 | 01 | 00 | Gaussian | 9.842103555712828e-4 | 0.09235975047806541 | 83620.23878378449 |
| 09 | 18 | 02 | 00 | Matern | 0.011759287449905759 | 0.24905085824886888 | 390523.22078412725 |
| 09 | 18 | 03 | 00 | Gaussian | 0.047893558148774155 | 0.5432326999256056 | 11970.979465265276 |
| 09 | 18 | 04 | 00 | Gaussian | 0.07523221018716486 | 0.7721760872198851 | 8433.2690678792 |
| 09 | 18 | 05 | 00 | Gaussian | 0.12643556050300703 | 0.71824992242145 | 13665.71413183987 |
| 09 | 18 | 07 | 00 | Matern | 0.053509690958318944 | 0.5311554713927645 | 14997.561629818232 |
| 09 | 18 | 08 | 00 | Matern | 0.05758758059928959 | 0.5869162050729152 | 8688.07395770549 |
| 09 | 18 | 09 | 00 | Matern | 0.04989119070212046 | 0.4366884148553105 | 7137.602033199394 |
| 09 | 18 | 10 | 00 | Matern | 0.01891929761368872 | 0.7220737746885656 | 37878.862054078745 |
| 09 | 18 | 11 | 00 | Matern | 0.0017636667410771808 | 4.440932476296048 | 744524.5427673823 |
| 09 | 18 | 12 | 00 | Matern | 0 | 0.44150355922419643 | 13200.567840368616 |
| 09 | 18 | 13 | 00 | Matern | 0.02337095949370199 | 4.297376735570598 | 196200.62094163624 |
| 09 | 18 | 14 | 00 | Matern | 0.04817494498632661 | 2.5921108927194125 | 82500.72778279989 |
| 09 | 18 | 15 | 00 | Matern | 0.02621978104974294 | 7.241017253672776 | 673216.1309333289 |
| 09 | 18 | 16 | 00 | Gaussian | 0.0025191661533738832 | 0.5913196581611858 | 50143.1165766948 |
| 09 | 18 | 17 | 00 | Gaussian | 5.872783514066073e-4 | 0.20967761002004973 | 70052.54554711074 |
| 09 | 18 | 19 | 00 | Gaussian | 0.010388017265601183 | 0.7027420583707918 | 73521.99530482468 |
| 09 | 18 | 20 | 00 | Matern | 0.011237237268814319 | 0.7898383543009939 | 56803.137729360555 |
| 09 | 18 | 21 | 00 | Matern | 0.006954085138245042 | 0.259723567051555 | 37799.65627860041 |
| 09 | 18 | 22 | 00 | Matern | 0 | 7.465834075618857 | 1968.6593824184527 |
| 09 | 18 | 23 | 00 | Spherical | 0.5791370473745403 | 7.8171884297103205 | 17226.818688996693 |
| 09 | 18 | 00 | 30 | Gaussian | 0.012836635119379965 | 0.1770576998929455 | 14971.114921755721 |
| 09 | 18 | 02 | 30 | Matern | 0.05869593104081579 | 0.24563526286462067 | 17346.820538077995 |
| 09 | 18 | 03 | 30 | Spherical | 0.052188735492383585 | 0.5333856748894908 | 19203.456622124424 |
| 09 | 18 | 04 | 30 | Spherical | 0 | 0.8164121043867002 | 25261.203607074727 |
| 09 | 18 | 05 | 30 | Matern | 0.12360044972365274 | 0.5052423685062346 | 9852.325508395132 |
| 09 | 18 | 06 | 30 | Matern | 0.014535247709443111 | 0.2037958253884233 | 13067.740864206555 |
| 09 | 18 | 07 | 30 | Matern | 0.04904546992322212 | 0.5216669735564596 | 9558.665604249918 |
| 09 | 18 | 08 | 30 | Matern | 0.07328700970048382 | 0.34283515812171195 | 9596.383073678087 |
| 09 | 18 | 09 | 30 | Gaussian | 0.08434921854075199 | 1.3260391110657266 | 15398.509382949365 |
| 09 | 18 | 10 | 30 | Matern | 0.0063375625666485065 | 1.2059151718985333 | 41584.208695222274 |

| | | | | | | | |
|---|---|---|---|---|---|---|---|
| 09 | 18 | 11 | 30 | Matern | 0 | 1.101097431590669 | 81720.22452210746 |
| 09 | 18 | 12 | 30 | Matern | 0.0633466001093679 | 1.8114495220447653 | 114329.20116258747 |
| 09 | 18 | 13 | 30 | Matern | 0.11544504147924162 | 5.820123905228986 | 266842.3527003298 |
| 09 | 18 | 14 | 30 | Matern | 0.06984308627284562 | 4.323958833629083 | 258555.45157712052 |
| 09 | 18 | 15 | 30 | Spherical | 0.0033658940584012464 | 12.953195264418964 | 11720998.217605209 |
| 09 | 18 | 16 | 30 | Matern | 0.0019670085978487706 | 0.20249376357446086 | 63958.08575181162 |
| 09 | 18 | 18 | 30 | Matern | 0.008614725397000188 | 0.5991595781598082 | 73731.33069601822 |
| 09 | 18 | 19 | 30 | Gaussian | 0.0011659483141111646 | 0.08096811111283121 | 76323.3048498064 |
| 09 | 18 | 20 | 30 | Matern | 0.012730387770643269 | 1.6180282045636605 | 51217.899232435375 |
| 09 | 18 | 21 | 30 | Matern | 1.9996221776728904 | 3.6687390684102708 | 143828.94021867603 |
| 09 | 18 | 22 | 30 | Spherical | 5.049850482773225 | 7.063416575986819 | 7716.918634020897 |
| 09 | 19 | 00 | 00 | Gaussian | 0.019797245490140496 | 1.2568929902896175 | 26355.703212026317 |
| 09 | 19 | 01 | 00 | Matern | 0.06899089685730235 | 0.8634248638595542 | 10122.183232657597 |
| 09 | 19 | 02 | 00 | Matern | 0.008080768391645215 | 0.3503752518831477 | 90552.2476314028 |
| 09 | 19 | 03 | 00 | Matern | 0.007065197455622464 | 0.32675080687587943 | 29671.88400271949 |
| 09 | 19 | 04 | 00 | Matern | 0.009875480388367192 | 1.5353819188998319 | 15333.133469162798 |
| 09 | 19 | 05 | 00 | Gaussian | 0.3026559197343126 | 1.9100762808875007 | 22171.431614726152 |
| 09 | 19 | 06 | 00 | Gaussian | 0.01645468055833708 | 1.475612315321865 | 39201.46290075405 |
| 09 | 19 | 07 | 00 | Spherical | 3.4622714721097014 | 8.180739946702207 | 5125.76543866575 |
| 09 | 19 | 08 | 00 | Matern | 2.630099369086186 | 3.515346140484216 | 31194.853696767073 |
| 09 | 19 | 09 | 00 | Gaussian | 0.062380187130612566 | 2.0003236142585585 | 34134.959116157384 |
| 09 | 19 | 10 | 00 | Gaussian | 0.05693665892490365 | 2.4574848005752816 | 34274.71614572726 |
| 09 | 19 | 11 | 00 | Gaussian | 0.0982161630861799 | 3.0301390892037205 | 33480.79520576668 |
| 09 | 19 | 12 | 00 | Gaussian | 0.12185915703460193 | 5.775115743970616 | 42823.571672114136 |
| 09 | 19 | 13 | 00 | Gaussian | 0.23151363095319133 | 4.7405196834727885 | 16340.374980779112 |
| 09 | 19 | 14 | 00 | Matern | 0.10827972501784554 | 3.1141726338572293 | 43928.31538113319 |
| 09 | 19 | 15 | 00 | Gaussian | 0.07151854493807089 | 0.9258612154399323 | 13011.397226802705 |
| 09 | 19 | 16 | 00 | Gaussian | 0.22068570353959313 | 2.674231296931478 | 20476.231780083283 |
| 09 | 19 | 17 | 00 | Gaussian | 0.19700975423055048 | 0.410917141181537 | 26731.290861307112 |
| 09 | 19 | 18 | 00 | Spherical | 0.20955816698818885 | 2.8898987264411873 | 5507.468600676413 |
| 09 | 19 | 19 | 00 | Matern | 0 | 0.426774711524469 | 41477.900134546966 |
| 09 | 19 | 20 | 00 | Matern | 1.0507695782499484e-4 | 0.6539830143431639 | 30303.503014001562 |
| 09 | 19 | 21 | 00 | Gaussian | 0.038315449037406454 | 1.2542842757214427 | 25726.87115720619 |
| 09 | 19 | 22 | 00 | Spherical | 2.687639853216663 | 8.96778426902262 | 7878.225205221274 |
| 09 | 19 | 23 | 00 | Gaussian | 0.14827296265804815 | 3.7093317630382097 | 18553.941936586307 |
| 09 | 19 | 00 | 30 | Gaussian | 0.007696832574420968 | 0.30051172236888724 | 31621.786724369515 |
| 09 | 19 | 01 | 30 | Matern | 0.057490944484730716 | 0.32166028152479575 | 9870.189232864312 |
| 09 | 19 | 02 | 30 | Matern | 0.00955522197762097 | 0.5659393001598564 | 38444.12335804846 |
| 09 | 19 | 03 | 30 | Matern | 0.027020461598791023 | 1.0925367989120456 | 14239.043378550034 |
| 09 | 19 | 04 | 30 | Gaussian | 0.019425434705320176 | 1.6840414750822943 | 22599.054415478025 |
| 09 | 19 | 05 | 30 | Gaussian | 0.0954486295230612 | 1.7482229551520503 | 27549.162049723363 |
| 09 | 19 | 06 | 30 | Matern | 1.5652307852483156 | 2.8422629719075925 | 174018.4740005117 |
| 09 | 19 | 07 | 30 | Matern | 0.1953493948786753 | 4.704564078393187 | 9624.847698681036 |
| 09 | 19 | 08 | 30 | Gaussian | 0.028247747877858147 | 1.5879680330690162 | 44311.8599866238 |
| 09 | 19 | 09 | 30 | Gaussian | 0.024893293687383293 | 2.260146573484708 | 34135.259331543515 |
| 09 | 19 | 10 | 30 | Gaussian | 0.08666239734756853 | 3.028749413030554 | 27660.209101342225 |
| 09 | 19 | 11 | 30 | Gaussian | 0.0659816001088736 | 4.032484178781777 | 42923.89216174248 |

| | | | | | | | |
|---|---|---|---|---|---|---|---|
| 09 | 19 | 12 | 30 | Matern | 0.18812093869634344 | 5.054189179292675 | 39784.4836427338 |
| 09 | 19 | 13 | 30 | Gaussian | 0.19964159150852132 | 5.500781049562925 | 23783.186568515215 |
| 09 | 19 | 14 | 30 | Matern | 0.09901204405865822 | 1.6826959211844381 | 16470.047938041822 |
| 09 | 19 | 15 | 30 | Matern | 0.03405543814375654 | 1.7388255831602477 | 17920.822025882455 |
| 09 | 19 | 16 | 30 | Gaussian | 0.24937555491704938 | 1.8161547180513358 | 22311.716311766686 |
| 09 | 19 | 17 | 30 | Spherical | 1.4332396767507485 | 9.4402542736817 | 12387.351640115592 |
| 09 | 19 | 19 | 30 | Gaussian | 0.013567673567282945 | 0.73993949864134 | 23130.479291301504 |
| 09 | 19 | 20 | 30 | Matern | 0.0011327649410850483 | 0.628335464255655 | 39645.446415011946 |
| 09 | 19 | 21 | 30 | Spherical | 0.6942163265364991 | 2.6674958402953473 | 6694.544202088519 |
| 09 | 19 | 22 | 30 | Matern | 0.18973304233537439 | 5.4099057067764695 | 12880.742667820825 |
| 09 | 19 | 23 | 30 | Gaussian | 0.16195226387585734 | 5.008256514628221 | 22961.579858303623 |
| 09 | 20 | 00 | 00 | Gaussian | 0.047076780640183176 | 1.9174614395618685 | 24519.15297265944 |
| 09 | 20 | 01 | 00 | Matern | 0.02665162860111574 | 0.38972229303740563 | 19154.681012186138 |
| 09 | 20 | 02 | 00 | Matern | 0 | 0.48800823833247287 | 2904.8134804490583 |
| 09 | 20 | 03 | 00 | Spherical | 0 | 4.595574254808019 | 3373.0348524624114 |
| 09 | 20 | 04 | 00 | Matern | 0.15973576911697873 | 1.5345987017809826 | 16486.715411786 |
| 09 | 20 | 05 | 00 | Matern | 0 | 0.7532931822583573 | 1192.133086597116 |
| 09 | 20 | 06 | 00 | Gaussian | 1.1431611576892904 | 1.8932705205595406 | 8655.658613071668 |
| 09 | 20 | 07 | 00 | Spherical | 0.008486200417859968 | 0.10817237735372923 | 57238.62241536371 |
| 09 | 20 | 08 | 00 | Matern | 0.11048581784613425 | 0.2077216929054031 | 42891.72645199338 |
| 09 | 20 | 10 | 00 | Gaussian | 0.23066474964413952 | 3.3222693619037726 | 12444.1110135563 |
| 09 | 20 | 12 | 00 | Gaussian | 0.08064573211915987 | 1.7581082811468607 | 53054.416075804445 |
| 09 | 20 | 14 | 00 | Gaussian | 0.004508880699299586 | 0.10264324470507767 | 17579.38784547792 |
| 09 | 20 | 15 | 00 | Gaussian | 0.0034319442485960545 | 0.3414655854346783 | 58936.67071207835 |
| 09 | 20 | 16 | 00 | Gaussian | 0.01523190626070853 | 1.0318007021520126 | 60591.35424249302 |
| 09 | 20 | 17 | 00 | Matern | 0.01515755435544875 | 390.74991660803136 | 56545060.083438516 |
| 09 | 20 | 19 | 00 | Matern | 7.029849952277487e-4 | 0.14501082193159756 | 147148.86205709862 |
| 09 | 20 | 00 | 30 | Gaussian | 0.034271428812797516 | 0.8352033399897368 | 18481.20548892252 |
| 09 | 20 | 01 | 30 | Matern | 0.004332574164407728 | 1184.5069033114528 | 15302556.178590545 |
| 09 | 20 | 02 | 30 | Matern | 0 | 5.767514930949129 | 2053.523056938436 |
| 09 | 20 | 03 | 30 | Spherical | 1.4699066952726665 | 5.3085512417474305 | 5507.073993860306 |
| 09 | 20 | 04 | 30 | Gaussian | 0.1511715478107978 | 0.3838701744228702 | 23626.389915624986 |
| 09 | 20 | 05 | 30 | Spherical | 0.8433936238709547 | 4.770493625348545 | 7310.472313539542 |
| 09 | 20 | 06 | 30 | Spherical | 0 | 1.7404239542314037 | 35842.55275511632 |
| 09 | 20 | 07 | 30 | Spherical | 0 | 0.07190755941932842 | 98908.92725725625 |
| 09 | 20 | 08 | 30 | Matern | 0 | 6.4755774007736635 | 1937.3537339550892 |
| 09 | 20 | 09 | 30 | Gaussian | 0.05230009396048997 | 0.5826769304101691 | 16742.30411268084 |
| 09 | 20 | 11 | 30 | Gaussian | 0.022298305682479924 | 1.381892477979014 | 36828.83904373766 |
| 09 | 20 | 12 | 30 | Gaussian | 0.04608085739043403 | 1.089082685633306 | 64273.62307114145 |
| 09 | 20 | 14 | 30 | Gaussian | 0.03396409339062696 | 0.4741799827363769 | 12390.93557780357 |
| 09 | 20 | 15 | 30 | Gaussian | 0.01874991813461311 | 0.8842029550163576 | 62907.683997199805 |
| 09 | 20 | 16 | 30 | Matern | 0 | 2.129397496287227 | 347338.21170804446 |
| 09 | 20 | 17 | 30 | Matern | 0.034134754034628574 | 68.02999422383733 | 3887572.5313999197 |
| 09 | 20 | 18 | 30 | Matern | 0.0038029175237447484 | 0.4141984053527101 | 165293.01170279566 |
| 09 | 21 | 04 | 00 | Spherical | 1.2891677085995712 | 5.798522035066699 | 7522.8930936936895 |
| 09 | 21 | 08 | 00 | Matern | 0.0010244342113148092 | 0.3068144577890016 | 159488.57947839558 |
| 09 | 21 | 10 | 00 | Matern | 0.0014105757725991904 | 43.39402999622677 | 5176090.288843799 |

| | | | | | | | |
|---|---|---|---|---|---|---|---|
| 09 | 21 | 14 | 00 | Matern | 0.003415159934859697 | 0.11803285568164405 | 113894.399606502 |
| 09 | 21 | 15 | 00 | Matern | 0.0032528654974497266 | 0.31685926487149296 | 132198.260775203 |
| 09 | 21 | 17 | 00 | Matern | 7.597814398065275e-4 | 0.251436281504776 | 135594.1884621588 |
| 09 | 21 | 19 | 00 | Matern | 0.0027284909997556187 | 0.4991373222627825 | 180839.89413239408 |
| 09 | 21 | 20 | 00 | Matern | 0.00414749083293049 | 121.64430665466992 | 12241935.382459862 |
| 09 | 21 | 21 | 00 | Matern | 0.00734907028952401 | 0.3116099015169749 | 76516.24642535669 |
| 09 | 21 | 23 | 00 | Matern | 8.001881510131956e-5 | 1.314686748475384 | 334154.01563565026 |
| 09 | 21 | 03 | 30 | Spherical | 0 | 2.3796702343148963 | 10340.40802309965 |
| 09 | 21 | 04 | 30 | Spherical | 0.21439910299358944 | 3.880122980536312 | 12438.25816784835 |
| 09 | 21 | 09 | 30 | Matern | 5.220554880459316e-4 | 0.45736812869822174 | 206373.2644875221 |
| 09 | 21 | 14 | 30 | Matern | 0.006414137573483952 | 0.3106307913859964 | 118442.6789823176 |
| 09 | 21 | 16 | 30 | Matern | 7.263850463953915e-4 | 0.17454820062399948 | 70352.74331256516 |
| 09 | 21 | 17 | 30 | Matern | 4.729776395960167e-5 | 0.4808348694333304 | 137803.740202766 |
| 09 | 21 | 18 | 30 | Matern | 6.600454728950624e-4 | 0.13315421135681485 | 90370.05553981518 |
| 09 | 21 | 19 | 30 | Matern | 0.0012759262970206036 | 25386.748244259317 | 149148072.29201415 |
| 09 | 21 | 20 | 30 | Gaussian | 0.01648184872873789 | 0.40937772754261753 | 88553.65028314557 |
| 09 | 21 | 22 | 30 | Matern | 2.819336187168547e-4 | 2.306087911317457 | 2461310.444661656 |
| 09 | 21 | 23 | 30 | Matern | 6.678956476482835e-4 | 0.3513781229322068 | 52721.11430685695 |
| 09 | 22 | 00 | 00 | Exponential | 0.018354591861478236 | 9.428280416163542 | 2721918.340128933 |
| 09 | 22 | 01 | 00 | Gaussian | 0.011494403326794096 | 0.22501619635687942 | 25333.890791410573 |
| 09 | 22 | 02 | 00 | Matern | 0 | 4.08114813390813 | 1668.2217357819723 |
| 09 | 22 | 03 | 00 | Matern | 0 | 1.1066763859703335 | 2131.5985256927584 |
| 09 | 22 | 05 | 00 | Matern | 6.158909090160806e-4 | 0.5513414215374002 | 81767.29516290227 |
| 09 | 22 | 06 | 00 | Matern | 0.0047078272951906076 | 0.1950122773825816 | 50568.21781389551 |
| 09 | 22 | 07 | 00 | Matern | 0.0032015960278400147 | 84.1454791689496 | 49637766.618373886 |
| 09 | 22 | 08 | 00 | Matern | 0.00473035642911489 | 0.19068969184987342 | 54671.46465605411 |
| 09 | 22 | 10 | 00 | Matern | 7.3662088724516e-4 | 2.8699046063785385 | 987956.5408656739 |
| 09 | 22 | 11 | 00 | Matern | 0.00477266314290517 | 0.5738974975599666 | 125731.0000588058 |
| 09 | 22 | 12 | 00 | Gaussian | 0.007908636478837543 | 0.9735158489854561 | 71867.69376870096 |
| 09 | 22 | 14 | 00 | Gaussian | 0.03481127336469722 | 1.8309165950504187 | 82900.57175903239 |
| 09 | 22 | 15 | 00 | Matern | 0.0045775537342557186 | 2.345438207405138 | 68460.75746988512 |
| 09 | 22 | 16 | 00 | Gaussian | 0.051593567573532735 | 1.9147399739233446 | 58876.261343097154 |
| 09 | 22 | 17 | 00 | Matern | 0.030063271393393935 | 1.9173232454418787 | 104725.46302002219 |
| 09 | 22 | 18 | 00 | Matern | 0.008286414254321146 | 1.0608943198444765 | 154973.0294016264 |
| 09 | 22 | 19 | 00 | Gaussian | 0.003239596951416818 | 0.570993317345389 | 108638.10867277396 |
| 09 | 22 | 20 | 00 | Gaussian | 0.016060722757950122 | 0.11897560936725088 | 20127.430537261596 |
| 09 | 22 | 21 | 00 | Matern | 0.001311540307025776 | 0.08528939806744902 | 127208.05462464676 |
| 09 | 22 | 23 | 00 | Gaussian | 0.018111496556925066 | 0.848069912153214 | 10205.23621910423 |
| 09 | 22 | 00 | 30 | Matern | 0.05828758663531457 | 0.3846604811453984 | 16354.589408503196 |
| 09 | 22 | 01 | 30 | Gaussian | 0.0307970884413708 | 0.46565112842105427 | 15885.180337467877 |
| 09 | 22 | 02 | 30 | Matern | 0 | 6.074841614718401 | 948.7268465927023 |
| 09 | 22 | 03 | 30 | Matern | 0.00158837292945012 | 0.5426684212999817 | 62946.008688143505 |
| 09 | 22 | 05 | 30 | Matern | 0.007739731116125603 | 0.21185447283815823 | 55894.1437359004 |
| 09 | 22 | 06 | 30 | Spherical | 0.003891414621445552 | 3.0294427695246626 | 2262266.9448245675 |
| 09 | 22 | 07 | 30 | Matern | 0.0018707653486737693 | 0.8711439618063445 | 370073.2479882154 |
| 09 | 22 | 08 | 30 | Matern | 0.0016808452870735314 | 0.0643892893732794 | 35573.38498041951 |
| 09 | 22 | 09 | 30 | Matern | 0.0011271126017526026 | 5.612061522254031 | 1001103.3260079838 |

| | | | | | | | |
|---|---|---|---|---|---|---|---|
| 09 | 22 | 10 | 30 | Matern | 7.574488294597336e-4 | 11.13736461025116 | 2454093.149528559 |
| 09 | 22 | 11 | 30 | Matern | 0.0010893656173111726 | 0.8479055981203121 | 111696.43891459538 |
| 09 | 22 | 12 | 30 | Matern | 0.010511937848442716 | 0.9067054559798474 | 36976.12178704665 |
| 09 | 22 | 13 | 30 | Matern | 0.02853292240708203 | 1.4636635772880286 | 66572.90126742466 |
| 09 | 22 | 14 | 30 | Matern | 0.00989773179069998 | 2.1891288407558838 | 75242.96591619693 |
| 09 | 22 | 15 | 30 | Matern | 0.038980996174575865 | 2.3385684025604077 | 67069.15753035249 |
| 09 | 22 | 16 | 30 | Matern | 0.07481572531304781 | 1.8337699611461615 | 72035.85602523279 |
| 09 | 22 | 17 | 30 | Matern | 0.03377095513109552 | 1.647782859132522 | 110003.35023702926 |
| 09 | 22 | 18 | 30 | Gaussian | 0.002812277233066645 | 0.5130317959004618 | 91214.02622742234 |
| 09 | 22 | 19 | 30 | Matern | 0.007819193991581055 | 140.98626852432034 | 53595590.971953586 |
| 09 | 22 | 20 | 30 | Matern | 8.239104498277074e-5 | 0.06330987404521343 | 157790.24041342366 |
| 09 | 22 | 21 | 30 | Matern | 8.972224662760559e-4 | 0.019851235668033117 | 112884.6057210643 |
| 09 | 22 | 23 | 30 | Matern | 0.03276981183425738 | 0.23845848103811407 | 9971.638508457052 |
| 09 | 23 | 04 | 00 | Gaussian | 0.029391121033973445 | 0.2441167920486472 | 15563.716631426776 |
| 09 | 23 | 05 | 00 | Gaussian | 0.002550167764334291 | 0.12547536993546693 | 22040.218330150034 |
| 09 | 23 | 06 | 00 | Matern | 1.7082249195544898e-4 | 3.10679147834842 | 2241361.213532208 |
| 09 | 23 | 08 | 00 | Matern | 0 | 5.795066273109794 | 230.93825758229568 |
| 09 | 23 | 09 | 00 | Gaussian | 0 | 8.026353268409574 | 2663.1443833485596 |
| 09 | 23 | 10 | 00 | Matern | 0.0356697524709061 | 4.90401600480206 | 8311.314284602164 |
| 09 | 23 | 11 | 00 | Matern | 0.10248226211800258 | 4.482967389595753 | 10502.163981257127 |
| 09 | 23 | 12 | 00 | Matern | 1.9490815493143059 | 8.913351613509922 | 11342.094948902759 |
| 09 | 23 | 13 | 00 | Spherical | 0.5003518594368769 | 8.7435316186201 | 11144.972369328412 |
| 09 | 23 | 14 | 00 | Spherical | 1.9663396557289214 | 7.887024027394452 | 6424.141659364913 |
| 09 | 23 | 15 | 00 | Matern | 2.8765698152938057 | 10.019717807084026 | 32777.52304725358 |
| 09 | 23 | 16 | 00 | Gaussian | 1.152937125734201 | 10.6510344428196 | 9571.13393867164 |
| 09 | 23 | 17 | 00 | Gaussian | 1.2210808490197915 | 8.71907900536246 | 11042.971865754665 |
| 09 | 23 | 18 | 00 | Gaussian | 1.0817357974742068 | 9.79271091361899 | 14489.866767839167 |
| 09 | 23 | 19 | 00 | Spherical | 1.0676280812127192 | 8.260283120584127 | 33552.31683347502 |
| 09 | 23 | 20 | 00 | Matern | 1.192396165008309 | 8.347610361877033 | 30492.651253606335 |
| 09 | 23 | 21 | 00 | Spherical | 1.189537496335853 | 5.799824833724662 | 9714.829208216472 |
| 09 | 23 | 22 | 00 | Gaussian | 2.74627227755712 | 2.74627227755712 | 52048.29657395149 |
| 09 | 23 | 23 | 00 | Matern | 2.3336589620508477 | 2.3336589620508477 | 52048.29657395149 |
| 09 | 23 | 02 | 30 | Matern | 5.365329822944007e-4 | 0.1835625009225899 | 30832.41516437088 |
| 09 | 23 | 03 | 30 | Gaussian | 0.0031564999524579702 | 0.13178242371001442 | 55190.4311874949 |
| 09 | 23 | 04 | 30 | Gaussian | 0.04322335894935637 | 0.4145865975035346 | 16884.334968130923 |
| 09 | 23 | 05 | 30 | Matern | 6.0477344253201775e-5 | 0.14772495144386003 | 96075.0677688935 |
| 09 | 23 | 06 | 30 | Matern | 0.0034170999597060536 | 0.33865039229112415 | 42801.06713791585 |
| 09 | 23 | 07 | 30 | Matern | 2.9835469532302814 | 3.446021043550885 | 137910.10562345406 |
| 09 | 23 | 08 | 30 | Matern | 0 | 3.926484091108798 | 5625.570971769766 |
| 09 | 23 | 11 | 30 | Matern | 1.3363369743800795 | 6.963474994275881 | 11860.584560078905 |
| 09 | 23 | 12 | 30 | Matern | 0.0694365566901451 | 8.589560330939435 | 10382.123523605504 |
| 09 | 23 | 13 | 30 | Spherical | 1.9168613311355402 | 8.880522610850086 | 14765.418041347117 |
| 09 | 23 | 14 | 30 | Matern | 0.4208700863928568 | 10.706519787516093 | 5388.419471464339 |
| 09 | 23 | 15 | 30 | Matern | 0.2574393779367094 | 9.115411193502341 | 18587.16143411853 |
| 09 | 23 | 16 | 30 | Matern | 0.8223494671264446 | 10.417532900893669 | 10438.67161646997 |
| 09 | 23 | 17 | 30 | Matern | 1.5910902129262565 | 8.150237276528772 | 27136.716431947025 |
| 09 | 23 | 18 | 30 | Spherical | 0.5617160132137217 | 9.189299633169842 | 28679.274517297 |

| | | | | | | | |
|---|---|---|---|---|---|---|---|
| 09 | 23 | 19 | 30 | Matern | 1.601361652934459 | 8.287391845265022 | 15278.07141230284 |
| 09 | 23 | 20 | 30 | Exponential | 0.20331062216433707 | 7.546666265104672 | 12284.976449410138 |
| 09 | 23 | 21 | 30 | Spherical | 1.9568065284637481 | 3.588880066015702 | 5001.91991140048 |
| 09 | 23 | 22 | 30 | Matern | 2.408920926857902 | 2.408920926857902 | 52048.29657395149 |
| 09 | 23 | 23 | 30 | Spherical | 1.919772984414915 | 3.402339664638588 | 5512.508166274655 |
| 09 | 24 | 00 | 00 | Spherical | 1.1614059102090692 | 4.600571327470081 | 8470.233220527856 |
| 09 | 24 | 01 | 00 | Gaussian | 0.29992725640781653 | 4.569336642793847 | 16254.124287344706 |
| 09 | 24 | 02 | 00 | Matern | 1.7144199286481396 | 9.525508369468612 | 5658.856657964458 |
| 09 | 24 | 03 | 00 | Matern | 0.05322829672799222 | 6.66372783510456 | 5585.6510795287195 |
| 09 | 24 | 04 | 00 | Matern | 0.628675841725945 | 7.3436329589506855 | 3758.6955918165213 |
| 09 | 24 | 05 | 00 | Matern | 0.8557711010954407 | 8.610633778537126 | 25481.500710797987 |
| 09 | 24 | 06 | 00 | Matern | 0 | 3.8413618689623648 | 7530.091603173101 |
| 09 | 24 | 07 | 00 | Matern | 0.5954453964956329 | 3.5242307244369355 | 12005.984436320623 |
| 09 | 24 | 08 | 00 | Matern | 1.244268629245773 | 4.002539479379513 | 13821.307860949035 |
| 09 | 24 | 09 | 00 | Gaussian | 0.8931022717478335 | 6.647926631571626 | 13797.751076894003 |
| 09 | 24 | 10 | 00 | Matern | 0.06263133579733181 | 3.928531656365689 | 9316.750509087096 |
| 09 | 24 | 11 | 00 | Spherical | 0.16436245024701646 | 2.361366394502106 | 113418.72271793596 |
| 09 | 24 | 12 | 00 | Matern | 0.15193873129721797 | 2.1712484015286244 | 25704.87107489138 |
| 09 | 24 | 13 | 00 | Spherical | 0.3958657610660607 | 4.961786192691815 | 19142.96040057096 |
| 09 | 24 | 14 | 00 | Gaussian | 1.2517687706632805 | 5.22693806689402 | 17815.19898669685 |
| 09 | 24 | 15 | 00 | Matern | 1.7241302914018206 | 4.535770827641457 | 19949.29321337974 |
| 09 | 24 | 16 | 00 | Matern | 0.25307626179375187 | 2.8036649102315945 | 48337.872077771375 |
| 09 | 24 | 17 | 00 | Spherical | 0.010233544361350924 | 0.5277428374471792 | 252942.2988873097 |
| 09 | 24 | 18 | 00 | Matern | 0.007051192533304171 | 1.3637538710291761 | 331121.30801336124 |
| 09 | 24 | 19 | 00 | Matern | 0.005442308770238621 | 1219.051565674222 | 435125370.4000765 |
| 09 | 24 | 20 | 00 | Matern | 0 | 1.5223509113029108 | 1687.9693054590232 |
| 09 | 24 | 21 | 00 | Gaussian | 1.3074412077251671 | 4.4500157304206756 | 7208.074056293827 |
| 09 | 24 | 22 | 00 | Matern | 1.8048776315208845 | 5.174641952875002 | 8117.806131740699 |
| 09 | 24 | 23 | 00 | Gaussian | 0.6616011791311781 | 1.870324548187427 | 33238.1321834213 |
| 09 | 24 | 00 | 30 | Spherical | 0.9406271452551592 | 4.400322680966685 | 13266.324438367048 |
| 09 | 24 | 01 | 30 | Spherical | 0.9346900922668703 | 6.5132378245787494 | 43940.104056974145 |
| 09 | 24 | 02 | 30 | Spherical | 0.23862715968446782 | 8.256217508499244 | 9521.439733015113 |
| 09 | 24 | 03 | 30 | Spherical | 0.8943209513899046 | 5.2305925935709325 | 9284.08099372351 |
| 09 | 24 | 04 | 30 | Matern | 0.041314337952407396 | 9.203820478527462 | 2985.763904538681 |
| 09 | 24 | 05 | 30 | Matern | 0.12767879069340568 | 5.305219965032866 | 12944.490071051228 |
| 09 | 24 | 06 | 30 | Exponential | 0.27296535263114347 | 5.035347254345563 | 7989.959417696343 |
| 09 | 24 | 07 | 30 | Matern | 0.9107543183434573 | 3.2748542177037003 | 33112.55631758801 |
| 09 | 24 | 08 | 30 | Spherical | 0.8410279960884763 | 4.291131377496091 | 36381.1862393631 |
| 09 | 24 | 09 | 30 | Matern | 0.7217933759252269 | 5.046322298066345 | 12562.725782345038 |
| 09 | 24 | 10 | 30 | Matern | 0.34127749780787336 | 2.876549133987227 | 45369.68604291366 |
| 09 | 24 | 11 | 30 | Spherical | 0.05517734556723571 | 2.337842365528462 | 56132.48814230197 |
| 09 | 24 | 12 | 30 | Spherical | 0.6721312200881101 | 3.8060527415049865 | 14322.778776086434 |
| 09 | 24 | 13 | 30 | Matern | 0.5366929732890571 | 3.1510153991075986 | 8893.967670523187 |
| 09 | 24 | 14 | 30 | Gaussian | 1.733064327637733 | 6.1888957748724405 | 22317.54560266421 |
| 09 | 24 | 15 | 30 | Spherical | 0.3810453261974518 | 4.11012535315474 | 79387.35393529471 |
| 09 | 24 | 16 | 30 | Matern | 0.11549366080102648 | 1.4228298807364639 | 64506.4059129473 |
| 09 | 24 | 17 | 30 | Gaussian | 0.011517967424160393 | 0.6088530250787704 | 106665.46875867936 |

| | | | | | | | |
|---|---|---|---|---|---|---|---|
| 09 | 24 | 18 | 30 | Matern | 0 | 14.147662219678923 | 3793193.3282846496 |
| 09 | 24 | 20 | 30 | Spherical | 0 | 4.096974873200154 | 5205.864656475771 |
| 09 | 24 | 21 | 30 | Matern | 0.06721370998220155 | 2.9322618314051314 | 5764.259530358321 |
| 09 | 24 | 22 | 30 | Spherical | 0.7866614503050898 | 3.283835000522243 | 11586.29266278565 |
| 09 | 24 | 23 | 30 | Gaussian | 0.058367623024813874 | 1.7537145151105895 | 47443.35475126869 |
| 09 | 25 | 00 | 00 | Matern | 0.11112949302513045 | 1.1464801003502099 | 52902.52312498349 |
| 09 | 25 | 01 | 00 | Matern | 0.4497093341264559 | 7.524051866258803 | 6766.144595687171 |
| 09 | 25 | 02 | 00 | Spherical | 0.6092325676192655 | 4.734241644255314 | 12013.857029604336 |
| 09 | 25 | 03 | 00 | Spherical | 0.6807368998962157 | 6.6832678265006695 | 14280.963396981551 |
| 09 | 25 | 04 | 00 | Gaussian | 0.3674230120686503 | 1.5925173093418796 | 14707.944214440053 |
| 09 | 25 | 05 | 00 | Spherical | 0 | 1.8581689468684364 | 5693.871483280049 |
| 09 | 25 | 06 | 00 | Spherical | 0.7993216582759387 | 5.2642968953878375 | 6696.503813999811 |
| 09 | 25 | 07 | 00 | Spherical | 0.6206503143379928 | 5.081269241427252 | 13051.214077938106 |
| 09 | 25 | 08 | 00 | Gaussian | 0.020871286146637216 | 0.977431920396539 | 17329.547849780174 |
| 09 | 25 | 09 | 00 | Gaussian | 0.024436876069346334 | 0.8935220606564357 | 27296.011967218543 |
| 09 | 25 | 10 | 00 | Spherical | 1.7846755913794066 | 5.122186878095053 | 6935.356455099231 |
| 09 | 25 | 11 | 00 | Gaussian | 1.2429913460191537 | 9.61856636614236 | 13494.253238934547 |
| 09 | 25 | 12 | 00 | Spherical | 2.721134087679743 | 4.7557958220795635 | 40752.09555776302 |
| 09 | 25 | 13 | 00 | Gaussian | 0.37498034401247177 | 5.2602793020063645 | 22144.581813860885 |
| 09 | 25 | 14 | 00 | Gaussian | 0.14173847938191594 | 4.142325683318109 | 55195.61828189117 |
| 09 | 25 | 15 | 00 | Matern | 0.02302358614694804 | 2.982625590991946 | 95210.16587579639 |
| 09 | 25 | 16 | 00 | Matern | 0.11229937793801599 | 2.936789631207628 | 113824.17425386336 |
| 09 | 25 | 17 | 00 | Gaussian | 0.09933136997448183 | 2.8128888966905774 | 90406.18222619448 |
| 09 | 25 | 18 | 00 | Matern | 0.019254749764641102 | 2.66345759985023 | 66283.28663392144 |
| 09 | 25 | 19 | 00 | Matern | 0.027045324777286744 | 1.4171978785578914 | 48121.472395767065 |
| 09 | 25 | 20 | 00 | Gaussian | 0.006177794683222593 | 0.20083299601313573 | 26628.50571656748 |
| 09 | 25 | 00 | 30 | Spherical | 0 | 3.4449776512422896 | 5336.552569659161 |
| 09 | 25 | 01 | 30 | Matern | 0.26926703794147716 | 6.240065812746762 | 3816.863533498444 |
| 09 | 25 | 02 | 30 | Matern | 0.8995412061742701 | 2.889909782517507 | 5463.067883625532 |
| 09 | 25 | 03 | 30 | Gaussian | 0.5418149907352549 | 3.8010824410993425 | 9252.25280132892 |
| 09 | 25 | 04 | 30 | Matern | 0 | 2.2105860139406133 | 1398.185979142086 |
| 09 | 25 | 05 | 30 | Gaussian | 0.27625823602034755 | 2.5562219945923768 | 18025.391724372676 |
| 09 | 25 | 06 | 30 | Matern | 1.249851875157783 | 4.958655826478467 | 7936.711809352712 |
| 09 | 25 | 07 | 30 | Gaussian | 0.06263702077929648 | 2.262697964812878 | 11723.386871061502 |
| 09 | 25 | 08 | 30 | Gaussian | 0.09443939225557987 | 0.9498126421069795 | 29828.450148154963 |
| 09 | 25 | 09 | 30 | Spherical | 0.3688797010730522 | 1.3152185971059938 | 7922.186819830244 |
| 09 | 25 | 10 | 30 | Spherical | 0.11272381745037649 | 8.741430003676651 | 23499.94575605305 |
| 09 | 25 | 11 | 30 | Gaussian | 2.583190787302449 | 6.536671145871017 | 15919.043984396167 |
| 09 | 25 | 12 | 30 | Spherical | 1.1195612301707314 | 4.96796466859074 | 46826.029604474796 |
| 09 | 25 | 13 | 30 | Gaussian | 0.26742741117604407 | 3.9696059389235585 | 20565.39254937122 |
| 09 | 25 | 14 | 30 | Matern | 0.09379961745059306 | 3.6785991093502703 | 81298.65032501043 |
| 09 | 25 | 15 | 30 | Matern | 0.06554604918272947 | 2.911651821106617 | 106453.48760416068 |
| 09 | 25 | 16 | 30 | Matern | 0.060735248999832875 | 47.6670948548346 | 1666798.1352372896 |
| 09 | 25 | 17 | 30 | Gaussian | 0.05101468336915924 | 3.1563516430002725 | 78521.8592491623 |
| 09 | 25 | 18 | 30 | Matern | 0.03590365582822388 | 2.1041729310326924 | 57565.44920677068 |
| 09 | 25 | 19 | 30 | Matern | 0.021144337639045916 | 0.6595319484921871 | 38559.57709957419 |
| 09 | 25 | 20 | 30 | Matern | 9.376995417723158e-4 | 0.040502749355097505 | 121306.70495987959 |

| | | | | | | | |
|---|---|---|---|---|---|---|---|
| 09 | 26 | 12 | 00 | Gaussian | 0.006534102667830396 | 0.6065136112402293 | 74542.81225825472 |
| 09 | 26 | 13 | 00 | Matern | 0.022622490149670205 | 1.0646713918304143 | 78048.73482238321 |
| 09 | 26 | 14 | 00 | Matern | 0.012880320011752728 | 1.140241738481867 | 88757.62363684966 |
| 09 | 26 | 15 | 00 | Matern | 0.00812764916781018 | 3.0872679092412976 | 431965.827813334 |
| 09 | 26 | 16 | 00 | Matern | 0.03349109549928136 | 1.109100208843376 | 557701.1104610754 |
| 09 | 26 | 17 | 00 | Matern | 0.021102488173080722 | 0.6753661452000964 | 109594.17070467293 |
| 09 | 26 | 18 | 00 | Matern | 0.00676959800911888 | 0.5380463746481197 | 91932.56527324117 |
| 09 | 26 | 21 | 00 | Matern | 0.004116641188886403 | 0.09763723428546715 | 38917.01081564442 |
| 09 | 26 | 22 | 00 | Gaussian | 0.012124421782912786 | 0.3060946672468172 | 39173.17495651904 |
| 09 | 26 | 23 | 00 | Gaussian | 0.011563748386327002 | 0.33106575986487846 | 44970.88975798637 |
| 09 | 26 | 11 | 30 | Matern | 0.006684691161663697 | 0.4156748490127123 | 73304.26159638923 |
| 09 | 26 | 12 | 30 | Gaussian | 0.007304229983834171 | 0.7845441281832098 | 77202.67904481008 |
| 09 | 26 | 13 | 30 | Gaussian | 0.014737401606559798 | 0.7549506559511243 | 87387.91314528661 |
| 09 | 26 | 14 | 30 | Gaussian | 0.009922413398138562 | 1.0233590152885905 | 102064.63192269082 |
| 09 | 26 | 15 | 30 | Matern | 0.00861980132670415 | 0.8387646042637052 | 128827.36261355437 |
| 09 | 26 | 16 | 30 | Matern | 0.037035595252295724 | 0.4010979985068594 | 114302.64650876146 |
| 09 | 26 | 17 | 30 | Matern | 0.016274487904473414 | 0.5142388375196744 | 105277.54781735859 |
| 09 | 26 | 18 | 30 | Matern | 0.004806095879212328 | 0.3151501179610345 | 100689.68492763772 |
| 09 | 26 | 20 | 30 | Matern | 0.0033566927658159906 | 0.03291084438110032 | 127992.85172311479 |
| 09 | 26 | 21 | 30 | Gaussian | 0.005147848041648822 | 0.1297961202891217 | 34167.96023284726 |
| 09 | 26 | 22 | 30 | Gaussian | 0.011567722962077719 | 0.3475827611244136 | 42176.306686630385 |
| 09 | 26 | 23 | 30 | Gaussian | 0.008758207740631315 | 0.2679628043821891 | 46421.4828183056 |
| 09 | 27 | 00 | 00 | Gaussian | 0.00899801793819921 | 0.3104878497990403 | 44161.71880193018 |
| 09 | 27 | 01 | 00 | Gaussian | 0.007848838820167642 | 0.22285955295758364 | 42359.454759834975 |
| 09 | 27 | 02 | 00 | Gaussian | 0.0062408798541484 | 0.236144700713719 | 38406.10265067725 |
| 09 | 27 | 03 | 00 | Gaussian | 0.004499018670324215 | 0.12337774601551917 | 33687.36010300833 |
| 09 | 27 | 04 | 00 | Gaussian | 0.0038596447759201083 | 0.2034155736635496 | 38366.16465639322 |
| 09 | 27 | 06 | 00 | Matern | 3.6099468683690393e-4 | 6.250391763535279 | 2437382.935897483 |
| 09 | 27 | 12 | 00 | Matern | 0.013268347431979697 | 499.15127913708574 | 38798746.77896619 |
| 09 | 27 | 13 | 00 | Matern | 0 | 5.689346571374861 | 523338.9336156271 |
| 09 | 27 | 14 | 00 | Matern | 0.012920193659803287 | 3.0831324760397707 | 116815.38714586203 |
| 09 | 27 | 15 | 00 | Matern | 0.012703351111271858 | 0.8404551451143729 | 57861.839564624286 |
| 09 | 27 | 16 | 00 | Gaussian | 0.05223983554362331 | 3.6413740105942494 | 27753.205255790548 |
| 09 | 27 | 17 | 00 | Matern | 0.321014403832097 | 5.960398878097246 | 11696.17001688862 |
| 09 | 27 | 18 | 00 | Spherical | 1.728027013890657 | 4.519245722719074 | 13132.605402473553 |
| 09 | 27 | 19 | 00 | Gaussian | 0.014042508647945684 | 0.13458184457372177 | 13366.67608820944 |
| 09 | 27 | 20 | 00 | Matern | 0.003161756884407139 | 0.13865713061642684 | 89979.99902633028 |
| 09 | 27 | 00 | 30 | Gaussian | 0.002311271243874518 | 0.14099014889564493 | 48391.080154446456 |
| 09 | 27 | 01 | 30 | Gaussian | 0.008555600387926122 | 0.28663269770571603 | 39867.438667435476 |
| 09 | 27 | 02 | 30 | Gaussian | 0.0024453726724383003 | 0.12481144245199952 | 37690.678471930216 |
| 09 | 27 | 03 | 30 | Gaussian | 0.006961749802035402 | 0.21075808265899146 | 37470.90037927519 |
| 09 | 27 | 11 | 30 | Matern | 0.005561226773681745 | 118.754144060016 | 4218635.463927403 |
| 09 | 27 | 12 | 30 | Matern | 0.005625152401996056 | 23.612881775656632 | 1909898.488307224 |
| 09 | 27 | 13 | 30 | Matern | 0.00534334127048233 | 3.6452220789872314 | 108532.62336917764 |
| 09 | 27 | 14 | 30 | Matern | 6.608367947531686e-4 | 1.6695117943113615 | 175651.27137653623 |
| 09 | 27 | 15 | 30 | Spherical | 0 | 1.3467677987937408 | 84149.0401236793 |
| 09 | 27 | 16 | 30 | Gaussian | 0.252708713238906 | 5.979623132881582 | 21006.359341228097 |

| | | | | | | | |
|---|---|---|---|---|---|---|---|
| 09 | 27 | 17 | 30 | Spherical | 0.5611566520625599 | 5.812266789599337 | 15215.648505304705 |
| 09 | 27 | 18 | 30 | Matern | 0.4460091735378397 | 2.3804156518164596 | 2032.0096172681347 |
| 09 | 27 | 19 | 30 | Matern | 0.004533947244828175 | 0.2656254325343996 | 77035.21737362826 |
| 09 | 28 | 02 | 00 | Matern | 0.020234215780989957 | 0.1374432562382781 | 22744.97123541692 |
| 09 | 28 | 03 | 00 | Matern | 0.04784564447349277 | 0.3391036519096159 | 28666.718661674644 |
| 09 | 28 | 04 | 00 | Matern | 0.03306607832442428 | 0.19393198924382904 | 31238.71901466519 |
| 09 | 28 | 05 | 00 | Gaussian | 0.03236127855193611 | 0.35056143729623046 | 29953.84522426406 |
| 09 | 28 | 06 | 00 | Matern | 0.06819458728601557 | 0.4491921424166789 | 26528.689068019063 |
| 09 | 28 | 07 | 00 | Matern | 0.01671164666017482 | 0.14784323789867998 | 38078.07251212748 |
| 09 | 28 | 08 | 00 | Matern | 0.0012884140785773314 | 19.98225954135552 | 3136688.767392331 |
| 09 | 28 | 09 | 00 | Matern | 0.002119033174942321 | 791.9762325226757 | 80356844.69258845 |
| 09 | 28 | 10 | 00 | Matern | 0.06892093544632329 | 2966.793448172426 | 33722936.13612171 |
| 09 | 28 | 11 | 00 | Matern | 0.06626116381908818 | 2.2694644794386085 | 165727.88195987142 |
| 09 | 28 | 12 | 00 | Matern | 0.019353009146067513 | 1.1724973864362336 | 76745.98294216984 |
| 09 | 28 | 13 | 00 | Gaussian | 0.1519583136034309 | 3.8597236092848806 | 21249.46653496912 |
| 09 | 28 | 14 | 00 | Matern | 0.36199167482996386 | 9.995331023853732 | 15809.910957321848 |
| 09 | 28 | 15 | 00 | Gaussian | 6.0216583937126105 | 15.4034896970057 | 22878.622290873052 |
| 09 | 28 | 16 | 00 | Matern | 0.6124873646927357 | 5.823654041642802 | 12566.553198577454 |
| 09 | 28 | 17 | 00 | Spherical | 0.776515890554948 | 1.5383075406471174 | 10674.884859106256 |
| 09 | 28 | 18 | 00 | Gaussian | 0.003956115140258215 | 0.6919656782642476 | 151539.47081404965 |
| 09 | 28 | 19 | 00 | Matern | 0.03695381758233472 | 68.0792512066363 | 17669810.16785989 |
| 09 | 28 | 20 | 00 | Matern | 0 | 13.648290275664994 | 6793004.882077542 |
| 09 | 28 | 21 | 00 | Matern | 0.01741862354539654 | 15.16577075779546 | 11812979.436817253 |
| 09 | 28 | 22 | 00 | Spherical | 0.1505216122630336 | 1.162729988745398 | 154407.41683988133 |
| 09 | 28 | 23 | 00 | Spherical | 0 | 3.229528828091309 | 109194.91711944576 |
| 09 | 28 | 02 | 30 | Gaussian | 0.052667372916975326 | 0.30538595247153294 | 19829.31450280889 |
| 09 | 28 | 03 | 30 | Matern | 0.01305485392915241 | 0.2286596428426926 | 25929.25219447974 |
| 09 | 28 | 04 | 30 | Spherical | 0.027489598616339376 | 0.38906867485500957 | 49751.0019271802 |
| 09 | 28 | 05 | 30 | Gaussian | 0.06219006908367282 | 0.40043490922633845 | 24008.68065390396 |
| 09 | 28 | 06 | 30 | Matern | 0.05484150177738929 | 0.31613986711705266 | 27800.269302920835 |
| 09 | 28 | 07 | 30 | Matern | 0.0013591672724357132 | 1614.3039045145101 | 118161364.48552665 |
| 09 | 28 | 08 | 30 | Matern | 0.0011448726290669774 | 16.85552836271548 | 2623822.2208525026 |
| 09 | 28 | 09 | 30 | Matern | 0.025299481402382647 | 154.4381289415854 | 30568011.432085518 |
| 09 | 28 | 10 | 30 | Matern | 0.020913744605647894 | 37.053784094099086 | 2126301.1458304687 |
| 09 | 28 | 11 | 30 | Matern | 0.028319538405041027 | 2.423186753949613 | 201243.32429680682 |
| 09 | 28 | 12 | 30 | Matern | 0.0016210030746500472 | 1.3110389722762241 | 57375.04233093868 |
| 09 | 28 | 13 | 30 | Gaussian | 0.3131525229759112 | 5.6802781128668 | 19354.86705068909 |
| 09 | 28 | 14 | 30 | Matern | 0.39048789443549775 | 12.276423966874665 | 10006.704794061841 |
| 09 | 28 | 15 | 30 | Matern | 0 | 13.542199778054679 | 16895.7737591166 |
| 09 | 28 | 16 | 30 | Matern | 2.605143760765631 | 4.1037032154010085 | 4421.204976224167 |
| 09 | 28 | 17 | 30 | Matern | 0 | 0.38708840038331305 | 98300.11057611625 |
| 09 | 28 | 18 | 30 | Matern | 0.02395287049233408 | 0.764913800616055 | 114166.44917910978 |
| 09 | 28 | 19 | 30 | Matern | 0.0683725611182541 | 64.62077184314333 | 14334723.214746084 |
| 09 | 28 | 20 | 30 | Matern | 0.03915281845707544 | 51.22396736256926 | 19773997.060638156 |
| 09 | 28 | 21 | 30 | Matern | 0.11711922264151886 | 1.6173690078001544 | 81741.2687503644 |
| 09 | 28 | 22 | 30 | Matern | 0.08337642682727686 | 2.4619622935927836 | 43277.405863729095 |
| 09 | 28 | 23 | 30 | Gaussian | 0.048928312802281756 | 3.2270253844048478 | 53163.779746889006 |

| | | | | | | | |
|---|---|---|---|---|---|---|---|
| 09 | 29 | 00 | 00 | Matern | 0.03730469119608989 | 1.2989440854884537 | 39937.816831169235 |
| 09 | 29 | 01 | 00 | Matern | 0.08225583612121481 | 1.1894832111692393 | 87558.49921801468 |
| 09 | 29 | 02 | 00 | Matern | 0.07030445309257932 | 1987413.682669369 | 905578187.9751499 |
| 09 | 29 | 03 | 00 | Matern | 0.010689402697721114 | 2274.169165481115 | 207098846.08526778 |
| 09 | 29 | 04 | 00 | Matern | 0.009078174287234494 | 1.7002035217904417 | 288698.92243425635 |
| 09 | 29 | 05 | 00 | Matern | 0.01604754360196256 | 0.933864665321227 | 47461.0389270102 |
| 09 | 29 | 06 | 00 | Matern | 0.02008672655858285 | 0.9408199348758729 | 41389.16377075334 |
| 09 | 29 | 07 | 00 | Matern | 0.01745381006528882 | 0.6796235189134205 | 39703.916193196135 |
| 09 | 29 | 08 | 00 | Matern | 0.00525284472271006 | 0.3726648103437292 | 32682.968350898485 |
| 09 | 29 | 13 | 00 | Gaussian | 3.0850127249571765e-4 | 0.09875429019339262 | 72139.20795746484 |
| 09 | 29 | 14 | 00 | Gaussian | 0.016160459128989 | 0.9597666254227208 | 62633.197282184534 |
| 09 | 29 | 15 | 00 | Gaussian | 0.03901375333808988 | 1.1463106611824148 | 62543.91983456337 |
| 09 | 29 | 17 | 00 | Gaussian | 0.04163684334359011 | 8.319018866027935 | 12036.76112560767 |
| 09 | 29 | 18 | 00 | Matern | 0.09601158506275546 | 3.4819199002656163 | 29865.206237534905 |
| 09 | 29 | 19 | 00 | Gaussian | 0.024868279465160993 | 3.7718406314487924 | 61963.996788529 |
| 09 | 29 | 20 | 00 | Matern | 0.0011624465339015765 | 3.6775693640933182 | 115772.22486917097 |
| 09 | 29 | 21 | 00 | Matern | 0.03909205132026278 | 4.014063596304025 | 93854.95716118174 |
| 09 | 29 | 22 | 00 | Matern | 0.04701007425023849 | 3.6493266554201536 | 74155.24036102746 |
| 09 | 29 | 23 | 00 | Matern | 0.11962534541991925 | 3.864721474659424 | 109345.13186136089 |
| 09 | 29 | 00 | 30 | Matern | 0.030126581557406586 | 0.774125926379661 | 34133.068386631334 |
| 09 | 29 | 01 | 30 | Matern | 0.011525786506879746 | 111.14825289474975 | 26609698.844714712 |
| 09 | 29 | 02 | 30 | Matern | 0.044515060943364326 | 1442.6170772662292 | 60367731.542484656 |
| 09 | 29 | 03 | 30 | Matern | 0.016820914321482555 | 3.2966020130757543 | 552277.5156747338 |
| 09 | 29 | 04 | 30 | Matern | 0.03212576497871141 | 1.1726558175561999 | 99119.33483315028 |
| 09 | 29 | 05 | 30 | Matern | 0.016032821159616902 | 0.9082452888941321 | 42060.477935808485 |
| 09 | 29 | 06 | 30 | Gaussian | 0.015550194128379264 | 0.7420541031385341 | 67794.267356361 |
| 09 | 29 | 07 | 30 | Matern | 0.01322106173284186 | 0.46621404034443437 | 32476.211593859385 |
| 09 | 29 | 08 | 30 | Matern | 0.008672257378281173 | 0.164933676609855 | 34443.44893025911 |
| 09 | 29 | 13 | 30 | Gaussian | 0.0037807997964972085 | 0.32766924453986573 | 65247.65579186342 |
| 09 | 29 | 14 | 30 | Gaussian | 0.021277651289089955 | 1.343842169836974 | 62820.59940891542 |
| 09 | 29 | 15 | 30 | Matern | 0.01010846321096629 | 0.5110330170220139 | 35488.01248168992 |
| 09 | 29 | 17 | 30 | Gaussian | 0.33395066646583005 | 6.384071456202847 | 17517.724064706093 |
| 09 | 29 | 18 | 30 | Gaussian | 0.02561149325570769 | 5.061360131145913 | 67688.72720896048 |
| 09 | 29 | 19 | 30 | Matern | 0.019651270484279382 | 4.34521709804637 | 109037.29807498273 |
| 09 | 29 | 20 | 30 | Matern | 0.007550752733392669 | 3.7950272127621556 | 116157.97166269734 |
| 09 | 29 | 21 | 30 | Matern | 0.010384381582005713 | 3.7291922208225925 | 95440.19141055107 |
| 09 | 29 | 22 | 30 | Matern | 0.05067747466042634 | 4.456989345841006 | 77644.17836693375 |
| 09 | 29 | 23 | 30 | Matern | 0.11661438777818259 | 4.190383888800171 | 311436.7730204485 |
| 09 | 30 | 00 | 00 | Matern | 0.03738134991783178 | 57.22981548358988 | 137010598.41537315 |
| 09 | 30 | 01 | 00 | Gaussian | 7.367352865522093e-5 | 0.3220417084882015 | 84422.86405384367 |
| 09 | 30 | 10 | 00 | Matern | 6.217485560434744e-4 | 12.167901517369176 | 1723697.5722930708 |
| 09 | 30 | 11 | 00 | Matern | 5.248621397548217e-4 | 0.8355053283462545 | 224235.0445815155 |
| 09 | 30 | 12 | 00 | Matern | 0.0024150113122426912 | 0.37804795260547924 | 57863.648899189466 |
| 09 | 30 | 13 | 00 | Matern | 0.012019758327289624 | 0.8268635496666803 | 38879.783880372284 |
| 09 | 30 | 15 | 00 | Gaussian | 0.4124776050753226 | 4.760138021425107 | 14730.460039985413 |
| 09 | 30 | 16 | 00 | Spherical | 1.204833145073028 | 8.151786308909763 | 18552.833515034654 |
| 09 | 30 | 17 | 00 | Spherical | 2.024571766729958 | 5.837214647255413 | 23188.30957990148 |

| | | | | | | | |
|---|---|---|---|---|---|---|---|
| 09 | 30 | 18 | 00 | Matern | 0.17934094355799882 | 6.854910863904765 | 75455.5861464124 |
| 09 | 30 | 19 | 00 | Matern | 3.608224395437469 | 6.513968911282317 | 49496.75476168134 |
| 09 | 30 | 20 | 00 | Matern | 0 | 4.505752333359115 | 3472.9857250550717 |
| 09 | 30 | 21 | 00 | Gaussian | 3.2597365154744904 | 3.2597365154744904 | 52048.29657395149 |
| 09 | 30 | 22 | 00 | Matern | 0 | 0.5871182661249729 | 1748.1549149507484 |
| 09 | 30 | 00 | 30 | Matern | 0.1383122844163948 | 0.9470044045014334 | 130911.15581579352 |
| 09 | 30 | 01 | 30 | Matern | 0.017365381866653182 | 0.06832690792567286 | 164352.37571909244 |
| 09 | 30 | 10 | 30 | Matern | 7.393091747334054e-4 | 4253.262373335592 | 38247054.79414531 |
| 09 | 30 | 12 | 30 | Matern | 0.009785962914284026 | 1.0138688540882372 | 48813.3238726512 |
| 09 | 30 | 13 | 30 | Matern | 0.018588956351191416 | 2.08992302336551 | 13785.214930735881 |
| 09 | 30 | 15 | 30 | Spherical | 1.1144763335130188 | 7.725750166697938 | 14038.298350486553 |
| 09 | 30 | 16 | 30 | Spherical | 0.25737824890733035 | 7.887029335111917 | 19124.541975796557 |
| 09 | 30 | 17 | 30 | Gaussian | 1.7974921425530483 | 4.617236122488284 | 12840.292169191865 |
| 09 | 30 | 18 | 30 | Matern | 1.2349097604467827 | 8.810126651222058 | 268894.14144961553 |
| 09 | 30 | 19 | 30 | Matern | 2.98872185814467 | 5.9296879558051305 | 60075.81705401792 |
| 09 | 30 | 20 | 30 | Gaussian | 3.5194541076065486 | 3.9100953535519754 | 7362.554057054762 |
| 09 | 30 | 21 | 30 | Matern | 0 | 1.7723890241166826 | 1705.0598006186872 |
| 10 | 01 | 01 | 00 | Matern | 5.4612163481340646e-5 | 0.08503270932884581 | 134376.3950659847 |
| 10 | 01 | 05 | 00 | Gaussian | 0.023758905638433574 | 0.07182715753659082 | 22295.888260045234 |
| 10 | 01 | 06 | 00 | Matern | 0.052930751917485454 | 0.15334864278154597 | 21527.387189052213 |
| 10 | 01 | 10 | 00 | Matern | 0.031028775311748285 | 0.031028775311748285 | 52048.29657395149 |
| 10 | 01 | 11 | 00 | Spherical | 0.050225715755139365 | 0.2566797345612427 | 15158.66313098858 |
| 10 | 01 | 12 | 00 | Spherical | 0.032287009384978735 | 0.21157530735190422 | 8465.506908270068 |
| 10 | 01 | 13 | 00 | Gaussian | 0.03716080238290754 | 0.4791437008110319 | 46757.66779513139 |
| 10 | 01 | 14 | 00 | Gaussian | 0.12450069812514086 | 2.634868051247932 | 39000.71354009104 |
| 10 | 01 | 15 | 00 | Gaussian | 2.361663542158582 | 8.275613737021768 | 11587.597219823705 |
| 10 | 01 | 16 | 00 | Gaussian | 0.4768108266919377 | 7.278315863679024 | 16271.809223293247 |
| 10 | 01 | 17 | 00 | Matern | 0.04537283486088378 | 4.819427384127921 | 44774.84283423693 |
| 10 | 01 | 18 | 00 | Matern | 2.0064868399015583 | 14.854189140491632 | 6243.954109838663 |
| 10 | 01 | 19 | 00 | Matern | 2.1601469824750335 | 9.27359550679722 | 4932.220249920076 |
| 10 | 01 | 20 | 00 | Gaussian | 0.22145259575072823 | 4.296587004860873 | 24885.522189929543 |
| 10 | 01 | 21 | 00 | Matern | 0.02926728808848971 | 0.8072461668728843 | 41546.35882858289 |
| 10 | 01 | 22 | 00 | Gaussian | 0.030285415674182355 | 1.1581506949547151 | 37956.87584807961 |
| 10 | 01 | 23 | 00 | Matern | 0.0023294721598577685 | 0.6615417076950645 | 30726.268078653266 |
| 10 | 01 | 05 | 30 | Gaussian | 0.05249897112591672 | 0.14916534553959693 | 24413.074514746713 |
| 10 | 01 | 10 | 30 | Gaussian | 0.0036891668960675663 | 0.17679642871913515 | 11610.991568812533 |
| 10 | 01 | 12 | 30 | Spherical | 0.007255712867116669 | 0.11099586661599804 | 101815.4892352959 |
| 10 | 01 | 13 | 30 | Gaussian | 0.08747110194945223 | 1.3769319942810287 | 37779.465766295994 |
| 10 | 01 | 14 | 30 | Gaussian | 0.26496294030670275 | 4.272514330220983 | 15373.291944931949 |
| 10 | 01 | 15 | 30 | Gaussian | 2.210824021199471 | 10.381209312572281 | 14439.53687919155 |
| 10 | 01 | 16 | 30 | Gaussian | 0.17485489576250018 | 5.272958269894925 | 26175.039886662253 |
| 10 | 01 | 17 | 30 | Gaussian | 0 | 7.444914096036645 | 2479.2613742935737 |
| 10 | 01 | 18 | 30 | Matern | 1.1566274594290487 | 11.557002652918364 | 5170.1692759700745 |
| 10 | 01 | 19 | 30 | Spherical | 1.4748352378202543 | 4.998559824188108 | 48903.28093121271 |
| 10 | 01 | 20 | 30 | Matern | 0.30662761262049887 | 2.000628962648215 | 17053.893365808555 |
| 10 | 01 | 21 | 30 | Gaussian | 0.013080473947724401 | 0.8800549034759351 | 42508.20611831988 |
| 10 | 01 | 22 | 30 | Matern | 0.009122334315478648 | 1.0456963912925754 | 31384.363272739305 |

| | | | | | | | |
|---|---|---|---|---|---|---|---|
| 10 | 01 | 23 | 30 | Spherical | 8.869934961079877e-4 | 0.07005512873065997 | 85894.57605431722 |
| 10 | 02 | 04 | 00 | Matern | 0 | 0.1839225411592642 | 84895.9749278011 |
| 10 | 02 | 05 | 00 | Matern | 0.0319890008990418 | 0.5414795699279694 | 200159.3361971751 |
| 10 | 02 | 06 | 00 | Exponential | 0.012869546183576061 | 16.133728698255723 | 5211554.451119574 |
| 10 | 02 | 15 | 00 | Matern | 0.0019506776147396746 | 0.2898860396298925 | 69344.9997486739 |
| 10 | 02 | 16 | 00 | Gaussian | 0.002958095881377676 | 0.4464352375259863 | 45765.694981957924 |
| 10 | 02 | 17 | 00 | Matern | 0 | 1.4884408666082152 | 259316.28796658493 |
| 10 | 02 | 23 | 00 | Matern | 0.0020130504870459103 | 0.1777633856824915 | 50869.662939294256 |
| 10 | 02 | 04 | 30 | Matern | 0.0020201453295419724 | 0.3655847307471977 | 126866.55721699509 |
| 10 | 02 | 05 | 30 | Matern | 0.018923576915543645 | 2.9549249140662193 | 1096040.2483584422 |
| 10 | 02 | 06 | 30 | Matern | 0.026366448161834272 | 1.0254692914371215 | 528124.4723039669 |
| 10 | 02 | 14 | 30 | Matern | 0.001111800912423838 | 0.08795566572836772 | 72284.53252760648 |
| 10 | 02 | 16 | 30 | Exponential | 0.0010910147594610114 | 126.81921556237461 | 55908371.26904817 |
| 10 | 02 | 17 | 30 | Matern | 0 | 0.9808417889127622 | 193922.70688851128 |
| 10 | 02 | 22 | 30 | Matern | 0.0023735980777019666 | 0.1629085237238696 | 52743.742670618994 |
| 10 | 03 | 04 | 00 | Matern | 0.17846154507158724 | 0.778267617372042 | 30832.702236030975 |
| 10 | 03 | 05 | 00 | Matern | 0.1581584719739962 | 0.7171062865910588 | 27176.069286727183 |
| 10 | 03 | 06 | 00 | Gaussian | 0.13975729121112276 | 0.6004549367117432 | 22753.947125590672 |
| 10 | 03 | 07 | 00 | Matern | 0.11178228910811637 | 0.18711534295605847 | 35608.078288280536 |
| 10 | 03 | 11 | 00 | Matern | 0.00222606295768361 | 1.4997637679875904 | 203660.38503168646 |
| 10 | 03 | 12 | 00 | Matern | 0 | 1.3901373117672682 | 224554.5817400517 |
| 10 | 03 | 13 | 00 | Matern | 0.2555006296289448 | 1.5999781201114989 | 63399.49749482975 |
| 10 | 03 | 14 | 00 | Matern | 0.2039224069479943 | 2.4677947921719796 | 16089.69759408667 |
| 10 | 03 | 15 | 00 | Matern | 0.10054107914630826 | 2.556601336777682 | 21545.191622262475 |
| 10 | 03 | 16 | 00 | Gaussian | 0.677787886946088 | 7.455549187859541 | 32769.572219712325 |
| 10 | 03 | 17 | 00 | Matern | 1.0894271464737901 | 6.025482513694104 | 21776.580096941332 |
| 10 | 03 | 18 | 00 | Spherical | 0.7241983682243712 | 4.077313106624795 | 15717.790313559906 |
| 10 | 03 | 19 | 00 | Matern | 1.7288606203826136 | 2.510876821559111 | 2727.2232739161927 |
| 10 | 03 | 20 | 00 | Gaussian | 0.25289433330336436 | 2.1985025292836453 | 36568.544570309416 |
| 10 | 03 | 21 | 00 | Matern | 0.2511183612927385 | 1.7731234155619984 | 35161.99282182603 |
| 10 | 03 | 22 | 00 | Gaussian | 0.013732164894994167 | 2.323684806133842 | 17051.228404768823 |
| 10 | 03 | 23 | 00 | Gaussian | 0.16215195888693545 | 1.0956337679982306 | 18544.838643281582 |
| 10 | 03 | 04 | 30 | Gaussian | 0.18319817969788643 | 0.8000133629510813 | 29209.459481706475 |
| 10 | 03 | 05 | 30 | Gaussian | 0.1480685200232457 | 0.7233305423694316 | 27319.011391051263 |
| 10 | 03 | 06 | 30 | Matern | 0.1766247143257712 | 0.43014541278438473 | 26108.66673317192 |
| 10 | 03 | 10 | 30 | Matern | 0.09426379842994961 | 204.33794809869792 | 3766673.0658678645 |
| 10 | 03 | 12 | 30 | Matern | 0.00992078356866224 | 1.7559602987325638 | 80261.31487694012 |
| 10 | 03 | 13 | 30 | Matern | 0.21951521217002326 | 1.5346471433372357 | 21306.3432543901 |
| 10 | 03 | 14 | 30 | Matern | 0.19386069537311668 | 3.899864838661116 | 25671.651566003642 |
| 10 | 03 | 15 | 30 | Matern | 0.8883956836774942 | 4.7659900060384235 | 23221.74106104229 |
| 10 | 03 | 16 | 30 | Gaussian | 1.2103807505405093 | 7.6745305889751485 | 36625.43941388414 |
| 10 | 03 | 17 | 30 | Matern | 1.2709647987433412 | 5.855609999717645 | 11642.130813512658 |
| 10 | 03 | 18 | 30 | Matern | 1.118105419885747 | 4.237168607438296 | 12340.332797700634 |
| 10 | 03 | 19 | 30 | Matern | 0.3212764272046553 | 2.0911597313006407 | 43831.55712637539 |
| 10 | 03 | 20 | 30 | Gaussian | 0.25268100883654854 | 2.4005291271109224 | 42709.700105109536 |
| 10 | 03 | 21 | 30 | Gaussian | 0.29447453937764534 | 1.1360852549791152 | 19586.55532955081 |
| 10 | 03 | 22 | 30 | Gaussian | 0.012039504507416223 | 2.251764313346663 | 17365.258281249022 |

| | | | | | | | |
|---|---|---|---|---|---|---|---|
| 10 | 03 | 23 | 30 | Spherical | 0 | 0.16000047157067165 | 51162.04741286561 |
| 10 | 04 | 00 | 00 | Gaussian | 0 | 0.8250351521165215 | 36069.75569867342 |
| 10 | 04 | 01 | 00 | Gaussian | 0.3467412886953562 | 0.5760871178868328 | 7723.016501899176 |
| 10 | 04 | 02 | 00 | Spherical | 0 | 2.875094890428795 | 8610.59747662315 |
| 10 | 04 | 12 | 00 | Matern | 0.16497779507081797 | 1.3613543674894748 | 45612.19524070163 |
| 10 | 04 | 13 | 00 | Matern | 0 | 0.5524973730650767 | 27162.70838717049 |
| 10 | 04 | 14 | 00 | Gaussian | 0 | 0.0691267633223854 | 17641.172105833473 |
| 10 | 04 | 15 | 00 | Gaussian | 0.1633104680258894 | 0.8988706973717595 | 27348.568473574614 |
| 10 | 04 | 16 | 00 | Gaussian | 0.10902159964581463 | 2.576214133467704 | 31118.988712979255 |
| 10 | 04 | 17 | 00 | Matern | 0.1907056212183338 | 3.48218646628926 | 41815.656951335295 |
| 10 | 04 | 18 | 00 | Matern | 0.3170344805433747 | 2.1835864732077925 | 43483.22010969567 |
| 10 | 04 | 19 | 00 | Matern | 0 | 3.5099603494915566 | 85335.31389829465 |
| 10 | 04 | 20 | 00 | Matern | 0.3695427468492504 | 1.3389756907053365 | 40514.8518042922 |
| 10 | 04 | 21 | 00 | Matern | 0.045350492435505305 | 0.6091077803666458 | 26516.622869353072 |
| 10 | 04 | 01 | 30 | Gaussian | 0 | 2.659208420886435 | 3419.968119210158 |
| 10 | 04 | 02 | 30 | Gaussian | 0 | 2.094338407474486 | 2789.733217857815 |
| 10 | 04 | 12 | 30 | Matern | 0.38314381941854275 | 1.4892314292681268 | 50231.815911923244 |
| 10 | 04 | 13 | 30 | Gaussian | 0.007190812753488348 | 0.5008285849524331 | 19576.496145130663 |
| 10 | 04 | 14 | 30 | Matern | 0.09479660341490206 | 0.7014955706130916 | 37806.044572332816 |
| 10 | 04 | 15 | 30 | Gaussian | 0 | 2.941491395658371 | 27957.150257318695 |
| 10 | 04 | 16 | 30 | Matern | 0.27825665989856363 | 2.7929513024762267 | 25050.374092148068 |
| 10 | 04 | 17 | 30 | Matern | 0.22388363426201954 | 3.0099548003728156 | 39790.792504767036 |
| 10 | 04 | 18 | 30 | Spherical | 0.45811337971839405 | 2.145638964444848 | 100930.40378028573 |
| 10 | 04 | 19 | 30 | Spherical | 0.1290407179881433 | 2.3293050004154505 | 97009.8772704212 |
| 10 | 04 | 20 | 30 | Matern | 0.1399242341796242 | 1.1594017120832159 | 22816.389835192993 |
| 10 | 04 | 21 | 30 | Matern | 0 | 0.3114803692823429 | 48569.18087874378 |
| 10 | 04 | 22 | 30 | Gaussian | 0 | 0.3554335472057895 | 53741.30614207952 |
| 10 | 05 | 00 | 00 | Matern | 0 | 0.30452731682807055 | 8974.622987666082 |
| 10 | 05 | 12 | 00 | Matern | 0.0031136041603015154 | 0.2779042869775526 | 209148.2847117068 |
| 10 | 05 | 13 | 00 | Matern | 9.702445712155598e-5 | 0.19131130273961955 | 150039.7624014909 |
| 10 | 05 | 15 | 00 | Gaussian | 0.06894310097677499 | 1.9081918202866945 | 42183.22310707844 |
| 10 | 05 | 16 | 00 | Gaussian | 0.043826453866488375 | 4.877579928101031 | 41780.617322137376 |
| 10 | 05 | 17 | 00 | Gaussian | 0.015670590243719973 | 3.88075185918588 | 35475.64677015398 |
| 10 | 05 | 18 | 00 | Matern | 0.0031424598941389805 | 0.6134415209560956 | 73519.9422798123 |
| 10 | 05 | 19 | 00 | Gaussian | 0.0047525210331106306 | 0.7294286999201728 | 69884.89213218295 |
| 10 | 05 | 20 | 00 | Matern | 0 | 1.2910727900888632 | 397617.23919541336 |
| 10 | 05 | 21 | 00 | Matern | 0.0017892697598379228 | 0.15614381968029908 | 52334.39488021303 |
| 10 | 05 | 23 | 00 | Matern | 0.0015241516543392898 | 3.1494888837500845 | 1067026.557341073 |
| 10 | 05 | 13 | 30 | Matern | 0.005471380930438471 | 0.18643632945087052 | 65722.30549023529 |
| 10 | 05 | 14 | 30 | Matern | 0.008691868286224962 | 1.296776280445522 | 52373.535338345115 |
| 10 | 05 | 15 | 30 | Gaussian | 0.08979287953357609 | 4.102329301347668 | 37880.2176519321 |
| 10 | 05 | 16 | 30 | Gaussian | 0.017539312120375815 | 4.2559623236837725 | 37133.47256794912 |
| 10 | 05 | 17 | 30 | Gaussian | 0.009684516898237223 | 1.8374825552678036 | 43470.5388397648 |
| 10 | 05 | 18 | 30 | Matern | 0.0026291987637845245 | 0.5642011984226555 | 80919.54832374083 |
| 10 | 05 | 19 | 30 | Matern | 4.333682053674695e-4 | 0.7730237777173715 | 135373.34670625953 |
| 10 | 05 | 20 | 30 | Matern | 0.007944515014613907 | 0.34613191195847143 | 61345.307314858685 |
| 10 | 06 | 03 | 00 | Matern | 5.106106077348851e-4 | 0.7198712111265032 | 181800.4935431812 |

| | | | | | | | |
|---|---|---|---|---|---|---|---|
| 10 | 06 | 06 | 00 | Matern | 0.013634365521490546 | 29.38773243780946 | 6318082.904204048 |
| 10 | 06 | 07 | 00 | Matern | 0.019996216014357922 | 126.901920626954 | 38801326.34007088 |
| 10 | 06 | 08 | 00 | Matern | 0.003328092054356876 | 3.7978757768903315 | 3853263.829421897 |
| 10 | 06 | 12 | 00 | Gaussian | 0.008616222174300208 | 0.8095948087188155 | 20057.429671104786 |
| 10 | 06 | 13 | 00 | Gaussian | 0.09652992817512172 | 2.0106627463540874 | 21636.59753013755 |
| 10 | 06 | 14 | 00 | Gaussian | 8.101247173222236 | 8.101247173222236 | 52048.29657395149 |
| 10 | 06 | 15 | 00 | Matern | 0.22667653827878778 | 10.249335288137159 | 2769.341134101046 |
| 10 | 06 | 16 | 00 | Matern | 3.109334356778181 | 8.337071253163312 | 19989.00829672751 |
| 10 | 06 | 17 | 00 | Spherical | 2.586364913239018 | 6.549627163604024 | 47284.35542356578 |
| 10 | 06 | 18 | 00 | Spherical | 1.3667995269924467 | 6.087356452790269 | 75501.91631575735 |
| 10 | 06 | 19 | 00 | Gaussian | 0.9005865474502288 | 2.1146178717026762 | 74837.62323715974 |
| 10 | 06 | 20 | 00 | Gaussian | 0.009286589849233305 | 0.6932042542799949 | 71148.52470308663 |
| 10 | 06 | 02 | 30 | Matern | 6.124327079401268e-4 | 12.298310026092162 | 2172234.648359034 |
| 10 | 06 | 03 | 30 | Matern | 3.420390928442288e-5 | 0.3372560829731147 | 160046.294989769 |
| 10 | 06 | 05 | 30 | Gaussian | 0.001377911245535645 | 0.02209065766091241 | 56005.579501835826 |
| 10 | 06 | 06 | 30 | Matern | 0.01868104643529954 | 490.2148455103195 | 63388754.76310063 |
| 10 | 06 | 07 | 30 | Gaussian | 0.01705291437590056 | 2.4991033653528683 | 731896.1142446504 |
| 10 | 06 | 11 | 30 | Gaussian | 0.005414811572441987 | 0.2267857419321212 | 79214.84681131018 |
| 10 | 06 | 12 | 30 | Gaussian | 0.01567355946085592 | 1.1923659360538987 | 23041.604483234947 |
| 10 | 06 | 13 | 30 | Gaussian | 0.14088344970566782 | 3.35880223662179 | 16454.395734658574 |
| 10 | 06 | 14 | 30 | Matern | 0 | 16.010970273782554 | 2350.2959937633705 |
| 10 | 06 | 15 | 30 | Gaussian | 3.6695194932200916 | 8.87979358288317 | 13468.13463489468 |
| 10 | 06 | 16 | 30 | Spherical | 3.0635787325713015 | 7.057647014000574 | 67054.749130487 |
| 10 | 06 | 17 | 30 | Matern | 1.902383288989267 | 6.774946003555857 | 24287.906685589733 |
| 10 | 06 | 18 | 30 | Spherical | 1.096792485404977 | 3.965383715847393 | 85463.65888752829 |
| 10 | 06 | 19 | 30 | Gaussian | 0.014625370959134125 | 1.311897519541964 | 71279.61125185051 |
| 10 | 06 | 20 | 30 | Gaussian | 0.004069016750201505 | 0.0750847078116335 | 66358.77518878228 |
| 10 | 07 | 11 | 00 | Matern | 0 | 0.34857717876413524 | 3455.5736024510816 |
| 10 | 07 | 12 | 00 | Matern | 0 | 0.07522113283001611 | 1717.373414160682 |
| 10 | 07 | 13 | 00 | Matern | 0.008021717641193233 | 0.9901470456516831 | 112340.36215612489 |
| 10 | 07 | 14 | 00 | Gaussian | 0.01133137365797566 | 0.7993601419144676 | 109843.91666376685 |
| 10 | 07 | 15 | 00 | Gaussian | 0.018255903853262926 | 0.7677510784730027 | 47715.576648527924 |
| 10 | 07 | 16 | 00 | Matern | 0.03452483806404855 | 0.8142881102958158 | 60382.87944398114 |
| 10 | 07 | 17 | 00 | Matern | 0.10324546660426516 | 164.32146930949855 | 32282832.377283216 |
| 10 | 07 | 18 | 00 | Gaussian | 0.007509880478231326 | 1.4375780307971642 | 45279.34912076392 |
| 10 | 07 | 19 | 00 | Matern | 0.03240971798573126 | 1.9577128917073214 | 34178.47969470601 |
| 10 | 07 | 20 | 00 | Gaussian | 0.07922130298955202 | 4.069337386018671 | 12487.975314289471 |
| 10 | 07 | 22 | 00 | Matern | 0.21118187785212997 | 10.006224523661588 | 22037.918632621655 |
| 10 | 07 | 23 | 00 | Gaussian | 1.5994310478227107 | 8.513934773079436 | 13811.724074030566 |
| 10 | 07 | 10 | 30 | Spherical | 0.022868192621231426 | 0.11439222461931121 | 7677.990439298904 |
| 10 | 07 | 11 | 30 | Gaussian | 0 | 0.28766717600206776 | 2752.537821740809 |
| 10 | 07 | 12 | 30 | Matern | 0.0045300950351746935 | 0.6538838813250926 | 146936.97027375552 |
| 10 | 07 | 13 | 30 | Gaussian | 0.009644151475550141 | 0.6086920668702227 | 97199.71296349855 |
| 10 | 07 | 14 | 30 | Matern | 0.018513320640630247 | 0.8018599856638341 | 105705.76187605593 |
| 10 | 07 | 15 | 30 | Gaussian | 0.024683377109847044 | 0.800056388964287 | 47073.358646937144 |
| 10 | 07 | 16 | 30 | Exponential | 0.0724089585876409 | 5.987268328548921 | 394725.9208644823 |
| 10 | 07 | 17 | 30 | Gaussian | 0.030884486467236186 | 1.6348652532469945 | 42370.55548584835 |

| | | | | | | | |
|---|---|---|---|---|---|---|---|
| 10 | 07 | 18 | 30 | Matern | 0.014111524825344737 | 1.4518425262535053 | 42794.49372515608 |
| 10 | 07 | 19 | 30 | Matern | 0.05875375885239316 | 3.0700167777683807 | 22273.326987808523 |
| 10 | 07 | 20 | 30 | Gaussian | 0.01610128039180536 | 6.27664808066249 | 13074.448434996744 |
| 10 | 07 | 21 | 30 | Matern | 0.15371561093333033 | 10.829362810341872 | 3256.942317711059 |
| 10 | 07 | 22 | 30 | Matern | 1.383605160309046 | 10.689914767784776 | 15653.382711925675 |
| 10 | 07 | 23 | 30 | Matern | 0.27047767071347 | 5.745478010350533 | 2878.0679135807873 |
| 10 | 08 | 00 | 00 | Matern | 2.1422687988955604 | 3.0964042570543953 | 107278.06615067234 |
| 10 | 08 | 01 | 00 | Matern | 0.04964205232248133 | 1.4919386949957854 | 75633.93732171835 |
| 10 | 08 | 02 | 00 | Matern | 0.007066415544962833 | 0.9736859059721251 | 83917.9691135784 |
| 10 | 08 | 03 | 00 | Matern | 0.0037001814311360846 | 0.16551402163354825 | 60158.3635803329 |
| 10 | 08 | 06 | 00 | Gaussian | 2.3320562147541302e-4 | 0.18895553504965298 | 150433.23442592582 |
| 10 | 08 | 14 | 00 | Matern | 0.002537770846826123 | 0.2780779500387385 | 84818.5343015875 |
| 10 | 08 | 15 | 00 | Matern | 0.008385959613959831 | 0.5850812388533227 | 61935.88186524002 |
| 10 | 08 | 16 | 00 | Matern | 0.0564721116080921 | 1.3935465342847266 | 91506.03786569198 |
| 10 | 08 | 17 | 00 | Gaussian | 0.06139820698509251 | 2.0508485149665696 | 48099.818762677794 |
| 10 | 08 | 18 | 00 | Matern | 0.06368443532526695 | 2.8469501450943038 | 61382.824720132776 |
| 10 | 08 | 19 | 00 | Matern | 0.13914344728144085 | 3.016574475701205 | 54316.94048282731 |
| 10 | 08 | 22 | 00 | Matern | 0 | 0.12420381587591578 | 114666.96888744809 |
| 10 | 08 | 00 | 30 | Gaussian | 0.03229346237245713 | 2.1411096761548314 | 67902.62795441083 |
| 10 | 08 | 01 | 30 | Matern | 0.01651636932650616 | 1.197848008504054 | 72572.53332602956 |
| 10 | 08 | 02 | 30 | Matern | 0.004005298692957918 | 0.39082756669115115 | 73039.66767230043 |
| 10 | 08 | 05 | 30 | Matern | 0.003069828986786739 | 0.5347261897436348 | 156558.0290600224 |
| 10 | 08 | 14 | 30 | Matern | 0.0028385566406516167 | 0.4300665817204036 | 66735.04875390344 |
| 10 | 08 | 15 | 30 | Matern | 0.02142238450005122 | 0.39354038730254387 | 80987.68746018966 |
| 10 | 08 | 16 | 30 | Matern | 0.03509446834761933 | 2.9462211468093025 | 154356.6883375405 |
| 10 | 08 | 17 | 30 | Gaussian | 0.07224093583206127 | 1.9992261459466891 | 49551.2831139481 |
| 10 | 08 | 18 | 30 | Matern | 0.06956364181640558 | 3.3826833160694902 | 56687.816480737056 |
| 10 | 08 | 19 | 30 | Matern | 0.014978390980316643 | 1.2872354589576012 | 35994.48337662567 |
| 10 | 09 | 04 | 00 | Matern | 0 | 0.1311051267934963 | 130691.70568201205 |
| 10 | 09 | 15 | 00 | Gaussian | 0.00651440070261658 | 0.9617062159329863 | 70300.69311666056 |
| 10 | 09 | 16 | 00 | Gaussian | 0.04404436244930254 | 3.025191615819052 | 66319.37256327987 |
| 10 | 09 | 17 | 00 | Gaussian | 0.08469989277669769 | 5.095507385596119 | 50419.38858473455 |
| 10 | 09 | 18 | 00 | Matern | 0.08695281637182999 | 5.0334683661010695 | 61121.087792772305 |
| 10 | 09 | 19 | 00 | Gaussian | 0.04514508431092629 | 3.3660260942700364 | 57097.21941895934 |
| 10 | 09 | 20 | 00 | Gaussian | 0.016859070422960122 | 2.16347984133957 | 70956.06195388942 |
| 10 | 09 | 21 | 00 | Gaussian | 0.00807970057896903 | 0.6203186635089414 | 52040.146488553204 |
| 10 | 09 | 22 | 00 | Matern | 0.0011588446072687282 | 0.11043999659838631 | 35922.209392058336 |
| 10 | 09 | 03 | 30 | Matern | 0 | 0.09364274649814311 | 134964.924075583 |
| 10 | 09 | 04 | 30 | Matern | 0.0014733253006746075 | 0.10273221004972426 | 91652.47765086596 |
| 10 | 09 | 15 | 30 | Gaussian | 0.019916745839140014 | 2.2804158700508212 | 67137.53569921125 |
| 10 | 09 | 16 | 30 | Gaussian | 0.06680533992961533 | 4.413810008855386 | 61918.64229805003 |
| 10 | 09 | 17 | 30 | Gaussian | 0.07975830434592535 | 4.561264922835645 | 46903.60995428759 |
| 10 | 09 | 18 | 30 | Matern | 0.05026221848733997 | 4.643038228391191 | 63512.98217179856 |
| 10 | 09 | 19 | 30 | Gaussian | 0.03307001413062904 | 2.3482322922910677 | 66623.17024566531 |
| 10 | 09 | 20 | 30 | Gaussian | 0.01929891581077417 | 1.1626843630917247 | 63294.02537770159 |
| 10 | 09 | 21 | 30 | Gaussian | 0.00739889446606217 | 0.33522384484376183 | 49657.30133291504 |
| 10 | 10 | 00 | 00 | Matern | 0.0031260142874698026 | 0.09084811255903093 | 149913.05954722853 |

| | | | | | | | |
|---|---|---|---|---|---|---|---|
| 10 | 10 | 01 | 00 | Matern | 0 | 0.08810687099993061 | 87355.77554557884 |
| 10 | 10 | 07 | 00 | Matern | 9.50977252674178e-4 | 2.7739470141381695 | 1059682.9129973312 |
| 10 | 10 | 13 | 00 | Matern | 0.004284530409747536 | 0.09858218384153794 | 68138.3595060519 |
| 10 | 10 | 14 | 00 | Gaussian | 0.035663292239887213 | 0.7701353731210122 | 77899.87553349443 |
| 10 | 10 | 15 | 00 | Matern | 0.03392944526415513 | 1.8497626621025023 | 73755.8806695633 |
| 10 | 10 | 16 | 00 | Matern | 0.010524885289314917 | 4.991786606202403 | 264005.8689654208 |
| 10 | 10 | 17 | 00 | Matern | 0.03812300486626516 | 4.374281560426433 | 87364.54772884776 |
| 10 | 10 | 18 | 00 | Gaussian | 0.03810934451248594 | 1.679437092809841 | 42781.85556875126 |
| 10 | 10 | 19 | 00 | Gaussian | 0.009300974202768873 | 1.479289274572385 | 49147.444535270355 |
| 10 | 10 | 20 | 00 | Gaussian | 0.010881624461403358 | 1.6695170323599522 | 49043.41887177317 |
| 10 | 10 | 21 | 00 | Gaussian | 0.035817246476773625 | 1.3348068431005922 | 58899.30214795914 |
| 10 | 10 | 22 | 00 | Matern | 0.0010995385289018205 | 0.1747669511483776 | 88526.32086031149 |
| 10 | 10 | 01 | 30 | Matern | 1.2926746685423063e-5 | 0.1927577856425212 | 51174.04430695313 |
| 10 | 10 | 12 | 30 | Spherical | 0 | 0.0358146439381715 | 164762.36876205727 |
| 10 | 10 | 13 | 30 | Gaussian | 0.009858031469860841 | 0.36424339827232266 | 69411.27976251369 |
| 10 | 10 | 14 | 30 | Matern | 0 | 1.1405161422542356 | 54819.35245139265 |
| 10 | 10 | 15 | 30 | Matern | 0.08050731875838495 | 3.832640208538973 | 231942.29744968837 |
| 10 | 10 | 16 | 30 | Matern | 0.024697318712252232 | 3.496550108211922 | 98953.64270819779 |
| 10 | 10 | 17 | 30 | Matern | 0.060216016460799555 | 3.163123214534251 | 40182.745742786086 |
| 10 | 10 | 19 | 30 | Gaussian | 0.00347984582334931 | 2.1230531311434118 | 52565.11999379165 |
| 10 | 10 | 20 | 30 | Matern | 0.05389914225611267 | 1.6879075759755704 | 46735.89759267305 |
| 10 | 10 | 21 | 30 | Matern | 0.008825397943529652 | 0.30145922345100623 | 62786.45630179834 |
| 10 | 11 | 01 | 00 | Matern | 0.005998958260373808 | 0.2875483417477372 | 94656.82051207441 |
| 10 | 11 | 02 | 00 | Matern | 0.011280723990768049 | 0.7330243136679316 | 133391.9513542718 |
| 10 | 11 | 03 | 00 | Gaussian | 0.007487271083472704 | 0.6919698892648347 | 110831.6797628374 |
| 10 | 11 | 04 | 00 | Matern | 0.00888970496094999 | 0.26808502861179273 | 112747.15024659885 |
| 10 | 11 | 05 | 00 | Matern | 0.03543104773858028 | 0.31845152842472335 | 162781.58680457485 |
| 10 | 11 | 06 | 00 | Spherical | 0.0311417773767313 | 0.11507781712962345 | 8866.662775713961 |
| 10 | 11 | 07 | 00 | Spherical | 3.519748433990559e-4 | 0.5092230129582836 | 2821992.5465808185 |
| 10 | 11 | 09 | 00 | Gaussian | 4.633475830560147e-4 | 0.06974213290063994 | 77215.11288720595 |
| 10 | 11 | 10 | 00 | Matern | 0.007882451049244333 | 2.7168896517124757 | 1448475.7325023653 |
| 10 | 11 | 11 | 00 | Matern | 0.06977753334042554 | 0.5392741349758244 | 9661.660038576387 |
| 10 | 11 | 12 | 00 | Gaussian | 0.33782524830669836 | 1.5369210038060754 | 13317.754207576018 |
| 10 | 11 | 13 | 00 | Matern | 0.2093646174668126 | 5.44318358890774 | 17585.576255895605 |
| 10 | 11 | 15 | 00 | Gaussian | 0.218872179119834 | 6.432489177230399 | 28045.516337145484 |
| 10 | 11 | 16 | 00 | Matern | 0.7440688670333689 | 4.561386020448963 | 17291.873172705382 |
| 10 | 11 | 17 | 00 | Matern | 2.7701782711474663 | 4.160043460459094 | 4974.467232406958 |
| 10 | 11 | 18 | 00 | Gaussian | 2.9907283929555346 | 3.172837615581098 | 4711.535426862839 |
| 10 | 11 | 19 | 00 | Spherical | 0.5416488612758014 | 1.0115717912346032 | 10344.400941970473 |
| 10 | 11 | 20 | 00 | Spherical | 1.0488267339027622 | 1.4923462942272123 | 8224.947380279993 |
| 10 | 11 | 21 | 00 | Matern | 0.0020393915735193264 | 0.6041897453799164 | 91604.25095256322 |
| 10 | 11 | 22 | 00 | Matern | 0.003958034628651865 | 0.4823176185006949 | 84981.49407927206 |
| 10 | 11 | 23 | 00 | Matern | 0.0088900540075293 | 0.379814581338208 | 128461.13450317652 |
| 10 | 11 | 01 | 30 | Gaussian | 0.015567561696061338 | 0.6281021106056578 | 131864.48361797558 |
| 10 | 11 | 02 | 30 | Gaussian | 0.013343758203796885 | 0.5856399088344793 | 96221.54608066624 |
| 10 | 11 | 03 | 30 | Gaussian | 0.011053899965466766 | 0.5052251980286181 | 105189.42626863447 |
| 10 | 11 | 04 | 30 | Matern | 0.0016874971248946266 | 0.3088393364730095 | 122247.189433521 |

# A | Additional figures

| | | | | | | | |
|---|---|---|---|---|---|---|---|
| 10 | 11 | 05 | 30 | Spherical | 0.016379387108926412 | 0.0911226608562628 | 6348.145767311208 |
| 10 | 11 | 06 | 30 | Matern | 0.005740496864243756 | 0.17073436887857735 | 142540.79439672772 |
| 10 | 11 | 09 | 30 | Gaussian | 8.108593764491531e-4 | 0.10786295074525964 | 98830.6576045069 |
| 10 | 11 | 10 | 30 | Spherical | 0.01777863562215222 | 1.5840108505156318 | 600739.7911597666 |
| 10 | 11 | 11 | 30 | Matern | 0.15138887329891945 | 1.0395841075215293 | 12838.140860762658 |
| 10 | 11 | 12 | 30 | Gaussian | 0.26665554468711733 | 2.5710378719468476 | 14106.067006545332 |
| 10 | 11 | 13 | 30 | Gaussian | 0.06554171042623838 | 6.7160738474556 | 19581.52393570643 |
| 10 | 11 | 14 | 30 | Gaussian | 0.14335765977985584 | 6.381383056882307 | 28047.95935028272 |
| 10 | 11 | 15 | 30 | Matern | 0.29197028250467594 | 5.77021819413312 | 21382.68011253194 |
| 10 | 11 | 16 | 30 | Gaussian | 1.2332299628019385 | 4.4815932287232485 | 10271.723429269372 |
| 10 | 11 | 17 | 30 | Matern | 3.453625039376253 | 4.308962122573776 | 15323.415034582858 |
| 10 | 11 | 18 | 30 | Spherical | 1.4486126786571916 | 1.832927946150788 | 9042.238319301727 |
| 10 | 11 | 19 | 30 | Matern | 0.6696718980848294 | 1.1735609343358022 | 5295.813174665491 |
| 10 | 11 | 20 | 30 | Spherical | 0.7485857556735938 | 1.2252637260585555 | 8888.088117377829 |
| 10 | 11 | 21 | 30 | Gaussian | 0.009337479659576667 | 0.44063910403241574 | 79983.07199613194 |
| 10 | 11 | 23 | 30 | Matern | 0.009158012036774205 | 10.427866797385935 | 2406848.0288290596 |
| 10 | 12 | 04 | 00 | Matern | 1.5383989584127233e-4 | 0.1041007950111921 | 115004.51571237114 |
| 10 | 12 | 12 | 00 | Spherical | 0.048847001109433213 | 0.2096203912933588 | 12461.543993343868 |
| 10 | 12 | 13 | 00 | Matern | 0.06761875628383035 | 0.4046659316551184 | 108374.95559263333 |
| 10 | 12 | 14 | 00 | Matern | 0.022483010143495512 | 1.3454109122954425 | 54555.63561868316 |
| 10 | 12 | 15 | 00 | Gaussian | 0.011882585840785744 | 4.2662412782080015 | 23232.00588807093 |
| 10 | 12 | 16 | 00 | Gaussian | 0.1106811242506547 | 5.712188092760884 | 21854.960091317476 |
| 10 | 12 | 17 | 00 | Matern | 0.1564923249390624 | 6.3585591676234925 | 30679.359312241424 |
| 10 | 12 | 18 | 00 | Matern | 3.7945819373052085 | 5.5705354581482425 | 61873.10467805849 |
| 10 | 12 | 19 | 00 | Spherical | 0 | 5.21146045240515 | 118653.6979703675 |
| 10 | 12 | 20 | 00 | Matern | 0.029809002323313776 | 3.6636954462706153 | 77753.72067831105 |
| 10 | 12 | 21 | 00 | Matern | 0.013203743722880901 | 3661.095711581722 | 132036195.3413361 |
| 10 | 12 | 22 | 00 | Matern | 0 | 0.2678160893159283 | 151062.40480947983 |
| 10 | 12 | 04 | 30 | Gaussian | 0.002617809033457425 | 0.050315192890495665 | 90632.69987340784 |
| 10 | 12 | 11 | 30 | Spherical | 0.044895727974243155 | 0.08900453315684945 | 12979.652469684497 |
| 10 | 12 | 13 | 30 | Spherical | 0.003535173087320143 | 0.5227456422728881 | 155889.49158285485 |
| 10 | 12 | 14 | 30 | Gaussian | 0.04504810519515065 | 2.2941279678589734 | 27811.370935195897 |
| 10 | 12 | 15 | 30 | Gaussian | 0.08101559845556784 | 5.002466604212468 | 21441.760912858772 |
| 10 | 12 | 16 | 30 | Gaussian | 0.09897076967676578 | 6.445341051065697 | 27224.0371215361 |
| 10 | 12 | 17 | 30 | Gaussian | 1.4688470317449882 | 6.756840990038168 | 47083.675864761324 |
| 10 | 12 | 18 | 30 | Spherical | 1.364328009799264 | 5.402054036014759 | 90058.46035348976 |
| 10 | 12 | 19 | 30 | Gaussian | 0.01855857286635817 | 3.9077687878636627 | 53703.440885564174 |
| 10 | 12 | 20 | 30 | Exponential | 0.028195097705078248 | 9.723669979030896 | 479788.64334496146 |
| 10 | 12 | 21 | 30 | Matern | 0 | 4.70152742703779 | 1214188.2706647322 |
| 10 | 13 | 02 | 00 | Matern | 0.0013214704174527192 | 0.177049010646197 | 65268.23364680092 |